



Politecnico  
di Bari

Department of Electrical and Information Engineering  
INDUSTRY 4.0 Ph.D. Program  
SSD: ING-INF/04-AUTOMATICA

Final Dissertation

---

# Control Techniques for Collaborative and Cooperative Robotic Systems

---

by

Silvia Proia



---

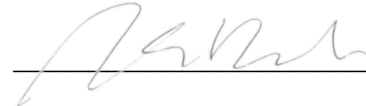
Referees:

Prof. Engr. Federica Pascucci

Prof. Engr. Karl von Ellenrieder

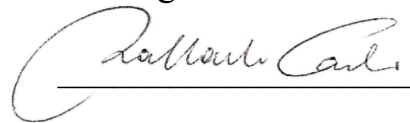
Supervisors:

Prof. Engr. Mariagrazia Dotoli



---

Dr. Engr. Raffaele Carli



---

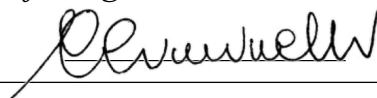
Dr. Engr. Graziana Cavone



---

*Coordinator of Ph.D Program:*

*Prof. Engr. Caterina Ciminelli*



---

Course n°36, 01/11/2020-31/10/2023



LIBERATORIA PER L'ARCHIVIAZIONE DELLA TESI DI DOTTORATO

Al Magnifico Rettore  
del Politecnico di Bari

Il/la sottoscritto/a Silvia Proia nato/a Piedimonte Matese (CE) il 23/10/1995, residente a Piedimonte Matese in viale della libertà n.35, e-mail [silvia.proia@poliba.it](mailto:silvia.proia@poliba.it), iscritto al 3° anno di Corso di Dottorato di Ricerca in Industria 4.0 ciclo 36 ed essendo stato ammesso a sostenere l'esame finale con la prevista discussione della tesi dal titolo:  
Control Techniques for Collaborative and Cooperative Robotic Systems

**DICHIARA**

- 1) di essere consapevole che, ai sensi del D.P.R. n. 445 del 28.12.2000, le dichiarazioni mendaci, la falsità negli atti e l'uso di atti falsi sono puniti ai sensi del codice penale e delle Leggi speciali in materia, e che nel caso ricorressero dette ipotesi, decade fin dall'inizio e senza necessità di nessuna formalità dai benefici conseguenti al provvedimento emanato sulla base di tali dichiarazioni;
- 2) di essere iscritto al Corso di Dottorato di ricerca Industria 4.0 ciclo 36, corso attivato ai sensi del "Regolamento dei Corsi di Dottorato di ricerca del Politecnico di Bari", emanato con D.R. n.286 del 01.07.2013;
- 3) di essere pienamente a conoscenza delle disposizioni contenute nel predetto Regolamento in merito alla procedura di deposito, pubblicazione e autoarchiviazione della tesi di dottorato nell'Archivio Istituzionale ad accesso aperto alla letteratura scientifica;
- 4) di essere consapevole che attraverso l'autoarchiviazione delle tesi nell'Archivio Istituzionale ad accesso aperto alla letteratura scientifica del Politecnico di Bari (IRIS-POLIBA), l'Ateneo archiverà e renderà consultabile in rete (nel rispetto della Policy di Ateneo di cui al D.R. 642 del 13.11.2015) il testo completo della tesi di dottorato, fatta salva la possibilità di sottoscrizione di apposite licenze per le relative condizioni di utilizzo (di cui al sito <http://www.creativecommons.it/Licenze>), e fatte salve, altresì, le eventuali esigenze di "embargo", legate a strette considerazioni sulla tutelabilità e sfruttamento industriale/commerciale dei contenuti della tesi, da rappresentarsi mediante compilazione e sottoscrizione del modulo in calce (Richiesta di embargo);
- 5) che la tesi da depositare in IRIS-POLIBA, in formato digitale (PDF/A) sarà del tutto identica a quelle **consegnate**/inviata/da inviarsi ai componenti della commissione per l'esame finale e a qualsiasi altra copia depositata presso gli Uffici del Politecnico di Bari in forma cartacea o digitale, ovvero a quella da discutere in sede di esame finale, a quella da depositare, a cura dell'Ateneo, presso le Biblioteche Nazionali Centrali di Roma e Firenze e presso tutti gli Uffici competenti per legge al momento del deposito stesso, e che di conseguenza va esclusa qualsiasi responsabilità del Politecnico di Bari per quanto riguarda eventuali errori, imprecisioni o omissioni nei contenuti della tesi;
- 6) che il contenuto e l'organizzazione della tesi è opera originale realizzata dal sottoscritto e non compromette in alcun modo i diritti di terzi, ivi compresi quelli relativi alla sicurezza dei dati personali; che pertanto il Politecnico di Bari ed i suoi funzionari sono in ogni caso esenti da responsabilità di qualsivoglia natura: civile, amministrativa e penale e saranno dal sottoscritto tenuti indenni da qualsiasi richiesta o rivendicazione da parte di terzi;
- 7) che il contenuto della tesi non infrange in alcun modo il diritto d'Autore né gli obblighi connessi alla salvaguardia di diritti morali od economici di altri autori o di altri aventi diritto, sia per testi, immagini, foto, tabelle, o altre parti di cui la tesi è composta.

Luogo e data Bari, 02/01/2024

Firma

Il/La sottoscritto, con l'autoarchiviazione della propria tesi di dottorato nell'Archivio Istituzionale ad accesso aperto del Politecnico di Bari (POLIBA-IRIS), pur mantenendo su di essa tutti i diritti d'autore, morali ed economici, ai sensi della normativa vigente (Legge 633/1941 e ss.mm.ii.),

**CONCEDE**

- al Politecnico di Bari il permesso di trasferire l'opera su qualsiasi supporto e di convertirla in qualsiasi formato al fine di una corretta conservazione nel tempo. Il Politecnico di Bari garantisce che non verrà effettuata alcuna modifica al contenuto e alla struttura dell'opera.
- al Politecnico di Bari la possibilità di riprodurre l'opera in più di una copia per fini di sicurezza, back-up e conservazione.

Luogo e data Bari, 02/01/2024

Firma

# Abstract

Over the years, the industrial landscape has experienced significant evolutions driven by advancements in technology, economic fluctuations, shifts in societal and environmental dynamics, and evolving consumer preferences. These changes have resulted in fundamental alterations in the way businesses operate, impacting various aspects of the industry, including the adoption of technology, labor practices, business models, and sustainability initiatives.

The ever-changing industrial environment is marked by several emerging frontiers that embrace on the one hand the incorporation of digital technologies, cyber-physical systems, artificial intelligence, and the internet of things into manufacturing processes with the potential for future developments, such as Industry 5.0, which emphasizes the advancement of collaborative robotic systems. Industry 5.0, in particular, places a significant emphasis on *human-robot collaboration* (HRC) by valuing human input.

On the other hand, the leading-edge frontiers involve incorporating sensors and data analytics into intelligent infrastructure, which serves to elevate maintenance standards, minimize downtime, and enhance safety. This also entails leveraging cooperative robot-machine systems, such as drones and diagnostic trains, for infrastructure inspections. These measures contribute to cost reduction and efficiency enhancement in the monitoring and maintenance processes. In the industrial sector, a realm of new prospects is emerging, driven by the innovative development of last-mile delivery solutions, encompassing drone deliveries, autonomous delivery vehicles, and smart lockers, all designed to streamline urban logistics.

As a result, this thesis is dedicated to solving two of the most important research challenges in designing decision and control techniques for collaborative and cooperative robotic systems and in particular for HRC and aerial-ground mobile robotic systems.

In the first part, this thesis aims to address the gaps identified in the existing literature regarding safe, ergonomic, and efficient HRC, which have been brought to light through a comprehensive review conducted in this field. In particular, the developed contributions regard the conceptualization and development of novel architectures and control techniques for HRC, in presence or absence of optimization. The central aim is to concurrently optimize the three key objectives, i.e., safety, ergonomics, and efficiency in tasks associated with addressing the trajectory planning problem formulated as second-order cone programming problem and solved with the direct transcription method, while respecting the *speed and separation monitoring* (SSM) ISO safety requirement and guaranteeing the ergonomic optimal position of the operator during the collaborative phase. Expanding upon the essential criteria for a safe and ergonomic HRC to encompass the emerging domain of collaboration between human and drone, the second goal involves creating control algorithms, i.e., *linear quadratic regulator* (LQR) controllers, for systems involving humans and drones within indoor industrial settings like warehouses 4.0.

The second part of this thesis is focused on the cooperation between a fleet of drones or an individual drone and a ground mobile robotic system (i.e., train, truck) that entails these entities working in harmony to achieve specific objectives or tasks in a coordinated manner. Particular emphasis is placed on the critical phase of drones returning to and landing on a moving train or truck. Thus, ad-hoc control techniques, i.e., consensus algorithm, LQR and receding horizon LQR controllers, are presented to tackle such complex tasks in an efficient and effective way.

*Faber est suae quisque fortunae.*  
Gaio Sallustio Crispo

# Contents

Preface	v
List of Papers Written by the Author	v
Acronyms	viii
<b>1 Introduction</b>	<b>1</b>
1.1 Collaborative vs Cooperative Robotic Systems . . . . .	2
<b>Part 1</b>	
<b>Collaborative Robotic Systems: Human-Robot Collaboration</b>	
<b>2 A Literature Review on Control Techniques for Safe, Ergonomic, and Efficient Human-Robot Collaboration in the Digital Industry</b>	<b>10</b>
2.1 Introduction . . . . .	10
2.2 Research Methodology . . . . .	14
2.3 Control Techniques for Safety in HRC Systems . . . . .	15
2.4 Control Techniques for Ergonomics in HRC Systems . . . . .	23
2.5 Control Techniques for Efficiency in HRC Systems . . . . .	26
2.6 Discussion and Future Developments . . . . .	30
2.7 Conclusions . . . . .	36
<b>3 A Multi-objective Optimization Approach for Trajectory Planning in a Safe and Ergonomic Human-Robot Collaboration</b>	<b>45</b>
3.1 Introduction . . . . .	45
3.2 Related Works and Contributions . . . . .	46
3.3 Proposed Methodology . . . . .	48
3.4 Case Study . . . . .	56
3.5 Conclusions . . . . .	60
<b>4 A Safe and Ergonomic Collaboration between Human and Drone in Warehouses</b>	<b>64</b>
4.1 Introduction . . . . .	64
4.2 Related Works and Contributions . . . . .	65
4.3 Quadrotor Model and Tasks . . . . .	67
4.4 Ascent and Descent Control Problem . . . . .	70
4.5 Free Flight Control Problem . . . . .	70
4.6 Descent for Human Collaboration with Drone Control Problem . . . . .	73
4.7 Case Study . . . . .	76
4.8 Conclusions . . . . .	79
<b>Part 2</b>	
<b>Cooperative Robotic Systems: Aerial - Ground Mobile Robotic Systems Cooperation</b>	
<b>5 Optimal Control of Drones for a Train-Drone Railway Diagnostic System</b>	<b>85</b>
5.1 Introduction . . . . .	85
5.2 Related Works and Contributions . . . . .	86
5.3 System Modelling and Tasks . . . . .	87
5.4 Control strategies . . . . .	90
5.5 Numerical experiments . . . . .	92

---

5.6	Conclusions . . . . .	94
<b>6</b>	<b>Optimal Control of Drones for a Hybrid Truck-Drone Delivery System</b>	<b>96</b>
6.1	Introduction . . . . .	96
6.2	Related Works and Contributions . . . . .	97
6.3	System Modelling and Tasks . . . . .	98
6.4	Control Strategy . . . . .	99
6.5	Numerical Experiments . . . . .	100
6.6	Conclusions . . . . .	102
<b>7</b>	<b>Conclusions</b>	<b>105</b>

# Preface

This thesis is submitted in fulfillment of the requirements for the degree of *Philosophiae Doctor* in Industry 4.0 at the *Politecnico di Bari*.

The research presented in this dissertation was conducted at the *Decision and Control Laboratory* in the Department of Electrical and Information Engineering of the Politecnico di Bari under the supervision of Professors **Mariagrazia Dotoli**, **Raffaele Carli**, and **Graziana Cavone** between November 2020 and October 2023.

This work is to the best of my knowledge original, except where acknowledgments and references are made to previous work. Most part of this thesis has been published during these three years in different scientific publications where I am one of the authors. The papers are preceded by an introductory chapter (Chapter 1), that relates them to each other and provides background information and motivation for the work. A version of Chapters 2, 3, and 4 have been presented in International Journals [1]–[3] while Chapters 5 and 6 have been published in the proceedings of International Conferences [4], [5]. A concluding chapter (Chapter 7) summarizes the main outcomes and findings for future developments.

Professors **Mariagrazia Dotoli**, **Raffaele Carli**, and **Graziana Cavone** were involved in the early stages of concept formation, as well as data collection, numerical implementation, analysis of experiments, and composition of the above-mentioned manuscripts.

In addition to the works presented in this thesis, I am one of the authors of further manuscripts on collaborative robotics [6], [7] and on human-drone interaction [8], that are the preliminary versions of [1], [2], and [3], respectively.

Finally, during these three years, I also had the opportunity to follow additional research directions leading to the publication of [9] that focuses on the game-theoretic control of power grids and energy communities.

The full list of papers written by the author is reported hereafter.

## List of Papers Written by the Author

### International Journal Articles

- [1] Proia, S., Carli, R., Cavone, G., and Dotoli, M., “Control techniques for safe, ergonomic, and efficient human-robot collaboration in the digital industry: A survey,” *IEEE Transactions on Automation Science and Engineering*, vol. 19, no. 3, pp. 1798–1819, 2022. DOI: [10.1109/TASE.2021.3131011](https://doi.org/10.1109/TASE.2021.3131011).
- [2] Proia, S., Cavone, G., Scarabaggio, P., Carli, R., and Dotoli, M., “Safety compliant, ergonomic and time-optimal trajectory planning for collaborative robotics,” *IEEE Transactions on Automation Science and Engineering*, 2023, (in press). DOI: [10.1109/TASE.2023.3331505](https://doi.org/10.1109/TASE.2023.3331505).
- [3] Proia, S., Cavone, G., Scarabaggio, P., Carli, R., and Dotoli, M., “A control framework for safe and ergonomic human-drone interaction in warehouses 4.0,” *IEEE Transactions on Automation Science and Engineering*, 2023, (under preparation).

### International Conference Proceedings

- [4] Proia, S., Cavone, G., Carli, R., and Dotoli, M., “Optimal control of drones for a train-drone railway diagnostic system,” in *2023 IEEE 19th International Conference on Automation Science and Engineering (CASE)*, Auckland, New Zealand, 2023, pp. 1–6. DOI: [10.1109/CASE56687.2023.10260390](https://doi.org/10.1109/CASE56687.2023.10260390).

- 
- [5] Proia, S., Cavone, G., Tresca, G., Carli, R., and Dotoli, M., “Automatic control of drones’ missions in a hybrid truck-drone delivery system,” in *2023 9th International Conference on Control, Decision and Information Technologies (CoDIT)*, 2023, pp. 1477–1482. DOI: [10.1109/CoDIT58514.2023.10284110](https://doi.org/10.1109/CoDIT58514.2023.10284110).
- [6] Proia, S., Carli, R., Cavone, G., and Dotoli, M., “A literature review on control techniques for collaborative robotics in industrial applications,” in *2021 IEEE 17th International Conference on Automation Science and Engineering (CASE)*, Lyon, France, 2021, pp. 591–596. DOI: [10.1109/CASE49439.2021.9551600](https://doi.org/10.1109/CASE49439.2021.9551600).
- [7] Proia, S., Cavone, G., Carli, R., and Dotoli, M., “A multi-objective optimization approach for trajectory planning in a safe and ergonomic human-robot collaboration,” in *2022 IEEE 18th International Conference on Automation Science and Engineering (CASE)*, Mexico City, Mexico, 2022, pp. 2068–2073. DOI: [10.1109/CASE49997.2022.9926513](https://doi.org/10.1109/CASE49997.2022.9926513).
- [8] Proia, S., Cavone, G., Camposeo, A., Ceglie, F., Carli, R., and Dotoli, M., “Safe and ergonomic human-drone interaction in warehouses,” in *2022 IEEE/RSJ International Conference on Intelligent Robots and Systems (IROS)*, Kyoto, Japan, 2022, pp. 6681–6686. DOI: [10.1109/IROS47612.2022.9981469](https://doi.org/10.1109/IROS47612.2022.9981469).
- [9] Calefati, M., Proia, S., Scarabaggio, P., Carli, R., and Dotoli, M., “A Decentralized Noncooperative Control Approach for Sharing Energy Storage Systems in Energy Communities,” in *2021 IEEE International Conference on Systems, Man, and Cybernetics (SMC)*, IEEE, Melbourne, Australia, 2021, pp. 1430–1435. DOI: [10.1109/SMC52423.2021.9658851](https://doi.org/10.1109/SMC52423.2021.9658851).



# Acknowledgements

Engaging in this Ph.D. journey has been a profoundly life-changing experience, and I am certain that I would have abandoned it on numerous occasions had it not been for the invaluable support and guidance I received from various people.

First and foremost, I want to express my profound gratitude to Prof. Mariagrazia Dotoli for her pivotal role as my primary supervisor throughout my studies. Whenever I faced questions or uncertainties, she consistently possessed the knowledge or directed me towards the right solutions. I am truly thankful for her contributions to my professional growth and for imparting precious lessons on becoming a proficient researcher and an upright person.

I also extend my heartfelt appreciation to Prof. Raffaele Carli and Prof. Graziana Cavone for their remarkable patience while supervising me. Their guidance and constant suggestions on the next steps were instrumental in leading me in the right direction, even when circumstances did not align with the original plans. Their unwavering motivation played a significant role in my journey.

I would like to acknowledge the entire research group of the Decision and Control Lab for fostering a stimulating and enjoyable work environment. I always enjoyed coming to work, going to conferences, and joining others group activities with you. The participation in conferences has been truly enriching experiences.

Without the support of my parents, this endeavor would not have been possible. Their belief in me has been the driving force behind my progress. To my aunt Tina, my stern math teacher and lifelong role model, your support and encouragement have been immeasurable, far beyond what I can convey in words.

Last but not least, I want to acknowledge and appreciate myself for the resilience and determination that led me to never give up.

# Acronyms

- AC** *admittance control.* 16
- AGVs** *automated guided vehicles.* 65
- APF** *artificial potential field.* 64, 67
- BDT** *Bayesian decision theory.* 18
- CBFs** *control barrier functions.* 18
- CCU** *cognitive control unit.* 24
- CNN** *convolutional neural network.* 18
- CPS** *cyber-physical system.* 17
- D-DDPG** *double deep deterministic policy gradient.* 28
- DH** *Denavit Hartenberg.* 57
- DM** *decision-making.* 24
- DMPs** *dynamic movement primitives.* 20
- DOE** *design of experiments.* 49
- DOF** *degrees of freedom.* 4, 67, 87, 98
- DSP** *disassembly sequence planning.* 28
- DT** *digital twin.* 27
- ERGA** *elite real-coded genetic algorithm.* 19
- FDCC** *forward dynamics compliance control.* 20
- FFT** *fast Fourier transform.* 28
- FIR** *finite impulse response.* 21
- FOAC** *fractional order admittance controller.* 22
- FOL** *first order logic.* 29
- GASP** *graph-based assembly sequence planner.* 24
- GPU** *graphics processing unit.* 19
- GS** *graph-search.* 26
- HR** *human-robot.* 11
- HRC** *human-robot collaboration.* i, 2, 10, 11, 45, 64, 66, 105
- HRI** *human-robot interaction.* 11
- IBLF** *integral barrier Lyapunov function.* 16
- IC** *impedance control.* 17, 21
- ILP** *integer linear programming.* 24

- LfD** *learning from demonstration.* 29
- LQR** *linear quadratic regulator.* i, 5, 21, 64, 67, 84–86, 96, 97, 106
- LS** *least square.* 17
- LUBA** *postural loading on the upper body assessment.* 49, 73
- MDBA-Pareto** *modified discrete bees algorithm based on Pareto.* 28
- MESO** *modified extended state observer.* 18
- MILP** *mixed-integer linear program.* 24
- ML** *machine learning.* 19
- MOCA** *mobile collaborative robot assistant.* 27
- MOO** *multi-objective optimization.* 47
- MPC** *model predictive control.* 20, 67
- MPIC** *model predictive impedance controller.* 21
- MSDs** *musculoskeletal disorders.* 23
- NLP** *non-linear programming.* 20
- NMPC** *non-linear model predictive control.* 19
- NNs** *neural networks.* 16
- OCRA** *occupational repetitive action.* 49, 73
- PCA** *principal component analysis.* 28
- PFL** *power and force limiting.* 17, 45, 65
- PID** *proportional-integral-derivative.* 67
- POMDP** *partially observable Markov decision process.* 20
- RBF** *radial basis function.* 25
- RBFNNs** *radial basis function neural networks.* 16
- REBA** *rapid entire body assessment.* 46, 49, 66
- RF** *random forest.* 29
- RL** *reinforcement learning.* 20
- RNNs** *recurrent neural networks.* 16
- RRC** *robot-robot collaboration.* 2
- RULA** *rapid upper limb assessment.* 4, 8, 45, 46, 64, 66, 106
- SLQ** *sequential linear quadratic.* 72
- SMC** *sliding mode control.* 21, 72
- SNS** *saturation in the null space.* 17
- SOCP** *second-order cone programming.* 47
- SoS** *system of systems.* 2
- SSM** *speed and separation monitoring.* i, 4, 8, 17, 45, 64–66, 106
- STOMP** *stochastic trajectory optimizer.* 20
- SVM** *linear support vector machine.* 18, 25

**UAVs** *unmanned aerial vehicles.* 86, 96

**VBSMC** *variable boundary layer SMC.* 22

# Chapter 1

## Introduction

Since the dawn of Industry 4.0 in the manufacturing scenario less than a decade ago, the design and development of production systems are experiencing substantial changes towards full automation. This ongoing challenge is being tackled with the adoption of robots and their repercussions on society.

While robotics has traditionally possessed an air of esoteric allure, and automation has often been perceived as the diligent workhorse, primarily associated with manufacturing and lacking glamour, the year 1984 witnessed a pivotal moment when a visionary group of researchers orchestrated the union of these two fields.

Despite their differences, –i.e., “...*Robotics focuses on systems incorporating sensors and actuators that operate autonomously or semi-autonomously in cooperation with humans. Robotics research emphasizes intelligence and adaptability to cope with unstructured environments. Automation research emphasizes efficiency, productivity, quality, and reliability, focusing on systems that operate autonomously, often in structured environments over extended periods, and on the explicit structuring of such environments.*”– the union has thrived, and, akin to most married couples, the partners have cultivated numerous shared interests over time [1].

In essence, robotics involves employing machines to execute tasks typically undertaken by humans. This has unquestionably enabled the automation of intricate and repetitive tasks, culminating in accelerated production, diminished cycle times, and heightened throughput. Consequently, it has bolstered productivity and efficiency.

Nevertheless, due to their distinct characteristics, in order to keep the couple together, there is an emerging need for designing appropriate decision and control techniques.

Control manifests in both technical and non-technical systems. A system may constitute a singular entity, element, part, or an assemblage of objects linked or interdependent in some manner [2]. Hence, by definition [3], a system is *an arrangement of parts or elements that together exhibit behavior or meaning that the individual constituents do not.*

In short, a system is a structured and organized collection of interrelated components or elements that work together to achieve a specific set of objectives, functions, or purposes. In the context of engineering and control theory, a robot can be considered as a system [4], [5]. It encompasses various interconnected components, including mechanical elements like joints and actuators, sensory equipment for environmental perception, a control unit responsible for data processing and decision-making, and at times, software for programming and communication purposes. These components collaborate in a coordinated manner to fulfill specific functions or tasks. Similar to any system, a robot operates with inputs, often comprising sensor data, and produces outputs in the form of actions or movements in response to these inputs. Robots are essentially controlled systems, with the control unit or software program issuing commands to direct the robot's actions based on sensory input and predetermined algorithms or instructions. Many robots incorporate feedback mechanisms that enable real-time adjustments, mirroring the principles of a closed-loop control system. Ultimately, robots are designed with particular objectives or tasks in mind, ranging from basic functions like object manipulation to intricate tasks such as navigating complex, unstructured environments. In essence, a robot is subject to analysis and comprehension as a system due to its interconnected components working in unison to achieve predefined goals. Engineers and researchers draw upon principles from control theory, system theory, and robotics to create, assess, and enhance robotic systems for a wide array of applications.

When we are not referring to a self-contained system but to a *complex network or*

*collection of individual systems that collaborate to achieve a more extensive and complex set of goals*, we use the term *system of systems* (SoS). It is essentially a higher-level composite system comprised of multiple subsystems, each potentially intricate in its own right, that has both operational and managerial independence of its elements. When the SoS is deconstructed into its constituent systems, these individual components should possess the capability to function effectively on their own (operational independence of the components). Furthermore, these component systems not only have the capability to operate independently, but they also do so in practice. Each component system is procured and integrated separately, maintaining ongoing operational autonomy separate from the SoS (managerial independence of the components) [6], [7].

Various types of systems come together to collectively address complex challenges or achieve overarching goals. Hence, a SoS can be composed of a diverse class of systems, including collaborative, cooperative and non-cooperative systems. These constituent systems contribute to the overall functioning of the SoS based on their characteristics and the specific context. Collaborative systems involve multiple entities, which could be humans, machines, or a combination, working together in a coordinated manner to achieve a common objective. Similarly, some constituent systems within an SoS may be cooperative systems. They also involve multiple entities working together, but the emphasis is on entities that have their own distinct goals or objectives while contributing to a common purpose. Thus, collaboration involves entities that work simultaneously on a shared object in a shared space whereas cooperation engages entities that work towards a shared goal in partially or completely shared space. Not all systems within an SoS need to be collaborative or cooperative. Some systems may operate independently or without actively participating in coordination efforts. These non-cooperative systems can have their own goals and functions that are not directly aligned with the common objectives of the SoS.

In the realm of robotics, a SoS pertains to the integration and coordination of multiple robotic systems to accomplish intricate tasks or objectives. It involves the collaborative operation of these robotic systems within a broader context, often with the aim of addressing complex challenges beyond the capacity of a single robot.

An SoS in robotics encompasses diverse robotic subsystems, which can range from autonomous robots to collaborative robots and drones. These subsystems are interconnected or synchronized to enable communication, information sharing, and joint efforts towards common goals. They are commonly deployed for tasks that demand a higher degree of complexity, scalability, or extensive coverage. This might include coordinating multiple robots for tasks like large-scale exploration, search and rescue missions, or managing a fleet of vehicles. Interoperability is a key consideration, ensuring that the various robotic systems within the SoS can collaborate effectively. Furthermore, the interactions among these robotic subsystems within the SoS can lead to emergent behaviors and properties, making the entire system more adaptable and efficient. SoS in robotics finds applications in diverse fields, including multi-robot exploration and collaborative industrial automation. The aim is to harness the capabilities of multiple robotic systems to address complex challenges more effectively and efficiently.

## 1.1 Collaborative vs Cooperative Robotic Systems

Collaboration can take various forms depending on the entities involved. In *human-robot collaboration* (HRC), the collaboration entails a human working alongside one or more robots, with the interaction occurring directly between the human and the robot(s). The primary goal is to enhance the capabilities of both humans and robots, with robots assisting in tasks while humans contribute cognitive abilities. In contrast, *robot-robot collaboration* (RRC) involves collaboration exclusively among robots, with no direct human involvement. The interaction takes place solely between the robots, and the objective is to leverage the collective strengths of multiple robots to perform tasks efficiently and autonomously. This type of collaboration is commonly employed in scenarios where

robots need to work together to accomplish complex tasks. Finally, Robot-Machine Collaboration involves robots collaborating with other machines or automated systems, optimizing complex processes.

As becomes apparent from the emerging sustainable, human-centric and resilient industrial paradigm, collaboration between humans and robots is generally more challenging than collaboration between robots. This difficulty arises due to the stark contrast in their capabilities and characteristics. Humans possess complex cognitive skills, adaptability, and emotional intelligence, while robots excel in precision, speed, and repetitive tasks. Ensuring effective communication and coordination between these diverse entities can be intricate. Safety is a paramount concern when humans work alongside robots, necessitating the incorporation of safety features and protocols. Moreover, building trust between humans and robots is a crucial but often time-consuming endeavor. Collaboration environments involving humans and robots are frequently unpredictable and dynamic, further complicating the adaptation of robots to changing conditions. Additionally, these scenarios often require robots to perform tasks designed for human abilities, introducing complexities in task execution.

Similarly, cooperation can occur between robots and machines, taking two primary forms: (1) robot-robot cooperation that entails multiple robots working together in a coordinated manner. They collaborate by sharing information, coordinating actions, or specializing in different aspects of a task to achieve a common objective; (2) robot-machine cooperation in which robots collaborate with other machines or automated systems. The aim is to optimize complex processes (e.g., production processes, logistics processes, infrastructure monitoring) and enhance overall system efficiency by integrating robot capabilities with machine functions. These forms of cooperation leverage the strengths of robots and machines to improve task performance and productivity in various industrial and automation applications.

Within this specific context, cooperation between robots and machines can pose greater challenges compared to cooperation among robots. This heightened complexity arises from factors such as diverse interfaces, compatibility issues, synchronization requirements, safety considerations, scalability concerns, interoperability challenges, and the need for adaptability to varied tasks. These complexities stem from the unique characteristics and functions of both robots and machines, as well as the diverse contexts in which they cooperate.

As a result, since significant attention and effort need to be dedicated to HRC and robot-machine cooperation and there is an extreme need to fill the gaps in the related literature, this thesis follows two main research directions and thus, is structured in two main parts –anticipated by the present Introduction– as described in the sequel. Note that this thesis presents the results of research conducted and published in a series of conference and journal papers by the author.

### 1.1.1 Human-Robot Collaboration

The fourth industrial revolution, commonly referred to as Industry 4.0, is fundamentally transforming the way people live and work. It exerts a significant influence on the manufacturing landscape and is increasingly being embraced across global production, distribution, and commercialization networks [8].

The pivotal technology underpinning the realization of Industry 4.0 is undoubtedly collaborative robotics. This technology is also emerging as a cornerstone of the forthcoming Industry 5.0 [9], a revolution that actively reintegrates humans into the automation chain. Within this paradigm, the unique qualities and attributes of both humans, such as intelligence, creativity, and adaptability, and robots, including flexibility, precise accuracy, and tireless operation, are harmoniously melded to enhance the execution of a wide array of tasks. As a result, operators and robots are positioned to work together in significantly closer collaboration, introducing innovative *collaborative robot* (cobot) models that elevate the efficiency of production processes [10].

The collaboration between a human and a collaborative robot can be viewed through the lens of a SoS. In this scenario, human and cobot function as separate subsystems. The human represents a complex system with unique capabilities, decision-making processes, and objectives. Simultaneously, the cobot, serves as another distinct subsystem. Unlike conventional robots, which typically operate autonomously and are frequently restricted within safety enclosures, cobots seamlessly cohabit in shared spaces with humans, maintaining both safety and operational efficiency. Cobots are purposefully engineered not to augment or supplant human capabilities, but rather to concentrate on repetitive tasks, enabling human operators to concentrate their expertise on more intricate problem-solving endeavors.

The advancement of HRC in industrial contexts is a continuously evolving process with several notable trends. The European research highlights a substantial surge in digital and smart manufacturing initiatives, particularly in the creation of collaborative robotic systems for diverse applications. Clearly, the primary objectives of HRC in industrial settings revolve around enhancing employee safety and well-being, alongside boosting profitability and productivity [11]. On the one hand, the portability and compactness of cobots allow to optimize production processes saving space and improving efficiency and accuracy. On the other hand, physical and cognitive ergonomics are enhanced by minimizing mental stress and psychological discomfort, which could be provoked to operators that share their work space with robots [12].

Thus, designing a robotic controller and analyzing existing decision and control techniques are essential for creating innovative models and cutting-edge methodologies for a safe, ergonomic, and efficient HRC. **Chapter 2** aims at addressing the emerging challenges in this area and crafting novel HRC architectures and control methods. This includes scenarios with or without optimization, aiming to bridge the gaps identified in the comprehensive literature reviews [11], [13] conducted by the author.

The primary goal of my thesis illustrated in **Chapter 3** is to simultaneously address three critical objectives, i.e., safety, ergonomics, and efficiency, particularly in tasks related to trajectory planning problems, since the literature has shown that only a small fraction of scientific articles attempt to optimize all three aspects simultaneously in HRC tasks. To achieve this, we must consider mechanical aspects of industrial manipulators with an increasing number of *degrees of freedom* (DOF), such as statics, kinematics, and dynamics, and incorporate them into constrained optimal control problems [14]. From an ergonomic perspective, we integrate the *rapid upper limb assessment* (RULA) index as an assessment tool in optimal control problems to evaluate workers' exposure to ergonomic risk factors. Additionally, we adhere to safety standards for human workers during collaborations, following the *speed and separation monitoring* (SSM) ISO criterion [15].

Extending the key requirements of a safe and ergonomic HRC to the arising field of collaboration between human and drone, the second objective of my thesis shown in **Chapter 4** focuses on developing control algorithms for trajectory planning/re-planning problems and collision avoidance issues in human-drone systems, especially in indoor settings like warehouses [16].

### 1.1.2 Aerial - Ground Mobile Robotic Systems Cooperation

The cooperative robotic systems are considered as SoSs because they are composed of multiple interacting and interdependent subsystems (e.g., drone, train, truck), each with its own specialized function and capabilities.

The aforementioned systems offer a myriad of advantages compared to standalone systems. They streamline task completion by distributing work among multiple entities, leading to faster job turnaround and heightened overall productivity. Additionally, they provide redundancy and reliability, ensuring uninterrupted operation even if one entity encounters issues. They demonstrate scalability, effortlessly adapting to increased workloads and changing requirements, while enabling entities to specialize and optimize resource allocation. Furthermore, they exhibit adaptability in dynamic environments, making necessary adjustments in interactions and resource allocation. Cooperative



systems can also be a cost-effective solution, especially when redundancy or extensive coverage is essential. Heterogeneous cooperative systems, comprising entities with diverse capabilities, excel in a wide range of tasks and challenges and in critical scenarios, they reduce time pressure on individual entities, promoting safer and more deliberate actions [17].

In particular, the cooperative robotic systems examined in this thesis operate in challenging outdoor environments, with a particular focus on railway diagnostics (**Chapter 5**) [18] and last-mile delivery (**Chapter 6**) [19]. In both applications the fleet of drones or the drone that interacts with a ground mobile robotic system is considered as a subsystem of the SoS. Specifically, my goal (i.e., third objective of the thesis) is to optimally manage the crucial phase of drones returning to and landing on the moving train or truck that represents the second subsystem. To control the drones, a combination of consensus algorithms in the leader-following fashion employed for fleet formation, trajectory re-planning and tracking algorithms (i.e., *linear quadratic regulator* (LQR), Receding Horizon LQR) are studied and implemented in real simulations' scenarios by managing the real-time changes of the positions of the landing point and considering some possible moving obstacles (i.e., dynamic environments) like humans or birds.

## References

- [1] Goldberg, K., "What is automation?" *IEEE transactions on automation science and engineering*, vol. 9, no. 1, pp. 1–2, 2011.
- [2] Unbehauen, H., *Control systems, robotics and automation*. Eolss Publishers Company Limited Oxford, 2009.
- [3] Dori, D., Sillitto, H., Griego, R. M., *et al.*, "System definition, system worldviews, and systemness characteristics," *IEEE Systems Journal*, vol. 14, no. 2, pp. 1538–1548, 2020. DOI: [10.1109/JSYST.2019.2904116](https://doi.org/10.1109/JSYST.2019.2904116).
- [4] Spong, M. W., Hutchinson, S., and Vidyasagar, M., *Robot modeling and control*. John Wiley & Sons, 2020.
- [5] Sciavicco, L. and Siciliano, B., *Modelling and control of robot manipulators*. Springer Science & Business Media, 2001.
- [6] Maier, M. W., "Architecting principles for systems-of-systems," *Systems Engineering: The Journal of the International Council on Systems Engineering*, vol. 1, no. 4, pp. 267–284, 1998.
- [7] Boardman, J. and Sauser, B., "System of systems-the meaning of of," in *2006 IEEE/SMC international conference on system of systems engineering*, IEEE, 2006, 6–pp.
- [8] Xu, L. D., Xu, E. L., and Li, L., "Industry 4.0: State of the art and future trends," *Int. J. Prod. Res.*, vol. 56, no. 8, pp. 2941–2962, 2018.
- [9] Demir, K. A., Döven, G., and Sezen, B., "Industry 5.0 and human-robot co-working," *Procedia Comput. Sci.*, vol. 158, pp. 688–695, 2019.
- [10] Hentout, A., Aouache, M., Maoudj, A., and Akli, I., "Human-robot interaction in industrial collaborative robotics: A literature review of the decade 2008–2017," *Adv. Robot.*, vol. 33, no. 15-16, pp. 764–799, 2019.
- [11] Proia, S., Carli, R., Cavone, G., and Dotoli, M., "Control techniques for safe, ergonomic, and efficient human-robot collaboration in the digital industry: A survey," *IEEE Transactions on Automation Science and Engineering*, vol. 19, no. 3, pp. 1798–1819, 2022. DOI: [10.1109/TASE.2021.3131011](https://doi.org/10.1109/TASE.2021.3131011).
- [12] Gualtieri, L., Rauch, E., and Vidoni, R., "Emerging research fields in safety and ergonomics in industrial collaborative robotics: A systematic literature review," *Robot. Comput. Integr. Manuf.*, vol. 67, p. 101998, 2021.

- [13] Proia, S., Carli, R., Cavone, G., and Dotoli, M., “A literature review on control techniques for collaborative robotics in industrial applications,” in *2021 IEEE 17th International Conference on Automation Science and Engineering (CASE)*, Lyon, France, 2021, pp. 591–596. DOI: [10.1109/CASE49439.2021.9551600](https://doi.org/10.1109/CASE49439.2021.9551600).
- [14] Proia, S., Cavone, G., Carli, R., and Dotoli, M., “A multi-objective optimization approach for trajectory planning in a safe and ergonomic human-robot collaboration,” in *2022 IEEE 18th International Conference on Automation Science and Engineering (CASE)*, Mexico City, Mexico, 2022, pp. 2068–2073. DOI: [10.1109/CASE49997.2022.9926513](https://doi.org/10.1109/CASE49997.2022.9926513).
- [15] Proia, S., Cavone, G., Scarabaggio, P., Carli, R., and Dotoli, M., “Safety compliant, ergonomic and time-optimal trajectory planning for collaborative robotics,” *IEEE Transactions on Automation Science and Engineering*, 2023, (in press). DOI: [10.1109/TASE.2023.3331505](https://doi.org/10.1109/TASE.2023.3331505).
- [16] Proia, S., Cavone, G., Scarabaggio, P., Carli, R., and Dotoli, M., “A control framework for safe and ergonomic human-drone interaction in warehouses 4.0,” *IEEE Transactions on Automation Science and Engineering*, 2023, (under preparation).
- [17] Feng, Z., Hu, G., Sun, Y., and Soon, J., “An overview of collaborative robotic manipulation in multi-robot systems,” *Annual Reviews in Control*, vol. 49, pp. 113–127, 2020.
- [18] Proia, S., Cavone, G., Carli, R., and Dotoli, M., “Optimal control of drones for a train-drone railway diagnostic system,” in *2023 IEEE 19th International Conference on Automation Science and Engineering (CASE)*, Auckland, New Zealand, 2023, pp. 1–6. DOI: [10.1109/CASE56687.2023.10260390](https://doi.org/10.1109/CASE56687.2023.10260390).
- [19] Proia, S., Cavone, G., Tresca, G., Carli, R., and Dotoli, M., “Automatic control of drones’ missions in a hybrid truck-drone delivery system,” in *2023 9th International Conference on Control, Decision and Information Technologies (CoDIT)*, 2023, pp. 1477–1482. DOI: [10.1109/CoDIT58514.2023.10284110](https://doi.org/10.1109/CoDIT58514.2023.10284110).

**Part 1**  
**Collaborative Robotic Systems:**  
**Human-Robot Collaboration**

The design and development of manufacturing systems are experiencing substantial changes towards Industry 5.0. This ongoing challenge is being tackled by academia and industrial experts with the adoption of collaborative robots, where the skills and peculiarities of humans (e.g., intelligence, creativity, adaptability, etc.) and robots (e.g., flexibility, pinpoint accuracy, tirelessness, etc.) are combined to better perform a variety of tasks. Nevertheless, due to their different characteristics, there is an emerging need for designing suitable decision and control techniques to ensure a safe and ergonomic HRC, while keeping the highest level of productivity.

Health and safety in workplaces are business imperatives, since they ensure not only a safe collaboration between industrial machinery and human operators, but also an increased productivity and flexibility of the entire industrial process. Hence, investing in health is a real driver for business growth. The key enabling technologies of Industry 5.0, such as collaborative robotics, exoskeletons, virtual and augmented reality, require standardization and indispensable technical safety requirements that cannot ignore physical, sensory, and psychological peculiarities of the human worker and aspects like usability and acceptability of these technologies in performing their activities.

Against this background, the aim of **Chapter 2** is to provide researchers and experts with a reference source in the related field, which can help them designing and developing suitable solutions to control problems in safe, ergonomic, and efficient collaborative robotics. In particular, since there is no work cataloging the scientific articles from the point of view of automatic control in HRC, this chapter aims at classifying the most relevant and recent works developed by the scientific community according to three key objectives of HRC in the smart manufacturing systems that are, safety, ergonomics, and efficiency. The articles are then grouped by problem and type of control, indicating whether optimization techniques are adopted or not. Finally, the literature review draws conclusions on relevant and promising future research directions in each analyzed domain.

Since none of the reviewed articles in the literature review is simultaneously focused on all the three targets (i.e., safety, ergonomics, and efficiency) and only a small percentage of the related works are written accordingly to dual targets, HRC research will need to address all three of the previously mentioned objectives simultaneously.

Against this ongoing industrial challenge, the aim of **Chapter 3** is to provide researchers and experts with an innovative HRC trajectory planning methodology focused on enhancing production efficiency while respecting the *speed and separation monitoring* (SSM) ISO safety requirement and guaranteeing the ergonomic optimal position of the operator during an assembly task. Therefore, the proposed methodology can be a convenient solution to be deployed in industrial companies, since it can support human operators by drastically reducing work-related musculoskeletal disorders and augmenting their performance in the working environment. Specifically, a multi-objective optimization approach for the trajectory planning in safe and ergonomic HRC is defined, with the aim of finding the best trade-off between the total traversal time of the trajectory for the robot and ergonomics for the human worker, while respecting the SSM ISO safety requirements. The proposed approach consists of three main steps. First, the *rapid upper limb assessment* (RULA) ergonomic index is evaluated on a manikin designed on a dedicated software. The aim is to ensure a high quality of work in the considered HRC scenario with a consequent decrease of the musculoskeletal disorders associated with highly repetitive and dangerous activities. Second, a time-optimal and safety-constrained trajectory planning problem is defined as a second-order cone programming problem. Finally, a multi-objective control problem is formulated and solved to compute the trajectory that ensures the best compromise between time end ergonomics. The approach is applied to a real-life case study, and the ensuing results are deliberated upon, affirming the approach's efficacy.

As highlighted by the extensive literature review proposed in Chapter 2, safety is the primary need in HRC applications, followed by the efficiency and the ergonomics targets. In **Chapter 4**, an application of collaboration between human and drone in warehouses is presented with the fundamental goal of enhancing the operators' safety and well-being while simultaneously improving efficiency and reducing production costs.

Until recently, the predominant emphasis has been on the collaboration between human and drone in outdoor settings. Comparatively, there have been fewer contributions for indoor industrial applications. However, indoor drone utilization, particularly in warehouses, holds significant promise for tasks like inventory management, intra-logistics, and inspection and surveillance. This study specifically addresses the development of a safe and ergonomic human-drone architecture for the pick-and-place task within the intra-logistics sector. Hence, the aim of this chapter is to define a novel trajectory planning and tracking control algorithm for a quadrotor transporting items from the picking bay to the palletizing area and supporting the operator tasks inside a warehouse, while respecting the ISO safety requirements and physical ergonomics in approaching the operator during the collaboration with the human operator. More specifically, the SSM methodology is applied for the first time to the collaboration between human and drone, in analogy to the HRC ISO safety requirements as well as the RULA, for evaluating the operator's ergonomic posture during the collaboration with the drone. The outcomes of the simulations involving the human-drone architecture are presented comprehensively and discussed, demonstrating the efficacy of the proposed approach in ensuring a safe and user-friendly collaboration.

## Chapter 2

# A Literature Review on Control Techniques for Safe, Ergonomic, and Efficient Human-Robot Collaboration in the Digital Industry

### Abstract

The fourth industrial revolution, also known as Industry 4.0, is reshaping the way individuals live and work while providing a substantial influence on the manufacturing scenario. The key enabling technology that has made Industry 4.0 a concrete reality is without doubt *collaborative robotics*, which is also evolving as a fundamental pillar of the next revolution, the so-called Industry 5.0. The improvement of employees' safety and well-being, together with the increase of profitability and productivity, are indeed the main goals of *human-robot collaboration* (HRC) in the industrial setting. The robotic controller design and the analysis of existing decision and control techniques are crucially needed to develop innovative models and state-of-the-art methodologies for a safe, ergonomic, and efficient HRC. To this aim, this chapter presents an accurate review of the most recent and relevant contributions to the related literature, focusing on the control perspective. All the surveyed works are carefully selected and categorized by target (i.e., safety, ergonomics, and efficiency), and then by problem and type of control, in presence or absence of optimization. Finally, the discussion of the achieved results and the analysis of the emerging challenges in this research field are reported, highlighting the identified gaps and the promising future developments in the context of the digital evolution.

### Contents

2.1	Introduction . . . . .	10
2.2	Research Methodology . . . . .	14
2.3	Control Techniques for Safety in HRC Systems . . . . .	15
2.4	Control Techniques for Ergonomics in HRC Systems . . . . .	23
2.5	Control Techniques for Efficiency in HRC Systems . . . . .	26
2.6	Discussion and Future Developments . . . . .	30
2.7	Conclusions . . . . .	36

### 2.1 Introduction

Less than a decade has passed since the paradigm of Industry 4.0 faced the manufacturing scenario. Today, the fourth industrial revolution is riding its peak, and has become a flourishing reality thanks to the combination of production and network connectivity through internet of things (IoT) and cyberphysical systems (CPS). In the world economy, there is still a growing demand for Industry 4.0 to increase the degree of industrialization, informatization, and digitization, and thus, to achieve superior efficiency, competency, and competitiveness [1].

Since the dawn of Industry 4.0 in 2011, great emphasis was laid on the coexistence of humans and robots in the industrial environment [1]. Undoubtedly, the way humans work together with robots is becoming ever more important in the era of automation and



robotization. In fact, visionaries are already predicting the next revolution, the so-called Industry 5.0, that reinserts proactively humans back into the automation chain, allowing operators and robots to work significantly more closely together [2]. Therefore, humans are expected to work alongside new models of *collaborative robots (cobots)*, enhancing production. In contrast to robots that predominantly work independently from humans and often reside in a cage, cobots co-exist in the same environment together with humans, without renouncing to safety or efficiency [3]. A cobot is designed not necessarily to augment the operator's skills nor to replace her/him, but rather to focus on repetitive activities, so that the operator can focus on problem-solving tasks.

Cobots are the object of in-depth investigations both in the fields of *human-robot interaction (HRI)* and *human-robot collaboration (HRC)*, which are relatively recent research areas and exactly for this reason the corresponding acronyms are often used indistinctly and confusedly in the literature and have aroused much debate among researchers due to conceptual misunderstandings. However, there is a clear distinction in the two meanings [4]. *Collaboration* is the activity of two or more entities that work jointly and sought a common goal. Differently, *interaction* is the reciprocal influence of two or more entities that do not necessarily entail a common goal. Both collaboration and interaction are classes of coexistence, i.e., the entities share the same environment. Eventually, coexistence can entail no interaction of the coexisting entities. Summarizing, any collaborative action implies numerous interactions but there may be an interaction which does not imply any collaboration. Moreover, each interaction signifies a coexistence of the two intervening beings. However, human and robot can work in the same environment (coexistence) but without any interaction. In our survey we focus only on HRC in the manufacturing scenario so as not to mislead the research.

The industrial development of HRC is ongoing in several different areas. The latest trends of the European research show a significant rise in digital and smart manufacturing projects, including the development of cobots for several application areas. Obviously, increasing the profitability of production is the main goal of cobot evolution, which certainly depends on a safe and efficient HRC in a shared work place [5]. Indeed, the portability and compactness of cobots allow to optimize the production process, saving space and improving efficiency and accuracy. In addition, another significant purpose of the research on collaborative robotics and in general of HRC in the digital industry is to enhance physical and cognitive ergonomics by minimizing mental stress and psychological discomfort which could be provoked to operators while sharing the workspace with robots [6], [7].

In this context, decision and control techniques [8] play a vital role in ensuring a safe and ergonomic HRC while keeping the highest level of productivity [5]. Therefore, the aim of this work is to focus on the pivotal goals of cobotics in the manufacturing context – i.e., safety, ergonomics, and efficiency (Fig. 2.1) – and surveying in detail the main pertaining control methods presented in the related literature with the aim of identifying advantages and gaps.

### 2.1.1 Survey Positioning in the Related Literature

In the last few years several scientists have tried to review and classify the research content on industrial collaborative robotics (*cobotics*) from different perspectives.

For instance, Hentout *et al.* [3] present a literature review of the major recent works on *human-robot (HR)* interaction in the industrial context, conducted between 2008 and 2017. A classification of the contents of these works is proposed, ranging into several categories and sub-categories from hardware and software design of collaborative robotics systems to robotic programming approaches and virtual & augmented reality, from safety to cognitive HR interaction. The HRC progress and prospects are further suggested by Ajoudani *et al.* who present in their review [9] the state-of-the-art on bi-directional human-robot interfaces developed for improved human-robot perception and in particular, for the estimation of the human physical or cognitive state variations with the use of bio-signals such as electromyography, robot control modalities, control performances



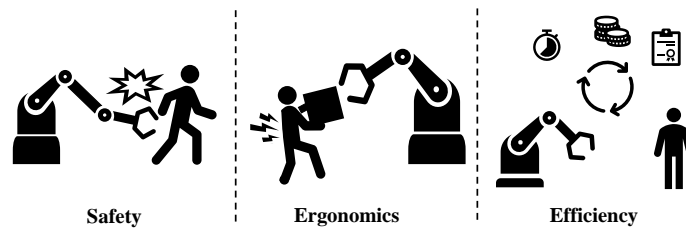


Figure 2.1: Main targets in HRC.

(system stability and transparency), benchmarking and relevant use cases. Aiming at presenting to the researchers all the application’s sectors and abilities to assist the workers in the HRC scenario, Tong and Liu analyze in detail in [10] the supernumerary robotic limbs (SRLs), which are a new type of wearable robots. In particular, the most recent control methods of SRLs are discussed and are firstly classified according to the control complexity into limb mapping control, electromyographic signal control and brain-machine interface control. Then they are further classified according to the control strategies into an iterative learning control strategy, phase-variable based control strategy or adaptive oscillator based control strategy.

Physical and cognitive collaboration in the industrial environment is the focus of the HRC extensive review proposed by Villani *et al.* [11]. From this work it emerges that the primary main challenge in HRC is undoubtedly safety, which must be taken into account by any approach implementing collaboration between humans and robots. In order to achieve a safe and flexible HRC, intuitive user interfaces can be properly drawn and appropriate design methods should be addressed, including control laws, sensors, task allocation and planning approaches. An overview of the state-of-the-art approaches for robot programming is also presented by the authors. Another survey proposed by Tsarouchi *et al.* [12] groups all the challenges, future trends, and techniques connected to task planning/coordination and intuitive programming in the manufacturing scenario such as human-robot task allocation, scheduling, and social aspects.

A systematic literature review is written by Gualtieri *et al.* [7] who investigate and categorize the recent research regarding safety and ergonomics or human factors for industrial collaborative robotics and describe a useful methodology to identify relevant papers for this study. A particular emphasis on the context of manufacturing is given in [5], where an overview of collaborative robotics towards manufacturing applications and the main industrial cases are depicted, and in [13], where the safety requirements in the manufacturing environment, the methods and challenges of safety assurance are discussed from the perspective of key functional requirements, collaboration variants, standardizations, and safety mechanisms.

Some literature reviews in the manufacturing context focus on the critical industrial process of assembly. For instance, Wang *et al.* [14] focus on symbiotic HRC assembly and present some existing communication methods like voice processing, gesture recognition, haptic interaction, and brainwave perception. Then, the authors illustrate the safety standards for collision avoidance and deep learning for classification, recognition, and context awareness identification. Challenges in the context of collaborative assembly are also highlighted by Papanastasiou *et al.* [15] who present a large variety of HRC technologies argued from a safety perspective in a real case study. Furthermore, Michalos *et al.* illustrate in [16] an approach in which high payload industrial robots and operators are employed for HRC assembly with a specific case study in the automotive sector and with all the safety guidelines described in detail.

Like the previously cited works, safety is considered the most critical concern in HRC and for this reason the potential strategies and methods for ensuring safety are also illustrated by Lasota *et al.* [17] from a different point of view. They classify the collection of existing works into four major categories: safety through control, motion planning, prediction, and consideration of psychological factors. Through this work, the



development of methods and techniques aimed at ensuring safety in the manufacturing setting is encouraged in order to reduce risks associated with HRC and thus facilitating the transfer of HRC systems from the research lab into the real world. The concept of safety also appears in [18], where the different safety measures and the technical standards relevant to HRC in the industrial production are highlighted. The in-depth conceptual categorization of the HRC aspects in awareness, intelligence, and compliance is certainly innovative in the HR taxonomy. Finally, Hashemi-Petroodi *et al.* [19] focus their work on operations management that aims at optimizing productivity and responsiveness in a company. Two main hybrid manufacturing systems, i.e., dual resource constrained and HRC optimization problems, are discussed, and different features of the workforce and machines/robots –such as heterogeneity, homogeneity, ergonomics, and flexibility– are introduced.

From the above analysis of existing surveys on HRC with particular attention to manufacturing, two crucial findings emerge. Firstly, safety appears to be the main target in the majority of reviews, like in [13],[17], [18], followed by ergonomics and efficiency, which are emphasized in [7] and [5],[19] respectively. Secondly, an evident gap surfaces from the literature. Despite the growing amount of review papers and surveys, there is no work cataloging the related articles from the point of view of automatic control in HRC systems. For the sake of coping with this gap, the current survey classifies the most relevant and recent works developed by the scientific community according to the three above described key objectives of HRC in the smart manufacturing systems (i.e., safety, ergonomics, and efficiency) that are also depicted in Fig. 2.1. All the articles are then grouped by problem and type of control, indicating whether optimization techniques are adopted or not. Finally, conclusions are drawn on promising future research directions in each domain.

### 2.1.2 Objective and Structure

The objective of this chapter is to present a systematic review of the control techniques used in collaborative robotics.

Control systems allow the coordinated movement and operation of different elements of the cobot, as well as the execution of a specific sequence of tasks, even in the presence of unpredicted events [20]. To ensure an effective HRC in the industrial scenario, an appropriate control method must be chosen and ad hoc controllers must be designed according to the desired specifications.

With the aim of providing the interested reader with a systematic guide to the control methods used for HRC in the industrial sector, we group the contributions by target (i.e., safety, ergonomics, and efficiency) and then by control problem per each target, reviewing the control techniques applied in each case, the obtained results, the corresponding advantages, and the eventual open issues.

First, in order to guarantee a safe HRC, no undesired contact must happen between robot and human. For this reason, several control algorithms have been proposed in the literature to prevent collisions by defining safety regions or tracking separation distance to guide robots away from humans and to detect collisions with the aim of reducing operator's injuries. Therefore, in cobotics, safety is understood as a fundamental requirement that allows operators to work side-by-side with “fenceless” robots in compliance with ISO/TS 15066 standards, i.e., limitation of maximum permissible forces or torques, speed reduction, and respect of a minimum protective separation distance.

Secondly, ergonomics aspects implying the psycho-physical well-being of workers are also of crucial importance. Cobots indeed reduce physical labor by helping operators with repetitive tasks but at the same time augment psychological stress connected to close HRC that can lead to a reduction in performance. Thus, physical and cognitive ergonomics must be taken into account in the design of HRC. Physical ergonomics is considered in collaborative robotics as the prevention of injuries associated with repetitive and dangerous tasks, and design and evaluation of workplaces; whereas cognitive ergonomics

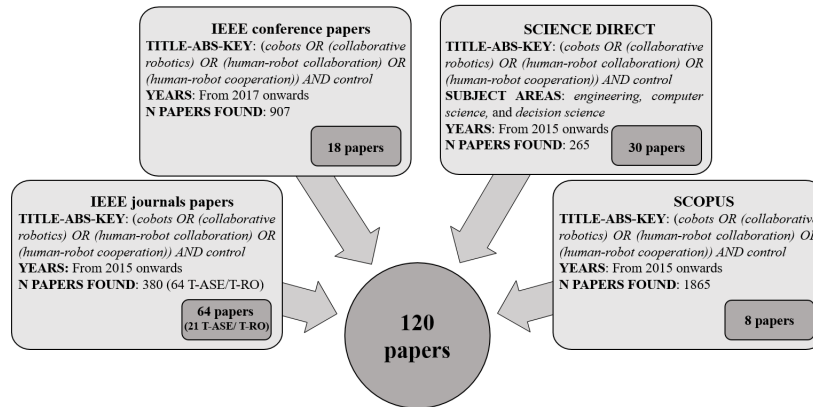


Figure 2.2: Search criteria and outcomes.

is associated with brain functions in the context of accident investigation or error analysis, mental workload, decision making, usability, and training [21].

Finally, HRC is aimed at increasing productivity, which has always been the primary goal of industrial companies. Cobots are certainly able to guarantee both a safe and ergonomic collaboration with humans, while significantly reducing the downtime, optimizing the production, and increasing the overall profitability. In the current analysis, efficiency is thus intended as the improvement of the entire industrial process or merely as the simplification of the operator's actions to complete a task by scheduling activities or planning the actions performed by the worker and the robot in the optimal way.

For the sake of providing the reader with an overview of the recent research activities in the field of cobotic control systems, the main findings of the selected works in the related literature are reported and summarized in the sequel. In particular, the remainder of this chapter is structured as follows. Section 2.2 delineates the research methodology used in this work. Each of the following sections –i.e., Section 2.3, Section 2.4, and Section 2.5– is dedicated to one of the above discussed HRC targets –i.e., safety, ergonomics, and efficiency, respectively– and it is structured in accordance with a higher-level classification into five main addressed problems: collision avoidance, collision detection, motion planning, control system design, and scheduling. Then, a lower-level categorization is applied to each problem aiming at highlighting the type of control and the eventual utilization of optimization methods. Section 2.6 identifies the gaps in the HRC research field regarding the developed control methods and provides an overview of emerging challenges for future investigation in this area. Finally, concluding remarks are reported in Section 2.7.

## 2.2 Research Methodology

This section presents in detail the methodology (see Fig. 2.2) used to select the most relevant works regarding the application of automatic control methods to ensure a safe, ergonomic, and efficient HRC. In particular, the well-known IEEE Xplore, Science Direct, and Scopus database have been consulted.

As for the IEEE Xplore database, the papers related to the HRC field in the control perspective were identified by using the ‘control’ keyword combined with the following ones: *cobots*, *collaborative robotics*, and *human-robot collaboration*. The research focused on papers published in the last ten years; nevertheless, it appears that the most significant works were published since 2015, when an exponential growth in the field of collaborative robotics is observed in the scientific community. Firstly, the research was limited to journals with a prominent interest for control engineering, such as IEEE Transactions on Automation Science and Engineering (T-ASE) and IEEE Transactions on Robotics (T-RO). This choice was made to focus on articles that present state-of-the-art control techniques in cobotics. As a result of this first research, we obtained 64 relevant papers. In

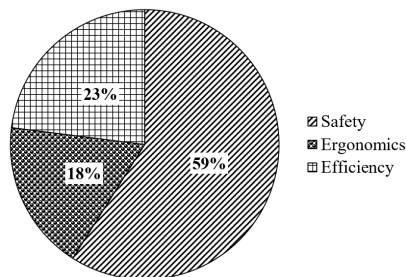


Figure 2.3: Percentage of analyzed papers per target in the present survey.

the second phase, the search was extended to all IEEE journals and the number of relevant papers increased to 380 articles. Among these, only those related to the manufacturing context were selected. To sum up, 64 IEEE journal papers (including 21 T-ASE and T-RO articles) were in total included in this survey. Then, we focused our study on the most relevant and cited IEEE conference papers from 2017 onwards and 18 of them were included in this literature review.

As for the Science Direct database, only contributions published in journals from 2015 onwards were selected with the same rule indicated for IEEE Xplore database and the search was further limited to the subject areas *engineering*, *computer science*, and *decision science*. Among the obtained 265 results, only those related to cobotics in the digital industry were identified and the 30 most relevant papers were reported here.

Finally, it is worth mentioning that the search was extended to Scopus in order to eventually identify other interesting journals related to the investigated HRC targets. As a result of this final step, 8 further journal papers were considered worthy of mention in the current review.

Summarizing, 120 papers were in total considered to be the most relevant by analyzing the corresponding contents and will be presented in detail in the current survey. In the last step, all the selected articles were categorized according to the three above described targets: safety, ergonomics, and efficiency. To this aim, the works were analyzed in detail by grouping them into tables with title, author, year, application, control system, and key findings. Finally, all the results were reported on a spreadsheet where they were organized by target and then by type of addressed control problem related to the specific target. According to the final analysis, 71 (59%) analyzed papers are related to safety, 21 (18%) to ergonomics and 28 (23%) to efficiency, as shown in Fig. 2.3. More specifically, as schematized in Fig. 2.4, the 71 articles from the safety perspective are divided into four problems: collision avoidance, collision detection, motion planning, and safety-oriented control system design. Conversely, both the classes of the 21 papers related to ergonomics and the 28 papers addressing the efficiency enhancement in HRC are grouped into three categories: motion planning, scheduling, and ergonomics/efficiency-oriented control system design. Furthermore, some papers focus on multiple targets, while occasionally several problems are simultaneously addressed in a single contribution. In such a case, the content of the articles is treated in different sections as long as the research contribution is significant to the corresponding addressed target.

### 2.3 Control Techniques for Safety in HRC Systems

In HRC applications, safety requirements are the primary need, as can be seen from the large number of articles focused on this concept, as highlighted in Fig. 2.3. For this reason, several control techniques and state-of-the-art control frameworks, schematized in Fig. 2.5, have been developed to meet the ‘*safety first*’ slogan in the digital industry. All the papers from the safety point of view are synthesized in this section outlining the relationships between them.

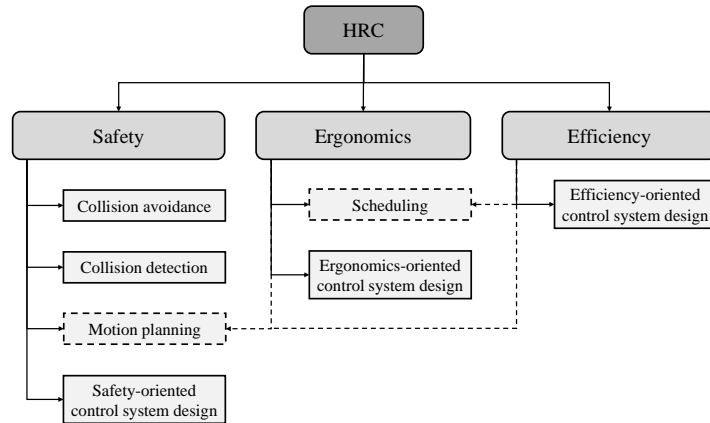


**Figure 2.4:** Taxonomy of control problems in HRC (the problems addressing multiple targets are shown by dashed boxes).

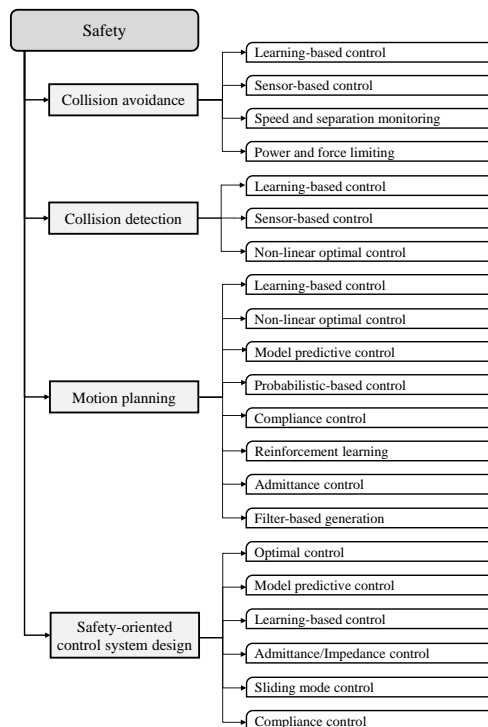


**Figure 2.5:** Overview of approaches in the safety target.

### 2.3.1 Collision Avoidance

A large amount of cobotics safety schemes rely on pre-collision systems, which aim at predicting the human intention, with the help of four classes of approaches: 1) learning-based techniques, 2) exteroceptive and proprioceptive sensors, 3) speed and separation monitoring and 4) power and force limiting (see Fig. 2.5), allowing the cobot to stop or modify its trajectory before impact occurs.

From a detailed search in the related literature, it is evident that the estimation of human impedance and motion intention is mostly achieved by learning-based techniques, i.e., *neural networks* (NNs), *recurrent neural networks* (RNNs), and *radial basis function neural networks* (RBFNNs). Yu *et al.* [22] present an adaptive neural *admittance control* (AC) for collision avoidance in HRC with position constraint, based on an *integral barrier Lyapunov function* (IBLF), that is adopted for improving tracking accuracy and interactive

compliance. An impedance model and a soft saturation function are used to generate a differentiable reference trajectory. A complete framework for safe HRC is developed in [23], where the robot's learning is applied not only to the human motion intention but also to the human impedance, estimated in real-time by RBFNNs and a *least square* (LS) method, respectively. The human impedance and motion intention are evaluated by the same research group in another paper [24]. In particular, the human stiffness obeying to the Gaussian distribution is estimated by using a Bayesian method and the human motion intention by knowing the dynamic relationship between human stiffness and motion intent. Yu *et al.* employ also in this paper NNs to handle model uncertainties in the robot's dynamics and *impedance control* (IC) to obtain an efficient HRC, while a stability analysis is performed by using Lyapunov function candidates. Furthermore, Yasar and Iqbal present in [25] a state-of-the-art sequence learning approach using RNNs which aims at predicting the motion of all agents in a given workspace. Its performance is compared to other motion prediction methodologies and it is shown that the model developed by the authors can prevent collisions more accurately by having a short-term performance and can plan the robot's actions more precisely by having a long-term performance. Another technique for human motion prediction in production lines, which combines RNNs and inverse kinematics, is presented by R. Liu and C. Liu in [26]. More specifically, the former is used to predict the wrist motion, whereas the latter expands the prediction to the full-arm. Finally, in [27], Liu and Wang present a context awareness-based collision-free HRC that is combined with a collision sensing module with sensor calibration algorithms. A learning-based algorithm is implemented in order to identify the human operator's pose during the assembly task.

As mentioned before, multi-sensor control systems are alternatively used to avoid collisions by detecting the human presence and evaluating in real-time the distance between the robot and the object in the workspace. In particular, two research groups implement this type of control technique for the complex robotic system in their works. Khatib *et al.* develop in [28] a multi-sensor control system for collision avoidance with both static and dynamic constraints and use a *saturation in the null space* (SNS) algorithm to categorize the tasks by priority's levels by giving the highest priority to collision avoidance of the whole robot body and then of the robot's end-effector. A mixed reality interface is also added to the system in order to facilitate HRC. Moon *et al.* also propose in [29] a control method for static and dynamic obstacle avoidance in real-time that employs a dual-type proximity sensor developed for HR distance evaluation. A trajectory planning scheme and a virtual force method are also presented and experimentally validated by the authors. Instead, Fernández *et al.* propose in [30] an optimization-based control scheme that integrates multi-sensor workspace monitoring and tracking algorithms together with collision avoidance algorithms: the resulting real-time solution allows the cobot movements to be free of self-collisions and collisions with external objects. The obstacle-robot distance evaluation in real-time is also the objective of the article [31] by Nascimento *et al.*, who develop a different control system architecture that uses a limitation of the repulsive force model with safety contour and of the paper [32] by Nikolakis *et al.* who focus on a *cyber-physical system* (CPS) for a safe HRC assembly. A closed-loop control system, based on the human's proximity to the robot is implemented in order to allow the safety assessment and to guarantee the collision avoidance. Optical sensors are also inserted in the CPS architecture to monitor the working space and to evaluate the human-robot distance. Furthermore, a new safety methodology called kinetostatic safety field is presented by Polverini *et al.* in [33] in order to introduce a straightforward safety measure for any moving rigid bodies. By combining the concept of safety field with a safety-oriented control strategy for redundant manipulators, the proposed approach is able to enhance safety in several real-time collision avoidance scenarios, including collision avoidance with potential obstacles, self-collision avoidance and safe HR coexistence.

In addition to the two above discussed approaches, some authors concentrate on methodologies that respect the new ISO standards related to the safety concept with the use of *speed and separation monitoring* (SSM) and *power and force limiting* (PFL). For instance, Liu *et al.* propose in [34] a dynamic risk assessment method based on modified

SSM that respects the safety regulations. An innovative collision avoidance strategy based on a dynamic risk index minimization using gradient descent is developed. The authors integrate the SSM and visual risk field in augmented reality to obtain an advanced HRC interface. Conversely, Ferraguti *et al.* exploit in their two works reported in this survey the theoretical framework of *control barrier functions* (CBFs) in order to guarantee collision-free trajectories along the robot. More in detail, they propose in the first paper [35] an optimization-based control algorithm where the difference between the nominal acceleration input and the commanded one is minimized. The human accelerations and velocities are computed with a bank of Kalman filters. In the second paper [36], the same authors provide an innovative control method that overcomes the limitations of SSM and PFL by developing a zeroing CBF optimization approach, which is compatible with the requirements of ISO/TS 15066, in order to act as a safety filter, by modifying the nominal control input only when safety can be a threat.

### 2.3.2 Collision Detection

Sometimes physical contact is required in HRC tasks. Therefore, learning-based methods and non-linear optimization problems (see Fig. 2.5) that provide safety by detecting collisions are developed to meet this need.

Haddadin *et al.* survey and discuss in detail in [37] the model-based algorithms for real-time collision detection, isolation, and identification that use only proprioceptive sensors. More specifically, the authors present the collision monitoring methods from scalar monitoring of robot energy to momentum-based observers, highlighting the advantages and disadvantages of each algorithm. The techniques are further evaluated and compared in simulations and experiments. On the other hand, a sensorless collision detection and coordinated compliance control method based on momentum observer for a dual-arm robot is proposed by Han *et al.* in [38]. Similarly to the collision avoidance problem (Section 2.3.1), learning-based control methodologies are the most employed techniques, since proprioceptive torque sensors are vital in identifying possible collisions. Furthermore, it is worth mentioning that the majority of the related works aims at designing an observer that provides an estimation of the internal state, which is surely needed to detect collisions. For instance, Ren *et al.* [39] introduce a collision detection method based on encoders and torque sensors by combining the robot dynamics and the design of a *modified extended state observer* (MESO). Another framework based on a deep learning approach, that is capable to monitor signal estimation and recognize any collision with a particular type of observer, is proposed by Heo *et al.* in [40]. A *convolutional neural network* (CNN) is adopted in order to achieve both high sensitivity to collisions and low susceptibility to false alarms. Park *et al.* [41] design two real-time learning-based detection methods, namely a *linear support vector machine* (SVM) and CNN. Only motor current measurements together with a robot dynamic model and a momentum observer are required. Thus, manual tuning collision detection thresholds for each joints can be avoided. Four further articles exploit learning-based control techniques. On the one hand, Sharkawy and Mostfa design in [42] a neural network for collision detection by examining the robot dynamics and by doing the training with the algorithm of Levenberg-Marquardt. More precisely, four NN's types are implemented by the authors, that are multilayer feedforward with one hidden layer and two hidden layers, cascaded forward, and recurrent NNs. A 1 *degree of freedom* (DOF) robot is chosen to test the proposed techniques which from the results appear to be very effective in detecting collisions. On the other hand, Lippi and Marino propose in [43] a solution based on RNNs that is able to detect and classify the nature of the contact with human, either intentional or accidental and to properly react. In particular, a long short term memory network is implemented to detect human contact. Furthermore, Zhang *et al.* design in [44] an online collision detection and identification scheme that consists of a signal classifier and an online diagnoser using supervised learning and *Bayesian decision theory* (BDT). Supervised learning NNs are also implemented in combination with signal filtering in [45] with the aim of improving the sensitivity of the system and reducing the computation time. In such a paper, Aivaliotis *et al.* present a



power and force limiting methodology for online collision detection without the use of external sensors. Another article written by Kouris *et al.* [46] is dedicated to developing a novel frequency domain scheme that aims at distinguishing unexpected dangerous collisions from voluntary contacts by detecting the external forces at the end-effector and the external joint torques with the help of proprioceptive torque sensors. With the same objective as the previous article, Mariotti *et al.* propose in [47] admittance control laws for a safe HRC in manual guidance mode by using 6D Force/Torque (F/T) sensor at the end-effector in addition to kinematic inputs information. Forces' detection prevents accidental collisions and avoids unintended contacts during robot movements. Hence, Gaz *et al.* present in [48] a control algorithm that allows the operator to reorient a work-piece held by the robot in polishing tasks of metallic surfaces and to distinguish the external torques acting at the robot joints in two components: the former is due to the polishing forces applied to the work-piece mounted on the end effector, whereas the latter depends on the reconfiguration of the manipulator arm. In order to detect the contact points on the robot and to evaluate the exchanged contact forces, Magrini and De Luca implement in [49] a parallel *graphics processing unit* (GPU) algorithm that monitors in real-time the dynamic distances between a robot and generic moving obstacles in the environment. A safety framework that includes safety measures and requirements is presented by Magrini *et al.* in [50], with the aim of ensuring HRC in open industrial robotic cells. To augment the level of safety, a depth-space algorithm for online monitoring of relative HR distance is implemented and combined with redundant sensing hardware, i.e., two laser scanners working in parallel in the cell. As a final contribution to the category of studies on the collision detection techniques without any optimization problem, the paper [51] by Labrecque *et al.* presents a macro-mini architecture with a novel passive mini mechanism to minimize the impedance, eliminate the nonlinear impedance and decouple HR dynamics. Advanced control collision detection strategies are specifically designed for this architecture.

Differently from the above, a collision detection approach based on constrained non-linear optimization is presented in [52], where a strategy to change speed is formulated by using a danger index and an *elite real-coded genetic algorithm* (ERGA) is used to guarantee the operator's safety.

### 2.3.3 Motion Planning

In collaborative applications, trajectory planning allows to reduce the risk of possible HR contacts, leveraging on the operator's motion prediction. The first part of this section deals with learning-based control and non-linear optimization problems, whereas the second one with model predictive control, probabilistic-based control, compliance control, reinforcement learning, admittance control and filter-based generation (see Fig. 2.5).

Most of the related works formulate the trajectory planning as a constrained optimization problem, whereas, as explained in Section 2.3.1, some ISO requirements must be respected to obtain a safe HRC in the manufacturing scenario. Oleinikov *et al.* propose in [53] a *non-linear model predictive control* (NMPC) approach for real-time planning based on SSM specifications for industrial applications. Sloth and Petersen present in [54] a method to compute a safe path velocity under the ISO/TS 15066 requirements for avoiding collisions between human and robot by implementing firstly an eigenvalue problem for stationary bodies and then a polynomial optimization combined with a line-search for moving bodies. The two different SSM and PFL strategies, mentioned in Section 2.3.1, are merged in the following two papers: in [55], where the initial velocity is optimally scaled to preserve the operator's safety and the path consistency of the robot trajectory, and in [56], where a *machine learning* (ML) method is proposed as a support for the combination of the two techniques in order to examine the human body movements. The use of the current methodology aims at reducing the safety zone's dimensions that are usually oversized for various simplifications in the practical applications. Another article [57] written by Costanzo *et al.* presents a strategy based on SSM. More precisely, safety through prediction is integrated with safety through control by combining tracking

separation distance and human actions prediction with safety regions and speed monitoring to avoid possible collisions. The authors implement a CNN that combines spatial and thermal information for human detection and an advanced fuzzy logic approach for robot speed scaling by monitoring the HR distance in real-time. The approach is verified in cooperative assembly of aeronautical structural parts. Furthermore, a kinematic control strategy based on metrics for safety assessment is proposed in [58] by Zanchettin *et al.* In order to respect the rules imposed by the minimum separation distance criterion, a set of constraints can be used in real-time to limit the velocity, according to the distance from the operator. The same research group proposes another trajectory generation algorithm in [59]. The pre-programmed trajectory can be modified by the robot controller in order to enforce the safety constraints, while anticipating task interruption.

An innovative safe minimum-time trajectory planning along specified paths in the HRC scenario is presented by Palleschi *et al.* in [60], where safety is iteratively guaranteed by using a safety module and a safety evaluation module. At every cycle, the high-speed motions are restored as soon as the safety issue is resolved. Non-linear optimization problems in real-time are presented in [61], where the trajectory planning problem is solved by using a decoupling method that transforms the original coupled optimization problem into multiple independent optimization problems, to reduce the computational burden. A *non-linear programming* (NLP) problem with human-in-the-loop constraints is also solved in the reference [62] in order to optimize the desired path subdivided into multiple segments. To ensure a flexible real-time use, a generalized method using *dynamic movement primitives* (DMPs) and the compliance of constraints is proposed. A proactive path planning for cobots is proposed in [63], where the robotic safe trajectory is optimized according to a prediction of the volume occupied by the human. Conversely, Kanazawa *et al.* [64] present an online motion planning system that computes an optimal trajectory to avoid collisions based on the probabilistic prediction of the worker's motion and the receding horizon scheme for the trajectory planning. Another receding horizon control approach is proposed by Ducaju *et al.* in [65]. In particular, the authors implement a *model predictive control* (MPC) fixed-time point-to-point online trajectory generation method with the addition of the null space motion that is used to guarantee a continuous movement of all joints during the entire trajectory task, to avoid joint stiction, and to facilitate the kinesthetic teaching in a redundant robot. A planning algorithm that depends on a *stochastic trajectory optimizer* (STOMP) is proposed by Mainprice *et al.* in [66]. The key of this approach is to predict the human motion for tasks not known a priori by learning an unknown cost function that describes the human movements. An integrated framework that includes plan recognition and trajectory prediction modules is proposed by Cheng *et al.* in [67]. More specifically, a robust plan recognition algorithm based on neural networks and Bayesian inference is implemented by the authors. Lastly, in [68] an algorithm that predicts human motions by combining the minimum jerk model with semi-adaptable neural networks is similarly used to estimate future positions of the human hand based on previous training.

As an alternative to the use of optimization, few works in this category rely on different techniques. For instance, in [69], a methodology to transfer human experience directly to the robot through a collaborative control system based on *forward dynamics compliance control* (FDCC) is presented. This framework is designed to exploit the operator's experience which is then applied to plan the trajectories for the robot. Similarly, Zhao *et al.* propose in [70] a *reinforcement learning* (RL) based method with a hazard estimator to balance task following and human safety with the aim of making a trade-off between following demonstrated path and adapting to human movements. Instead, Chen and Song develop in [71] a control framework for a collision-free trajectory in HRC scenarios which includes three main parts: 3D perception and object tracking, potential field generation composed of attractive and repulsive forces where the former is applied to reach the target position whereas the latter to avoid collisions, and a real-time motion planning under the Cartesian constraint of the environment. In [72], Ji *et al.* implement a *partially observable Markov decision process* (POMDP) for human-aware motion planning in industrial HRC where the robot executes the sequential decision making problems without being able



to fully observe the human state and especially the human intention. In [73], He *et al.* design a soft saturation function for path planning and an admittance-based controller in the constrained task space that involves integral barrier Lyapunov function that is implemented for tracking issues and radial basis function NNs that is used for dynamic uncertainties' approximation. Finally, Besset and Béarée [74] present a *finite impulse response* (FIR) filter-based trajectory generator which produce online time-optimal jerk-limited trajectories from arbitrary initial velocity and acceleration conditions, while respecting the kinematics constraints of position, velocity, acceleration and jerk. The methodology adopted by the authors is suitable for systems with a large DOF and in dynamic environments where the robot controller must quickly react to unpredictable events.

### 2.3.4 Safety-Oriented Control System Design

This sub-section includes all the works that aim at designing advanced controllers for a safe HRC without specifically referring to any of the control problems addressed in the previous sub-sections. The employed approaches are summarized in Fig. 2.5. They incorporate optimal control, MPC, learning-based control, AC/IC, *sliding mode control* (SMC), and compliance control.

To begin the discussion, a complete control framework with a large quantity of innovative robotics elements, i.e., trajectory optimization, admittance control, and image processing is presented to the reader. The article proposed [75] written by Cherubini *et al.* is certainly interesting for HRC researchers for its completeness and its practical application in the manufacturing scenario. The authors develop a control scheme for collaborative safe assembly that consists of two steps: the offline nominal trajectory generation step and the online controller for the assembly task.

In the following papers some constrained control frameworks are described, starting from a discrete controller developed by Roveda *et al.* [76] with a two layers' structure that can be used in both the free-motion and contact phases. The admittance regulator gains can be computed by solving a *linear quadratic regulator* (LQR) optimal control problem. The current method avoids force overshoots and instabilities. The objective of the next paper is to define a safe zone to move in without endangering the human. Aiming at this purpose, an innovative control scheme for HRC, which enforces dynamic constraints even in the presence of external forces, is designed in [77] by Kimmel and Hirche. Then, Bednarczyk *et al.* combine *impedance control* (IC) and MPC in [78], since this control field is relatively new for HRC and no research has been performed yet. Thus, a new controller named *model predictive impedance controller* (MPIC) is presented by the authors. The strong point of the MPIC is the ability to integrate different type of constrains like speed, energy, and jerk limits that can affect the operator's security. Furthermore, Reyes-Uquillas and Hsiao design in [79] an adaptive admittance law, for parameters tuning in manual guidance tasks, which enables to satisfy three typical HRC constraints that are singularities, joints, and workspace limits. The proposed methodology allows to tune the parameters during the normal operation area with the input forces/torques detected at the robot end-effector. On the other hand, Xiao *et al.* present in [80] a HRC assembly scheme without employing additional force/torque sensors and considering load and friction compensation with the aim of improving safety, compliance, and flexibility of the loaded robots.

In addition to the above discussed approaches that make use of optimization techniques, further related works focus on learning-based and sensor-based controllers that are designed to reactively adapt to continuous changes in the environment. For instance, a multi modal responsive and sensor-based controller is presented by Cherubini *et al.* [81]. The control framework operates by activating or deactivating various tasks, according to the sensed data and to the application's needs. A method able to detect and compensate for undefined behaviors due to collisions and other unexpected events is suggested by Suzuki *et al.* in [82]. The proposed compensation technique employs a switching function that allows to move from a learning-based to a model-based controller by using

internal representation of a task-trained RNN. A novel neural adaptive controller, that achieves globally asymptotically trajectory tracking for a flexible-joint robot with unknown dynamics, is presented by Chen and Wen in [83], where the tracking performance of the controller is improved by using the regressor online learning. Lastly, Cremer *et al.* [84] propose another neuroadaptive controller framework for stable and efficient HRC using a two-loop structure where both the robot dynamics and the human intent during collaboration are being evaluated online. Two NNs in the outer-loop predict human motion intent and estimate a reference trajectory for the robot that the inner-loop follows. A third NN is used in the inner loop to impose a prescribed error dynamics and feedback linearize the robot dynamics. Results show fast convergence of the proposed controller and a reduced position error and motion jerk compared to a standard admittance controller.

Various methodologies have been developed in the literature to investigate the stability limits of a robot under admittance control, during HRC. A model-free control scheme is proposed by Dimeas and Aspragathos for in [85] for detecting instabilities –i.e., introduction of the additional feedback term at high stiffness of the robot’s environment– of the admittance controller and for adjusting online the admittance parameters to stabilize the robot and thus, to obtain low effort HRC. A stability and steady-state analysis are outlined in another paper written by [86] in order to guarantee a safe HRC. Li *et al.* develop an impedance controller on the basis of PD control to realize the active compliance, while the passive one is achieved by a specially designed elastic element. The trade-off between stability and transparency is a core challenge addressed also in [87], where a new variable *fractional order admittance controller* (FOAC) is proposed to handle this trade-off. The designed controller displays stability robustness against the system disturbances. In addition to ensuring asymptotic stability, a controller design must be able to guarantee passivity. Raiola *et al.* [88] introduce a novel impedance controller which allows a safe HRC through energy and power limitations, assuring passivity through energy-tanks. The compliant joint manipulators can store a huge amount of energy potentially dangerous due to nonlinearities.

Other techniques based on SMC and AC have been implemented in the state-of-the-art controllers. For instance, an innovative controller, for a safe and performing control of compliant joint manipulators, is presented in [89]. The *variable boundary layer SMC* (VBSMC) allows to achieve various interaction levels while maintaining good tracking performances. Furthermore, Solanes *et al.* present in [90] an approach for HRC in transportation applications using multi-task, non-conventional SMC, admittance control, and the gradient projection method. A hybrid position-force scheme is designed since some coordinates of the robot pose are controlled via a position feedback loop, while others via a force feedback loop. Three tasks with different priority levels are defined in the controller to cooperatively perform the safe transportation of an object with a human worker. In [91], Liu *et al.* propose a generalized dynamic behavior control framework that incorporates four models: the task model, which includes role allocation, motion planning, control performance, and intentional interaction, the dynamic behavior control model, the robot model, and the human model. In this article, the authors not only concentrate on single-point HR interaction but also on multi-point HR interaction, both in the Cartesian space and joint space. In the second HR interaction scenario that consists of two main issues’ types, i.e., expected interaction and undesired collision, a smooth task transition algorithm is defined to ensure safety during the task switching process. To conclude, Fu and Zhao propose in [92] two different Maxwell model-based compliance control methods in HRC scenarios that minimize the effect of collisions compared to the conventional Voigt model. In particular, a Maxwell model-based Cartesian admittance control scheme is developed to generate an innovative plastic compliance of the robot end-effector and a Maxwell model-based null space admittance control approach for redundant manipulators is realized to obtain a plastic whole body compliance.

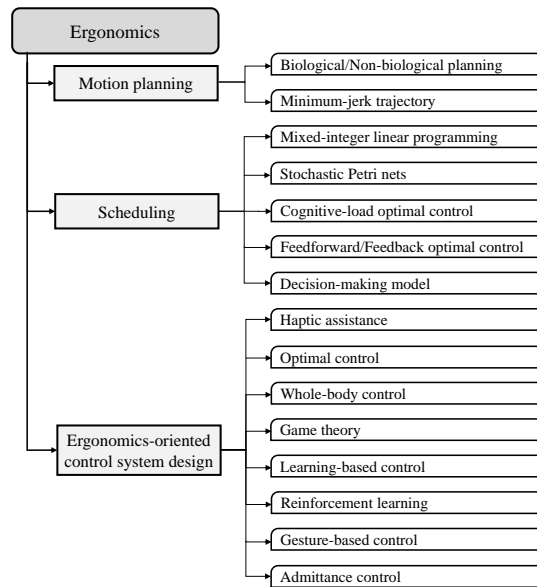


Figure 2.6: Overview of approaches in the ergonomics target.

## 2.4 Control Techniques for Ergonomics in HRC Systems

In the developed countries, the so-called work-related *musculoskeletal disorders* (MSDs) affect almost 50% of human workers. Aiming at minimizing MSDs, and other health issues and injuries provoked by poor ergonomics, collaborative robots are introduced in the manufacturing scenario. Cobots are increasingly adopted in tasks involving repetitive motions to reduce the operator’s fatigue, increment the overall level of comfort, and augment productivity by shortening a task time. However, close HRC can induce psychological stress in the operator that must be evaluated and analyzed in order to design robots adapt to human features and smooth interactions.

In this section a review of the articles with an ergonomic control perspective are discussed in detail. All the control approaches employed are synthesized in Fig. 2.6.

### 2.4.1 Motion Planning

Also in the ergonomics perspective, motion planning plays an important role both for the physical and cognitive HRC. Two main control methods are considered for motion planning: biological and non-biological trajectory optimization and minimum jerk trajectory planning (see Fig. 2.6).

As for the physical HRC, a crucial issue lies in how humans lead the movement and how the cobot motion can be controlled for efficient and intuitive collaboration. In this view, Maurice *et al.* [93] investigate quantitatively the human ability to non-biological patterns in robot movements. In particular, the human adaptability to biological and non-biological velocity profiles during an elliptic movement are examined, showing that a robot control oriented to the biological velocity profiles increases the physical ergonomics for the operator. Similarly, [94] –which mainly aims at improving the efficiency of the assembly process– focuses on the motion planning problem aiming at optimizing the handover between robot and human in the ergonomics perspective.

As for cognitive ergonomics, it is taken into account in [95], where Rojas *et al.* propose a novel trajectory-planning methodology that aims at ensuring both psychological and physical safety by using the minimum-jerk variational problem which is also able to minimize vibrations. The same research group proposes in a more recent work [96] a similar trajectory planning technique that seeks to reduce simultaneously the execution time and the psychological stress inducted on employees when working with cobots.

### 2.4.2 Scheduling

An excellent scheduling of activities is certainly a starting point for reducing physical and cognitive stress. For this reason, many researchers address the HRC scheduling problem from the ergonomic perspective, as reported in this sub-section. The control methods adopted in this context mainly rely on mixed-integer linear programming, Stochastic Petri nets, cognitive-load optimization, feedforward/feedback optimization, and *decision-making* (DM) model as shown in Fig. 2.6.

In contrast to the majority of the existing studies for scheduling and allocating tasks, which do not consider the ergonomic factors, Pearce *et al.* [97] firstly analyze the differences in skills between human and robot and the differential ergonomic impact of tasks on operators and then generate task assignments by using a *mixed-integer linear program* (MILP) scheduler. Aiming at improving ergonomics and reducing the worker's physical strain, the authors introduce a variation of the so-called strain index method as a measure of human physical stress of each work element in a task. Several other works focus on ergonomics-oriented scheduling; however, the underlying analysis relates to a specific application area. For instance, in [98] the risk for musculoskeletal disorders resulting from repetitive movements and excessive fatigue of the operator in the kitting process is alleviated by optimally allocating the tasks between human and robot with an online scheduling algorithm. A novel stochastic Petri net control framework is proposed by Hu and Chen [99] to solve an optimal task-allocation problem for the human-machine collaborative manufacturing process. The proposed stochastic framework allows to model the impact of human fatigue on the process dynamics. In addition, Faber *et al.* [100] develop a *cognitive control unit* (CCU) which is extended by a *graph-based assembly sequence planner* (GASP) in order to reduce the cognitive and physical risk in the collaborative assembly process. Similarly, Rahman and Wang [101] present a two-level (feedforward and feedback) optimization strategy for trust-based subtask allocation between the human and the robot in flexible lightweight assembly. Lastly, Jiang and Wang design in [102] a human-like DM under risk model that can be involved in HRC task allocation. A mathematical DM model is designed to enclose the psychological effects, including regret effects, probability weighting effects, and range effects and a fuzzy logic controller is employed to collect data from individual decision makers.

### 2.4.3 Ergonomics-Oriented Control System Design

This sub-section illustrates all the works aimed at designing advanced controllers for an ergonomic HRC, without specifically referring to any of the two ergonomics-oriented control problems addressed in the previous sub-sections. In particular, the majority of works minimize the human physical and cognitive discomfort in the collaboration with robots by designing optimal control strategies (i.e., haptic assistance, optimal control, whole-body control, and game theory), while the remaining ones aim at improving ergonomics by designing control strategies based on NNs, RL, gesture-based control, and admittance control (see Fig. 2.6).

The works that address the design of optimal control strategies to increase the ergonomics level of HRC typically integrate human factors in the HRC control schemes. In particular, Medina *et al.* in [103] minimize the human effort by designing a novel anticipatory model-based haptic assistance scheme that considers model uncertainty in the robot interaction control, while in [104], Ansari and Karayiannidis present a task-based role-adaptation control that can produce assistive robot forces based on the task's velocity profile in cooperative object manipulation. An assistive force can be applied by an active robot according to a similar task. In particular, in the latter work, the task executed by the human is identified in real-time and modeled as an *integer linear programming* (ILP) problem that is employed to detect the closest velocity profile to the ongoing velocity for an interval of time and is also able to compute the similarity factor for each task. Aiming at enhancing the working conditions for the human co-worker in co-manipulation and handover tasks, Peternel *et al.* propose in [105] an innovative dynamic HRC control

approach in which the human body configuration, that minimizes the overloading joint torques, is found. With the same overall aim, Kim *et al.* present in [106] a state-of-the-art HRC control strategy that allows the operator to work in a more ergonomic configuration during dexterous operations like drilling or polishing tasks. For this purpose, the authors develop an optimization problem that minimizes the overloading torques in the human joints by taking into account the worker's ergonomics aspects with the use of constraints, such as the human arm muscular manipulability. Since the operator's performance could vary due to factors such as individual strength, working pattern, and interaction with the robot, Sadrfaridpour and Wang [107] develop a novel framework which integrates physical and social HR interaction factors into the robot motion controller for HRC assembly tasks. To improve physical HR interaction the robot speed can be controlled with the aim of synchronizing its motion progress with that of the human during the task. For greater social HR interaction, human trust in robot and visual feedbacks are provided for a better performance and safety. Similarly, the work [75], already described from the safety control perspective, aims at improving the physical ergonomics in the development of the state-of-the-art control framework. Lastly, Messeri *et al.* propose in [108] a HRC framework in which the trade-off between human physiological stress and productivity is optimized in real-time by using a non-cooperative game theoretic approach.

In contrast to the previous contributions, the following ones still include human factors in the controller design but do not address any optimization problem. In particular, in [109] the human factors, –i.e., the weight perception in the control of HR systems– during the manipulation task of heavy objects are examined. The author develops an adaptive control algorithm based on human characteristics and uses RL to predict the control parameters producing the best control performance. To test the control system, a 1 DOF testbed power assist robotic system is defined and several position and force control strategies for the system are set and compared, showing the best performance of the method in case of position control. The complex influence of several human factors on the operator performance is also identified by using a neural network based learning approach in the paper [110] by Oliff *et al.*, where a framework that integrates intelligent control and data processing is developed to improve coexistence with human colleagues in the manufacturing context. In another article [111] by Shen *et al.*, an innovative framework is developed to improve HRC by endowing the robot with the capability of understanding human personalities during face-to-face interaction. The experimental protocol developed by the authors consists of the nonverbal feature extraction and the machine learning model training that uses the ridge regression and *support vector machine* (SVM) classifiers. Another original control framework that consists of two control loops is developed by Modares *et al.* in [112] with the aim of minimizing the human effort and achieving an optimal performance. The inner-loop neuro-adaptive controller is designed to make the nonlinear unknown robot dynamics behave like a prescribed robot impedance model whereas the outer-loop controller is developed to find the optimal parameters of the impedance model and minimize the tracking error. RL is also implemented to solve the LQR control problem that is formulated to find the optimal parameters of the impedance model. Furthermore, in the paper [84] by Cremer *et al.*, already mentioned from the safety point of view, the human effort is minimized by using the so-called human intent estimator that proactively helps the user follow the desired trajectory. The human factor analysis tools are also involved in the design of the gesture commands. For instance, Tang and Webb [113] develop a hand gesture robot control system which enables the user to perform motion control and simple programming of an industrial robot. As opposed to the previous authors, who paid attention to cognitive ergonomics, Zanchettin *et al.* focus on physical ergonomics in [114]. They present a control strategy for the robotic manipulator to minimize the muscular fatigue of the worker during the manipulation of bulky objects. The proposed method shows a significant mitigation of the musculoskeletal disorders' risks and a remarkable reduction in the cycle time and thus, an increase in productivity. To conclude, the article [115] by Yao *et al.* aims also at reducing the burden on the human with the help of *radial basis function* (RBF) by describing a dynamic model of an industrial robot in both dynamic and quasi-static mode that computes the external

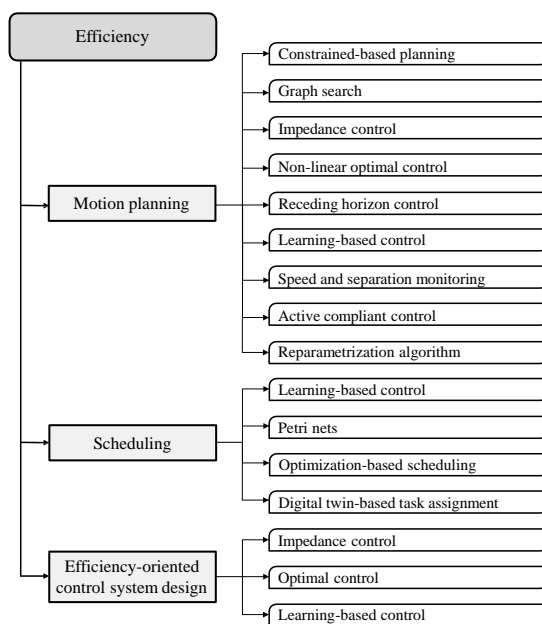


Figure 2.7: Overview of approaches in the efficiency target.

force produced by the human operator. Admittance control is implemented in order to transfer the detected external force into reference position and velocity of the robot.

## 2.5 Control Techniques for Efficiency in HRC Systems

In today's high-tech manufacturing scenarios, collaborative robotics is employed to augment productivity, flexibility, and profitability. The cycle times can be roughly halved using HRC as opposed to workers only and, as demonstrated in a research conducted by Shah [116], the idle time is shortened by 85% when operators work collaboratively with a human-aware robot rather than when working in all-human teams. Therefore, manufacturing processes, i.e., assembly, machine tending, and palletizing are faster, more efficient, and more cost-effective with cobots' application.

A large number of control techniques for HRC are developed to minimize costs and increase the overall level of productivity in the digital industry. In this section all the related papers written from an efficiency perspective are reported and described in detail. The taxonomy of the control approaches is synthesized in Fig. 2.7.

### 2.5.1 Motion Planning

This sub-section discusses the control techniques aimed at optimizing robot trajectories to minimize the time needed to complete an industrial task and/or improve the quality and comfort of collaborative tasks. The control methods applied to such purposes are various and largely depend on the specific application. They include constraint-based planning, graph-search, impedance control, non-linear optimization, receding horizon control, learning-based algorithms, speed and separation monitoring, active compliant control, and reparametrization algorithm (see Fig. 2.7).

Firstly, Raessa *et al.* propose in [94] a constraint-based incremental manipulation planning method to generate the motion for the robot system, while distributing efficiently the subtasks of a complex task to robots and humans. Differently, an online adaptive robot motion generation for a dyadic collaborative manipulation scenario is presented by Stouraitis *et al.* in [117] where *graph-search* (GS) methods are used in combination with



trajectory optimization. The current approach computes the optimal hybrid policy for the robot to complete manipulation tasks as a member of a dyad or alone.

On the other hand, Balatti *et al.* [118] focus on the complex problem of pallet jack recognition and re-positioning in order to enable the *mobile collaborative robot assistant* (MOCA) to execute the loco-manipulation tasks autonomously, or in collaboration with humans. The proposed framework consists of four main modules: pallet jack reaching, handle detection, handle preparation and pallet jack repositioning. A whole-body impedance controller and a trajectory planner, which considers the mobility constraints of the robot-pallet jack chain, are implemented for this purpose. The impedance control reveals particularly appropriate for such task where contact forces must be kept small, but accurate regulation is not required. Like in the previous article, Wu *et al.* present in [119] an innovative weighted whole-body cartesian impedance controller for the MOCA, which is used for a door opening task. In particular, three motion modes are defined –pure locomotion, manipulation, and coupled loco-manipulation– in addition to the classical loco-manipulation pattern.

Furthermore, it is worth mentioning here some works already discussed in the safety section as they are written according to dual targets. In [62], Weitschat and Aschemann solve a non-linear optimal problem by minimizing the time needed by the robot to reach the goal position under human-in-the loop constraints. In [64], the online computation and control of the optimal trajectory, that is based on a receding horizon, aims at decreasing the waste time, by incorporating and managing effectively the temporal requirements needed to predict the workers' behavior, and thus, at improving the work-time efficiency. In [27], the robotic path is planned combining the use of sensors and a learning based algorithm, not only to avoid obstacles but also to reach the target position in time by maintaining the assembly efficiency at the highest level. Also the authors of [34] aim at preserving productivity although the primary goal remains to avoid collisions along the robot's trajectory. In [58] and [55], the productivity is maintained at the maximum level, while guaranteeing safety. In [67], Cheng *et al.* aim not only at improving safety but also at minimizing the task completion time. Lastly, in [57] high profitability, efficiency, and reduced cycle time are obtained by minimizing unnecessary robot stops and slowdowns in case of false-positive human detection.

Differently from the above cited works, reference [120] describes a new optimization-free method for one of the most difficult disassembly tasks, i.e., the unfastening of screws. A cobot equipped with an adapted electrical nutrunner is used for this scope. A spiral search motion is performed to align, locate, and engage a nutrunner onto a hex screw with an initial positional error. The authors implement a control strategy combining torque and position monitoring with active compliance. To conclude, Rojas and Vidoni propose in [96] a non-linear reparametrization –based on the calculus of variations and the theory behind the Noether's Theorem– that aims at minimizing the execution time while controlling and preserving the degree of motion's smoothness.

## 2.5.2 Scheduling

Productivity can be optimized by implementing scheduling algorithms for HRC. The control methods used in this context are based on reinforcement learning (RL), convolutional neural network (CNN), Petri nets, optimization-based scheduling, and *digital twin* (DT)-based task assignment (see Fig. 2.7).

For instance, Yu *et al.* make in [121], an analogy between a chessboard and the assembly process. The selection of moves in the chessboard are compared with the HR decision-making. A self-play algorithm based on RL is used to obtain the optimal policy and a CNN is trained to predict the distribution of the priority of move selections and whether a working sequence is the one resulting in the highest HRC efficiency. On the other hand, the assembly planning and processes are modeled in [122] with the use of AND/OR graphs. Johannsmeier and Haddadin propose a HRC framework for task allocation at team and agent level by optimally combining the capabilities of humans and robots in industrial assembly tasks.

Casalino *et al.* propose in [123] a scheduler based on timed Petri nets to maximize the throughput and minimize the idle time of each agent involved in collaborative assembly tasks. Furthermore, the goal of the paper by Pearce *et al.* [97] is the optimization of production time -by minimizing the makespan (task completion time) and the worker's idle time - in addition to the ergonomics improvement.

Conversely, a recent work [124] by Zanchettin aims at minimizing the difference of the actual production from a reference one -i.e., the tracking error- rather than minimizing the idle time or maximizing the throughput. The author suggests a robust scheduling and dispatching rules for high-mix collaborative manufacturing systems by developing an optimization algorithm that is then tested with an assembly layout composed of six stations and four resources.

Reducing the planning time and the efficient spatial utilization is instead the purpose of the article written by Michalos *et al.* [125] who present a multi-criteria task assignment problem by considering the spatial layout of the assembly workplace. On the one hand, CAD models are utilized for the extraction of a product's assembly sequence, on the other hand, an algorithm is implemented for the generation and examination of alternative planning scenarios. An optimal study for an effective reconfiguration of the assembly cells is proposed by Tsarouchi *et al.* in [126]. The authors outline a method for the allocation of sequential tasks assigned to the robot and the operator placed in different workspaces and in particular in the assembly lines of an automotive industry. Conversely, Xu *et al.* propose in [127] an optimization problem to find the best disassembly sequence that is considered the key step in remanufacturing. The *disassembly sequence planning* (DSP) is computed by the *modified discrete bees algorithm based on Pareto* (MDBA-Pareto) with the aim of minimizing the disassembly time, cost, and difficulty.

A hierarchical task model from human demonstrations that is able to identify the sequential and parallel relationships of the task at all levels of abstraction in assembly scenarios is proposed by Cheng *et al.* in [128]. An optimization-based planner is also developed by the authors in order to minimize the completion time for the planning horizon by excellently assigning the parallel sub-tasks to the human and the robot.

Finally, some authors develop a digital twin with the aim of improving the efficiency of the HRC industrial processes. For instance, Wang *et al.* create in [129] a DT for human-robot interactive welding that includes the robot, the operator, and the welding scene in order to replicate the welding operations and analyze the welder behaviors after a welding skill level classification from demonstrated operation data. To this intent, a combination of *fast Fourier transform* (FFT), *principal component analysis* (PCA), and support vector machine (SVM) is proposed by the authors. Aiming at increasing the assembly flexibility, Bilberg and Malik design in [130] a digital twin of an assembly cell for skill-based tasks distribution between human and robot, task sequencing, and program development. Finally, an innovative framework based on digital twin is developed by Lv *et al.* in [131] to cope with the increasing demand for medical equipment in the COVID-19 era. The assembly process is segmented after analyzing each assembly element and the *double deep deterministic policy gradient* (D-DDPG) is chosen as an optimization method for learning the optimal HRC action sequence and action path for assembly task.

### 2.5.3 Efficiency-Oriented Control System Design

This last sub-section illustrates all the frameworks designed to augment the performance and efficiency of a cooperative task and, thus, productivity and profitability of the digital factory without specifically referring to any of the efficiency-oriented control problem addressed in the previous sub-sections. The available control systems design approaches are mainly based on impedance or optimal control combined with learning-based approaches (see Fig. 2.7).

A general framework based on Pareto optimization is proposed by Aydin *et al.* [132] in order to handle the trade-off between stability robustness and transparency of a closed-loop physical HR interaction. The proposed design not only enables to optimize the controller parameters for the best trade-off performance, but also allows the designer to make a



well thought decision by comparing all the interaction optimal controllers with different structures. The HR interaction performance is also optimized in [133], where a novel adaptive impedance control is employed for the robotic manipulator. The acquisition of an optimal impedance model of the individual arm is obtained by formulating the LQR that is then solved with integral reinforcement learning. A novel BLF based adaptive impedance control is developed for physical limits, transient perturbations, and time varying dynamics.

Except for the above cited studies, most of the related works in this category specifically focus on assembly, since it is one of the most critical process in the manufacturing scenario. For instance, a human-robot framework named FLEXHRC+ is designed for greater flexibility and scalability in assembly tasks by Darvish *et al.* in [134]. The authors implement a *first order logic* (FOL) based hierarchical AND/OR graph structure that makes the task representation suitable for any type of scenario. In order to avoid damaging the work-pieces, the flexibility of the robot is usually ensured by installing a six-dimensional force/torque sensor on the robot. In [135], Noohi *et al.* propose a model to improve HRC that computes the interaction force by measuring only the force applied by the human. Firstly, the scheme is embedded in an offline controller and then in an online-controller that estimates the interaction force in real-time. No difference in performance is shown between the two proposed controllers. Conversely, other works rely on sensorless solutions that allow the robot to learn and improve the industrial process. In particular, Zeng *et al.* propose in [136] a sensorless compliant control method for a 6 DOF robot which aims at reducing the costs connected to the sensors implementation. A unified impedance model of the robot and the environment is established and based on that, the virtual contact surface is proposed to optimize the assembly. Similarly, Roveda *et al.* [137] design a HRC framework for assembly task learning and optimization. The authors employ a task trajectory learning algorithm based on a few human's demonstrations (exploiting an hidden Markov model approach), and an autonomous optimization procedure of the task execution (exploiting Bayesian optimization). In this article, the sensorless Cartesian impedance controller is involved to perform the task execution. Furthermore, in order to simplify the assembly tasks, Polverini *et al.* [138] make use of a constraint-skill-based programming which allows to specify force control actions at task level and provide compliant capabilities, without the need to specify the motions of the robot. Thus, this approach helps simultaneously the skill developer to embed force control requirements within the specification of an assembly skill and the non-expert user to intuitively program a complex assembly task by simple sequence of assembly skills.

Cobots are not only employed in assembly tasks but also in palletizing as demonstrated in [139], where Lamon *et al.* propose an innovative HRC framework for mixed case palletizing by using a MOCA. Several problems linked to the box and pallet detection are addressed simultaneously by implementing firstly an optimization algorithm to maximize the number of boxes in a pallet, then a role allocation algorithm to assign three possible modes (i.e., autonomous MOCA mode, autonomous human mode, HRC mode). An impedance controller is used to manage the MOCA and visual perception algorithms are added to facilitate the entire process.

Finally, it is worthwhile mentioning that HRC can be improved by using learning-based approaches i.e., *learning from demonstration* (LfD) and RL. On the one hand, Al-Yacoub *et al.* present in [140] a LfD methodology that combines a machine learning algorithm –i.e., *random forest* (RF)– with stochastic regression, using haptic information captured from human demonstration. On the other hand, Ghadirzadeh *et al.* propose in [141] a RL based framework for a more time-efficient HRC that finds an optimal balance between timely actions and the risk of taking improper actions.

To conclude this sub-section, the HRC is improved in [142] by designing a controller that allows the human to choose what to focus on in a 6 DOF Cartesian space. The scheme is tested using a virtual reality system and the experiments show its efficiency and thus, its possible application in sophisticated HR collaborative tasks.

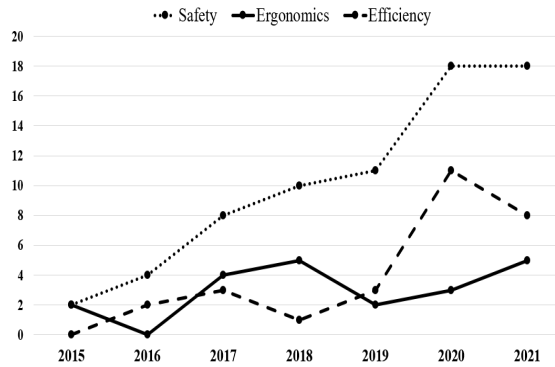


Figure 2.8: Annual distribution of the analyzed papers for each HRC target in the selected time span.

## 2.6 Discussion and Future Developments

In this section all the results of the previous examination are summarized and discussed. Then, outlooks from the control point of view for a safe, ergonomic, and efficient HRC are provided to identify the main lacks in the related literature.

### 2.6.1 Current Research Trends in HRC Control Systems

A large number of control approaches for HRC are examined by the authors of the papers reviewed in this survey and are experimented and tested in real case studies in laboratories or directly in the industrial setting. All the control techniques implemented by the respective authors, application, and cobot models employed for the simulation and/or experiment are summarized by target and problem in Tables 2.1, 2.2, and 2.3. In particular, Tables I, II, and III refer respectively to the safety, ergonomics, and efficiency targets. Each table summarizes the control problems related to the considered target (I column), the literature reference (II column), the authors of the contribution and the year of publication (III and IV column), the control techniques tested by researchers in the laboratory and/or in the industrial field (V column), the type of application (VI column), and the cobot model (VII column).

As a preliminary remark on the rapid and increasing research interest in HRC control, Fig. 2.8 reports the annual distribution of the surveyed papers for each analyzed target. From the figure it can be seen that since the beginning of the research on collaborative robotics, safety first has been the guiding principle, and nowadays it is a consolidated concept in the scientific community. In fact, as shown by the trends in Fig. 2.8, after a slight rise in the first years, a rapid growth from 2019, and a steady state period between 2020 and 2021, the search for a safe HRC continues to be the primary need in the digital industry. Over the years, the number of cobots in production as well as the distribution and commercialization chains has increased exponentially worldwide to cope with the change in the marketplace. The fundamental purpose of the digital industry is to obtain simultaneously in the shortest production time high quality of products, pinpoint accuracy, and optimal flexibility in the industrial process. All these goals can be achieved by improving efficiency and, in fact, from the graph in Fig. 2.8, it is evident that the total annual papers from an efficiency perspective exhibits lately a significant growth from 2019 until it reaches a peak in 2020. Compared to the well-established concepts of safety and efficiency, physical and cognitive ergonomics is still emerging in the scientific research. As a matter of fact, the number of existing works focused on ergonomics from the control perspective is lower than that of the other two targets. As depicted in Fig. 2.8, although the number of articles on the ergonomics point of view shows a fluctuating trend throughout the period considered in this survey, there seems to be a slight rise from 2019 which bodes well for the HRC research field and there will be surely a growth of papers based on this concern in the near future.

**Table 2.1:** Summary of recent studies related to safety-oriented HRC control techniques

Problem	Ref. No	Authors	Year	Control technique	Application	Cobot model
Collision avoidance	[22]	Yu <i>et al.</i>	2019	Neural-AC/IBLF	Manipulation	Baxter robot
	[23]	Yu <i>et al.</i>	2020	RBFNNs/LS	Co-transporting	Baxter robot
	[24]	Yu <i>et al.</i>	2021	Bayesian method/IC/NNs	Co-transporting	Baxter robot
	[25]	Yasar and Iqbal	2021	RNNs	Motion prediction	-
	[26]	R. Liu and C. Liu	2021	RNNs/IK	Assembly	5-DOF manipulator
	[27]	H. Liu and Wang	2021	Sensor/Learning-based alg.	Assembly	Virtual robot model
	[28]	Khatib <i>et al.</i>	2021	Sensor-based system/SNS	Coordinated motion	KUKA LWR4
	[29]	Moon <i>et al.</i>	2021	Sensor-based control	Multiple tasks	UR10 robot
	[30]	Fernández <i>et al.</i>	2017	Whole-body control	Handling/Assembly	Kuka LBR iwa
	[31]	Nascimento <i>et al.</i>	2021	Safety contour	HR distance evaluation	Kuka LBR iwa
	[32]	Nikolakis <i>et al.</i>	2019	Closed-loop control system	Assembly	COMAU Racer 7 robot
	[33]	Polverini <i>et al.</i>	2017	Kinostatic safety field	Pos./orient. tasks	ABB Frida
	[34]	Liu <i>et al.</i>	2020	Modified SSM	Path planning	Industrial robot
	[35]	Ferraguti <i>et al.</i>	2020	CBFs	HR sharing workspace	Universal robot UR5/Puma 260
	[36]	Ferraguti <i>et al.</i>	2020	CBFs	Human tracking	Universal robot UR5
	Collision detection	[37]	Haddadin <i>et al.</i>	2017	Collision monitoring methods	Multiple tasks
[38]		Han <i>et al.</i>	2019	Coordinated compliance control	Multiple tasks	ABB YuMi robot
[39]		Ren <i>et al.</i>	2018	MESO	Dynamic/quasi-static impact	7 DOF cobot
[40]		Heo <i>et al.</i>	2019	CNNs	Multiple tasks	6 DOF manipulator
[41]		Park <i>et al.</i>	2020	SVM/CNN	Multiple tasks	6 DOF cobot
[42]		Sharkawy and Mostfa	2021	NNs	Multiple tasks	KUKA LWR
[43]		Lippi and Marino	2020	RNNs	Multiple domestic tasks	Kinova Jaco2/3 fingers gripper
[44]		Zhang <i>et al.</i>	2020	Supervised Learning/BDT	Multiple tasks	Kuka LWR4+
[45]		P. Avalliotin <i>et al.</i>	2019	Supervised Learning NNs	Multiple tasks	COMAU Racer 7 robot
[46]		Kouris <i>et al.</i>	2018	Frequency domain approach	Multiple tasks	KUKA LWR
[47]		Mariotti <i>et al.</i>	2019	Admittance control	Cyclic, piecewise linear path	KUKA KR5 Sixx R650 robot
[48]		Gaz <i>et al.</i>	2018	HRC control algorithm	Polishing	Universal Robot UR10
[49]		Magrini and De Luca	2017	GPU algorithm	Multiple tasks	KUKA LWR
[50]		Magrini <i>et al.</i>	2020	Depth-space algorithm	Tasks in open industrial cells	6R ABB-IRB 4600-60 robot
[51]	Labrecque <i>et al.</i>	2017	Closed-loop system	Peg-in-hole assembly	uMan	
[52]	Chan and Tsai	2020	Danger index/ERGA	Pick & place	6 DOF industrial robot	
Motion planning	[53]	Oleinikov <i>et al.</i>	2021	NMPC	Pick & place	Kinova Gen3 robot
	[54]	Sloth and Petersen	2018	Optimization problem	Multiple tasks	3 DOF robot
	[55]	Lucci <i>et al.</i>	2020	SSM/PFL	Multiple tasks	ABB YuMi robot
	[56]	Lemmer <i>et al.</i>	2019	SSM/PFL/ML	Assembly	Manipulator PRBT
	[57]	Costanzo <i>et al.</i>	2021	CNN/Fuzzy control logic	Assembly	Yaskawa MOTOMAN SIA5F
	[58]	Zanchettin <i>et al.</i>	2015	Kinematic control	Manipulation/Assembly	ABB Frida
	[59]	Ragaglia <i>et al.</i>	2018	Trajectory generation	Pick & place	ABB IRB1 40 robot
	[60]	Palleschi <i>et al.</i>	2021	Time-optimal trajectory planning	Unwrapping task	Franka Emika Panda arm
	[61]	Zhang <i>et al.</i>	2020	Decoupled optimization	Manipulation	ABB IRB1 40 robot
	[62]	Weitschat and Aschemann	2018	NLP/DMPs	Path planning	8 DOF robotic system
	[63]	Casalino <i>et al.</i>	2019	Proactive path planning	Assembly	ABB YuMi robot
	[64]	Kanazawa <i>et al.</i>	2019	Adaptive control	Assembly	Two-link planar manipulator
	[65]	Ducaju <i>et al.</i>	2021	MPC	Multiple tasks	Franka Emika Panda arm
	[66]	Mainprice <i>et al.</i>	2016	STOMP	Assembly	PR2 robot
	[67]	Cheng <i>et al.</i>	2020	NNs/Bayesian inference	Assembly	FANUC LR Mate 200iD/7L
	[68]	Landi <i>et al.</i>	2019	Semi-Adaptable NN	Multiple tasks	FANUC LR Mate 200iD/7L
	[69]	Maric <i>et al.</i>	2020	FDC	Sanding	Kuka KR10
[70]	Zhao <i>et al.</i>	2021	RL	Assembly	UR5 robot	
[71]	Chen and Song	2018	Collision-free motion planning	Multiple tasks	Techman TM5	
[72]	Ji <i>et al.</i>	2020	POMDP	Assembly	ABB IRB1200	
[73]	He <i>et al.</i>	2020	AC/IBLF/RBFNN	Multiple tasks	Baxter robot	
[74]	Beset and Béarée	2017	FIR filtering	Multiple tasks	Kuka LBR iwa	
Control system design	[75]	Cherubini <i>et al.</i>	2016	Sensor-based/AC	Assembly	KUKA LWR IV
	[76]	Roveda <i>et al.</i>	2018	IC	Interaction tasks	KUKA LWR4+
	[77]	Kimmel and Hirche	2017	Invariance control	Multiple tasks	7 DOF Anthropomorphic robot
	[78]	Bednarczyk <i>et al.</i>	2020	MPIC	Multiple tasks	KUKA iwa 14
	[79]	Reyes-Uquillas and Hsiao	2021	Adaptive admittance law	Manual guidance task	HIWIN RA605
	[80]	Xiao <i>et al.</i>	2021	Sensorless scheme	Peg-in-hole assembly	6-DOF cobot
	[81]	Cherubini <i>et al.</i>	2015	Reactive sensor-based	Screwing	KUKA LWR IV
	[82]	Suzuki <i>et al.</i>	2021	RNN	Pick & place	Torobo ARM
	[83]	Chen and Wen	2020	Adaptive NN	Multiple tasks	Baxter robot
	[84]	Cremer <i>et al.</i>	2019	Adaptive NN	Assisted tasks	PR2 robot
	[85]	Dimeas and Aspragathosfor	2016	AC	Co-manipulation	KUKA LWR
	[86]	Li <i>et al.</i>	2017	IC based on PD	Medical tasks	4 DOF robotic arm
	[87]	Sirintuna <i>et al.</i>	2020	FOAC	Drilling	KUKA LBR iwa 7 R800
	[88]	Raiola <i>et al.</i>	2018	IC/Energy-tanks	Co-manipulation	KUKA LWR4+
	[89]	Makrini <i>et al.</i>	2016	VBSMC	Multiple tasks	Baxter robot
	[90]	Solanes <i>et al.</i>	2018	Non-conventional SMC/AC	Handling	Sawyer robot
[91]	Liu <i>et al.</i>	2021	Dynamic Behavior Control System	Manipulation	2-DOF robot	
[92]	Fu and Zhao	2021	Maxwell model	Domestic/Assembly/Puncturing tasks	KUKA LWR 4+/LBR iwa 14 R820	

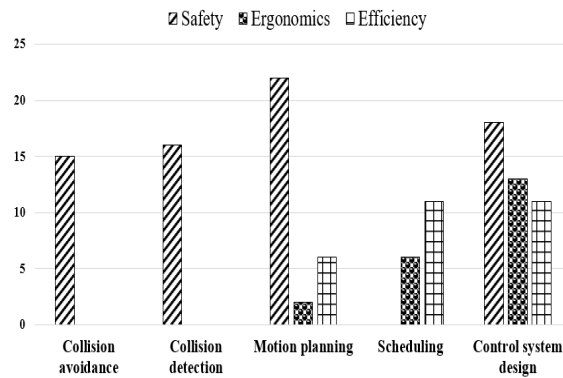


**Figure 2.9:** Number of papers related to the analyzed control problems for each HRC target in the 2015-2021 time span.

For the sake of identifying which of the analyzed control problem represents the most trending research field in HRC, Fig. 2.9 shows the distribution of the surveyed papers per control problem for each HRC target. According to Fig. 2.9, all three targets are mostly

**Table 2.2:** Summary of recent studies related to ergonomics-oriented HRC control techniques

Problem	Ref. No	Authors	Year	Control technique	Application	Cobot model
Motion planning	[93]	Maurice <i>et al.</i>	2017	Biological/Non-biological planning	Multiple tasks	User handle
	[95]	Rojas <i>et al.</i>	2019	Minimum-jerk trajectory	Assembly	Universal Robots UR3
Scheduling	[97]	Pearce <i>et al.</i>	2018	MILP	6 real-world factory tasks	Baxter Robot
	[98]	Maderna <i>et al.</i>	2020	MILP	Kitting	Robot manipulator
	[99]	Hu and Chen	2017	Stochastic Petri Nets	Assembly	-
	[100]	Faber <i>et al.</i>	2017	CCU/GASP	Assembly	-
	[101]	Rahman and Wang	2018	Feedforward/Feedback optimization	Assembly	Hybrid cell
Control system design	[102]	Jiang and Wang	2021	DM model	Multiple tasks	-
	[103]	Medina <i>et al.</i>	2015	Haptic assistance	Multiple tasks	-
	[104]	Ansari and Karayiannidis	2021	Integer linear programming	Rotation/Translation	UR10 robotic manipulator
	[105]	Peternel <i>et al.</i>	2017	Whole-body control	Co-manipulation/Handover tasks	KUKA-Pisa/IIT Softhand
	[106]	Kim <i>et al.</i>	2021	Optimization problem	Drilling/ Polishing	KUKA LBR IV+
	[107]	Sadrifaridpour and Wang	2018	Speed control	Assembly	Baxter Robot
	[108]	Messeri <i>et al.</i>	2021	Game theory	Assembly	ABB Yumi robot
	[109]	Rahman	2021	Position/Force control/RL	Manipulation	PAO
	[110]	Oliif <i>et al.</i>	2020	NN	Multiple tasks	-
	[111]	Shen <i>et al.</i>	2020	Machine learning	Personality assessment	Pepper robot
	[112]	Modares <i>et al.</i>	2015	Two-loops framework/RL/LQR	Point-to-point motion	PR2 robot
	[113]	Tang and Webb	2018	Hand gesture robot control	Multiple tasks	Universal Robot UR5
[114]	Zanchettin <i>et al.</i>	2019	Ergonomics-based control law	Painting	COMAU SmartSix	
[115]	Yao <i>et al.</i>	2018	Admittance control	Multiple tasks	KUKA KR 6 R700 sixx	

**Table 2.3:** Summary of recent studies related to efficiency-oriented HRC control techniques

Problem	Ref. No	Authors	Year	Control technique	Application	Cobot model
Motion planning	[94]	Raessa <i>et al.</i>	2020	Constrained planning	Assembly	UR3 arms
	[117]	Stouraitis <i>et al.</i>	2020	GS/trajectory opt	Dyadic manipulation	KukaLBRiwa 820 arms
	[118]	Balatti <i>et al.</i>	2020	IC/trajectory planning	Palletizing	MOCA
	[119]	Wu <i>et al.</i>	2021	Cartesian IC	Door opening	MOCA
	[120]	Li <i>et al.</i>	2020	Torque-position/compliance	Disassembly	KUKA LBR iwa 14 R800
	[96]	Rojas and Vidoni	2021	Reparametrization algorithm	Pick & pass	Universal Robot UR3
Scheduling	[121]	Yu <i>et al.</i>	2020	RL/CNN	Assembly	-
	[122]	Johannsmeier and Haddadin	2016	AND/OR graphs	Assembly	KUKA LWR
	[123]	Casalino <i>et al.</i>	2021	Time Petri nets	Assembly	ABB Yumi Robot
	[124]	Zanchettin	2021	Scheduling algorithm	Assembly	-
	[125]	Michalos <i>et al.</i>	2018	Multi-criteria task assignment	Assembly	-
	[126]	Tsarouchi <i>et al.</i>	2017	Task allocation	Assembly	SmartSix Comau Robots
	[127]	Xu <i>et al.</i>	2020	MDBA-Pareto	Disassembly	-
	[128]	Cheng <i>et al.</i>	2021	Hierarchical task model	Assembly/Shelving	FANUC LR Mate 200iD/7L
	[129]	Wang <i>et al.</i>	2020	DT-based/PFT/PCA/SVM	Welding	-
	[130]	Bilberg and Malik	2019	DT-based/Task allocation	Assembly	-
[131]	Lv <i>et al.</i>	2021	DT-based/D-DDPG	Assembly	-	
Control system design	[132]	Aydin <i>et al.</i>	2020	Pareto optimization	HR interaction tasks	UR5 Robot
	[133]	Li <i>et al.</i>	2017	BLF based aIC/LQR/IRL	Multiple tasks	Robotic exoskeleton
	[134]	Darvish <i>et al.</i>	2020	FOL based hierarchical AND/OR graph	Assembly	FLEXHRC+
	[135]	Noohi <i>et al.</i>	2016	IC	Dyadic manipulation	4 DOF WAM arm
	[136]	Zeng <i>et al.</i>	2019	Sensorless compliance/VCS	Peg-in-hole assembly	6 DOF cobot
	[137]	Roveda <i>et al.</i>	2021	IC-HMM/BO	Assembly	Franka EMKA panda manipulator
	[138]	Polverini <i>et al.</i>	2019	Constraint-based programming	Assembly	ABB Yumi Robot
	[139]	Lamon <i>et al.</i>	2020	Opt/IC/Visual perception	Palletizing	MOCA
	[140]	Al-Yacoub <i>et al.</i>	2021	LfD/RF	Assembly	Motoman SDA10D robot
	[141]	Ghadirzadeh <i>et al.</i>	2020	Deep RL	Packaging	ABB Yumi Robot
	[142]	Whitwell and Artemiadis	2017	RL	Multiple tasks	7DOF KUKA LBR iwa

focused on the design of state-of-the-art controllers. In particular, a safe collaboration of humans with robots is obtained by developing controllers that aim at speed and separation monitoring by defining safe zones to avoid unwanted HR contacts or adjusting the speed in the robot's proximity and at power and force limiting. Sometimes NNs are used to predict the human motion intent, other times energy tanks are involved to ensure stability and passivity. To improve the working conditions and reduce physical and psychological stress, HRC factors are integrated in the controllers that can also exploit human gestures commands. Learning-based frameworks and sensorless solutions are also designed to increase efficiency and the overall level of productivity. An ergonomics improvement is obtained with a perfect task allocation and scheduling of activities. In fact, as shown in Fig. 2.9, scheduling is a relevant issue in the ergonomics target. The optimal scheduling problem is also very important to minimize the downtime and augment the profitability. Looking at the literature from the safety perspective, the trajectory planning optimization problems are solved to react to sudden changes in the environment and to avoid the operator's injuries. For this reason, approximately 31% of the papers on safety belongs to this category. Collision detection and avoidance techniques with and without optimal control are widely studied by researchers in the field of robotics and in the last decade in collaborative robotics. In total, around 44% of the safety-oriented surveyed papers concern the implementation of algorithms to avoid or detect collisions.

## 2.6.2 Emerging Control Issues and Challenges

To collaborate together, humans and robots need a common view of their working environment. This requires that HRC control systems must rely, in an essential way, on tools and techniques such as sensing, data fusion, and deep learning to safely, ergonomically, and efficiently define, plan, execute, and optimize joint tasks.

Due to the recent growth on bio-inspired measurement technologies that have made sensors affordable and lightweight, as well as easy to use on robots, sensor-based methodologies are employed in a large number of HR collaborative tasks, as shown in Table 2.1, 2.2, and 2.3. Four different state-of-the-art types of modes (audio-based, touch-based, vision-based, and distance-based) are generally implemented in robotics systems where recently they are often combined with virtual and augmented reality to reduce the control's computational complexity and make interfaces more intuitive and readable by non-expert users.

Multiple sensors [28], [30], [31], [39], [46], [47], [75] are often involved in fully integrated robotic systems to collect and learn the huge amount of data over time that are used to predict the human movements during the collaboration with robots. Sometimes, learning-based solutions [27] are employed in decoding the sensors' signals to generate an intelligible representation of the phenomenon initially perceived. Other times, sensorless solutions [38], [80], [136], [137] often integrated in learning-based approaches [45] are exploited to overcome the limitations imposed by sensors' implementation that are visible degrees of hysteresis, non-stationarity, and other mechanical nonlinearities.

Without doubt, among all the techniques addressed by the surveyed papers, learning-based control methodologies are the most popular in the scientific community and it is foreseeable that these will continue to be addressed in the long term. It has to be specified that, in general, the learning-based techniques aim at introducing, in addition to motion/force control, an analysis of the human behavior to avoid unsafe situations or facilitate HRC by predicting in real time the human behavior and thus control accordingly the robot. Consequently, in case of learning-based control methods, the control of the robot benefits from the prediction of the human behavior to improve safety, efficiency, and ergonomics. From Tables 2.1, 2.2, and 2.3, it is evident that a large variety of NNs algorithms are applied to robot control problems where the training can be performed online or offline, depending on the type of task. On the one hand, offline training of NNs is more straightforward than the online approach, since the designed parameters are not adjusted according to the differences between expected and actual outputs; however, a successive online training is sometimes needed in order to achieve the real dynamics. On the other hand, online training is more precise than the offline approach but could deal with unknown dynamic uncertainties, i.e., payloads or frictions, that affect the robot's performance. As shown in the summaries (Tables 2.1, 2.2, and 2.3), RNNs [25], [26], [43], [82] are one of the most popular type of NNs employed in all the proposed targets, since they have feedback mechanisms that allow to avoid an offline training in the majority of real-time control problems. Aiming at compensating for unknown dynamic uncertainties, feedforward NNs with radial basis function [23], [73] are also employed for their effectiveness in solving dynamic and kinematic problems of robot manipulators. Due to the intrinsic structure of this type of networks, it is proven that they are faster than typical back propagation networks when trained by a supervised learning method like in [44], [45]. Alternatively, convolutional NNs [40], [41], [57], [121] are chosen for object detection and categorization, but it is demonstrated that in the majority of cases they cannot be applied in real-time and are used with a limited number of object categories.

All the aforementioned control strategies based on learning have been developed to address uncertainties and external disturbances that might provoke the robot's performance degradation by replacing the traditional proportional-integral-derivative controllers, typically characterized by a complicated tuning of control parameters. Since the above described methods suffer from several problems, ranging from a huge computation time to a limited generalizability or adaptability to unseen situations, NNs based on modern control theories –e.g., SMC [89], [90], Takagi-Sugeno fuzzy control



[57], and RL [70], [109], [112], [121], [133], [141]– are introduced in the literature and modeled to overcome these complex robot’s control issues. Obviously, also these innovative advanced techniques present limitations, such as chattering and sensitive problems for the SMC and possible instabilities for fuzzy approaches. Although learning-based algorithms present these limitations, they have recently gained in popularity thanks to the ability to learn from demonstrations [140], high generalization performance, and capability to approximate an arbitrary function with adequate number of neurons.

As a consequence, there is an emerging need of tackling uncertainties while keeping the controller’s performance and robustness at the highest level. To cope with this issue, hybrid control techniques that combine NNs with admittance/impedance control [22], [23], stochastic control techniques [24], [67], and optimization-based methods [56], [68] are introduced in some of the selected papers and could be the turning point in future research in collaborative robotics.

Impedance and admittance control methodologies [47], [75], [76], [85], [118], [119], [135] are widely employed to regulate interactive forces in HRC. The main difference between them is that the former controls motion after the force’s detection, especially in dynamic interaction with stiff environments, whereas the latter controls force after the measurement of motion or deviation from a set point in interaction with soft environments or operation in free space. In general, impedance controllers are modeled as open-loop force systems by avoiding the use of force sensors which are expensive and sensitive to drift and temperature change. However, this type of control can be affected by friction. In some articles presented in this survey, a variable impedance controller integrates an energy tank [88] –only a certain amount of energy that is stored in the system can be used to perform a task– as a tool for passivity-based control in order to guarantee asymptotic stability also in non-passive environments. Aiming at improving the robotic controllers’ efficiency, the awareness of the energy amount needed to perform a specific task can be integrated in the energy tank systems.

In other works described in the previous sections, stochastic approaches, i.e., Bayesian robot programming [24], [44], [137], hidden Markov model [137], and Gaussian mixture model are preferred by the authors to deal with incomplete and uncertain information in hard environments, due to their simplicity in implementation, clear theoretical foundations, rigorous programming methodology, and homogeneity of representations and resolution processes.

In a large number of the reviewed works, optimization-based methods are introduced to improve the calculator performance and develop high-speed algorithms. In a multitude of cases, they are used in combination with other techniques, e.g., learning-based and sensor-based, and change the cost function according to the target and problem analyzed. On the one hand, optimal control is implemented to respect the new ISO industrial safety requirements by exploiting CBFs [35], [36], that overcome the limitations of both SSM and PFL [34], [54]–[56], and in the future can be combined with human gesture prediction [113] and integrated with MPC [78] to plan the best safe behavior in the long term. As it is well-known, MPC is a high-tech control technique that solves at every time step a finite-horizon control problem with multiple constraints in multi-variable systems. Thanks to its flexibility in achieving complicated goals and implementing robust robot constraints, MPC [53], [65] has been recently introduced in HR interaction control, even if the concept of receding horizon has already been exploited for task-parameterized and multi-agent motion planning, and for haptic assistance – i.e., stochastic trajectory optimization for motion planning [66], incremental trajectory optimization for motion planning, particle swarm optimization –. Unfortunately, the MPC control technique has several drawbacks from the computational complexity – iterative calculation at each time step – and high number of control variables, to the derivation of the complex robot’s dynamic models. Aiming at solving these issues and also instabilities that can appear during HRC, MPC can be combined with other control methodologies i.e., impedance and admittance control or stochastic techniques. On the other hand, several optimization-based approaches are proposed for task allocations and scheduling problems by maximizing the productivity and minimizing the human effort, physical, and psychological stress. Aiming at assigning

tasks optimally and robustly by maximizing the throughput and minimizing the cycle time, sometimes ILP and MILP [97], [98] are chosen and other times graph search, timed [123] and stochastic Petri Nets [99] are implemented in robotics systems.

As a further remark, it is worthwhile mentioning that only a small quantity of papers summarized in this survey aims at optimizing multiple targets through the above discussed techniques. Specifically, none of the reviewed articles is simultaneously focused on all the three targets (i.e., safety, ergonomics, and efficiency). Approximately 12% (14 papers) of the selected works are written accordingly to dual targets. In particular, more than half of the dual targets' articles ([27], [34], [55], [57], [58], [62], [64], [67]) are formulated from the safety and efficiency control perspective; the remaining ones address the safety and ergonomics control perspective ([75], [84]) and ergonomics and efficiency control perspective ([94], [96], [97], [108]).

Aiming at filling this gap and thus at improving the cobots' performance in the industrial context, HRC research will have to try to deal with the three objectives at the same time. For instance, RULA (rapid upper limb assessment) [113] and REBA (rapid entire body assessment) [114], can be integrated as assessment tools in the optimization processes to evaluate the exposure of individual workers to ergonomic risk factors. With the expected coming of Industry 5.0, which is centered on sustainability and human perspective, there will certainly be an increase in the use of cobots in the manufacturing scenario since HRC will be the turning point of this new revolution. Therefore, researchers will continue to experiment with innovative control techniques to ensure operator's safety and well-being.

### 2.6.3 HRC Applications in Industry

The discussion about HRC control techniques is concluded with some remarks related to their applications in the digital industry. From Tables 2.1, 2.2, and 2.3, it emerges that, in almost all the reviewed articles, the control techniques are usually applied to the assembly or disassembly processes. In the near future the application context could be extended to other industrial processes which are under study and development by the leaders of robotics and cobotics worldwide. In particular, the most appreciated fields of development are: accurate assembly processes (e.g., screw driving, nut driving, part fitting, and insertion to painting, polishing, and sanding), material handling (i.e., packaging, palletizing, and kitting), material removal (i.e., grinding, milling, and drilling), welding, quality inspection and machine tending. In all such activities, the main aim is to reduce repetitive workplace injuries and to achieve greater productivity in the global market. For all the reported applications, cobots also offer higher speed and process quality, pinpoint accuracy and optimal flexibility, for multiple tasks in operations of every size. Consequently, their success can become unquestioned in the most varied sectors (e.g., automotive, electronics, agriculture, food processing, logistics, and metalwork). The main companies that are contributing to the development of cobots are ABB Robotics [143], which is the pioneer company in robotics, machine automation, and digital services, and Universal Robots [144] which is a Danish manufacturer of flexible industrial collaborative robot arms. In addition to these developers, also Rethink Robotics [145] –a pioneer in the field of collaborative robotic solutions which has recently entered into a joint development agreement with Siemens Technology Accelerator and Siemens Corporate Technology– and Omron [146] –a Japanese manufacturer in industrial automation, in the healthcare sector, and in electronic components– are developing new innovative cobotics technologies in several sectors and fields of application.

Lastly, only recently novel priority areas of application for cobots are emerging, such as the healthcare and pharmaceutical sectors for which cobots could be part of the regular cleaning cycle aiming at preventing and reducing the spread of infectious diseases, viruses, and bacteria. Moreover, given the current situation where COVID-19 is changing lives and habits, cobots can be included in areas such as sanitization and inventory to help workers maintain healthy work environments.



## 2.7 Conclusions

Collaborative robotics is currently the fastest growing segment of industrial robotics, as demonstrated by the increasing number of papers in the recent literature. The analysis of the state-of-the-art of cobotics is essential for researchers to identify gaps and future developments in this context of digital evolution. Thus, the categorization of the main works related to a safe, ergonomic, and efficient human-robot collaboration and the identification of the pertaining existing and trending decision and control techniques, which are the objective of this survey, will be useful to the scientific community to improve the current methodologies and seek alternative solutions.

## References

- [1] Xu, L. D., Xu, E. L., and Li, L., “Industry 4.0: State of the art and future trends,” *Int. J. Prod. Res.*, vol. 56, no. 8, pp. 2941–2962, 2018.
- [2] Demir, K. A., Döven, G., and Sezen, B., “Industry 5.0 and human-robot co-working,” *Procedia Comput. Sci.*, vol. 158, pp. 688–695, 2019.
- [3] Hentout, A., Aouache, M., Maoudj, A., and Akli, I., “Human–robot interaction in industrial collaborative robotics: A literature review of the decade 2008–2017,” *Adv. Robot.*, vol. 33, no. 15-16, pp. 764–799, 2019.
- [4] Castro, A., Silva, F., and Santos, V., “Trends of human-robot collaboration in industry contexts: Handover, learning, and metrics,” *Sensors*, vol. 21, no. 12, p. 4113, 2021.
- [5] Matheson, E., Minto, R., Zampieri, E. G., Faccio, M., and Rosati, G., “Human–robot collaboration in manufacturing applications: A review,” *Robotics*, vol. 8, no. 4, p. 100, 2019.
- [6] Kadir, B. A., Broberg, O., and Conceicao, C. S. da, “Current research and future perspectives on human factors and ergonomics in industry 4.0,” *Comput. Ind. Eng.*, vol. 137, p. 106 004, 2019.
- [7] Gualtieri, L., Rauch, E., and Vidoni, R., “Emerging research fields in safety and ergonomics in industrial collaborative robotics: A systematic literature review,” *Robot. Comput. Integr. Manuf.*, vol. 67, p. 101 998, 2021.
- [8] Dotoli, M., Fay, A., Miśkiewicz, M., and Seatzu, C., “Advanced control in factory automation: A survey,” *Int. J. Prod. Res.*, vol. 55, no. 5, pp. 1243–1259, 2017.
- [9] Ajoudani, A., Zanchettin, A. M., Ivaldi, S., Albu-Schäffer, A., Kosuge, K., and Khatib, O., “Progress and prospects of the human–robot collaboration,” *Auton. Robot.*, vol. 42, no. 5, pp. 957–975, 2018.
- [10] Tong, Y. and Liu, J., “Review of research and development of supernumerary robotic limbs,” *IEEE CAA J. Autom. Sinica*, vol. 8, no. 5, pp. 929–952, 2021.
- [11] Villani, V., Pini, F., Leali, F., and Secchi, C., “Survey on human–robot collaboration in industrial settings: Safety, intuitive interfaces and applications,” *Mechatronics*, vol. 55, pp. 248–266, 2018.
- [12] Tsarouchi, P., Makris, S., and Chryssolouris, G., “Human–robot interaction review and challenges on task planning and programming,” *Int. J. Comput. Integr. Manuf.*, vol. 29, no. 8, pp. 916–931, 2016.
- [13] Bi, Z., Luo, M., Miao, Z., Zhang, B., Zhang, W., and Wang, L., “Safety assurance mechanisms of collaborative robotic systems in manufacturing,” *Robot. Comput. Integr. Manuf.*, vol. 67, p. 102 022, 2021.
- [14] Wang, L., Gao, R., Váncza, J., *et al.*, “Symbiotic human-robot collaborative assembly,” *CIRP annals*, vol. 68, no. 2, pp. 701–726, 2019.

- 
- [15] Papanastasiou, S., Kousi, N., Karagiannis, P., *et al.*, “Towards seamless human robot collaboration: Integrating multimodal interaction,” *Int. J. Adv. Manuf. Technol.*, vol. 105, no. 9, pp. 3881–3897, 2019.
- [16] Michalos, G., Kousi, N., Karagiannis, P., *et al.*, “Seamless human robot collaborative assembly—an automotive case study,” *Mechatronics*, vol. 55, pp. 194–211, 2018.
- [17] Lasota, P. A., Fong, T., Shah, J. A., *et al.*, *A survey of methods for safe human-robot interaction*. Now Publishers, 2017.
- [18] Kumar, S., Savur, C., and Sahin, F., “Survey of human-robot collaboration in industrial settings: Awareness, intelligence, and compliance,” *IEEE Trans. Syst., Man, Cybern.*, 2020.
- [19] Hashemi-Petroodi, S. E., Thevenin, S., Kovalev, S., and Dolgui, A., “Operations management issues in design and control of hybrid human-robot collaborative manufacturing systems: A survey,” *Annu. Rev. Control*, 2020.
- [20] Ibrahim, A., Alexander, R., Shahid, M., Sanghar, U., Dsouza, R., and Souza, D., “Control systems in robotics: A review,” *Int. J. Eng. Inventions*, vol. 5, pp. 2278–7461, Apr. 2016.
- [21] Wilson, J. R., “Fundamentals of ergonomics in theory and practice,” *Applied ergonomics*, vol. 31, no. 6, pp. 557–567, 2000.
- [22] Yu, X., He, W., Xue, C., Li, B., Cheng, L., and Yang, C., “Adaptive neural admittance control for collision avoidance in human-robot collaborative tasks,” in *IEEE/RSJ Int. Conf. on Intelligent Robots and Systems (IROS)*, IEEE, 2019, pp. 7574–7579.
- [23] Yu, X., Li, Y., Zhang, S., Xue, C., and Wang, Y., “Estimation of human impedance and motion intention for constrained human–robot interaction,” *Neurocomputing*, vol. 390, pp. 268–279, 2020.
- [24] Yu, X., He, W., Li, Y., *et al.*, “Bayesian estimation of human impedance and motion intention for human–robot collaboration,” *IEEE Trans. Cybern.*, vol. 51, no. 4, pp. 1822–1834, 2021. DOI: [10.1109/TCYB.2019.2940276](https://doi.org/10.1109/TCYB.2019.2940276).
- [25] Yasar, M. S. and Iqbal, T., “A scalable approach to predict multi-agent motion for human-robot collaboration,” *IEEE Robot. Autom. Lett.*, vol. 6, no. 2, pp. 1686–1693, 2021. DOI: [10.1109/LRA.2021.3058917](https://doi.org/10.1109/LRA.2021.3058917).
- [26] Liu, R. and Liu, C., “Human motion prediction using adaptable recurrent neural networks and inverse kinematics,” *IEEE Contr. Syst. Lett.*, vol. 5, no. 5, pp. 1651–1656, 2021. DOI: [10.1109/LCSYS.2020.3042609](https://doi.org/10.1109/LCSYS.2020.3042609).
- [27] Liu, H. and Wang, L., “Collision-free human-robot collaboration based on context awareness,” *Robotics Comput. Integr. Manuf.*, vol. 67, p. 101997, 2021.
- [28] Khatib, M., Al Khudir, K., and De Luca, A., “Human-robot contactless collaboration with mixed reality interface,” *Robotics Comput. Integr. Manuf.*, vol. 67, p. 102030, 2021.
- [29] Moon, S. J., Kim, J., Yim, H., Kim, Y., and Choi, H. R., “Real-time obstacle avoidance using dual-type proximity sensor for safe human-robot interaction,” *IEEE Robot. Autom. Lett.*, 2021.
- [30] Gea Fernández, J. de, Mronga, D., Günther, M., *et al.*, “Multimodal sensor-based whole-body control for human–robot collaboration in industrial settings,” *Rob. Auton. Syst.*, vol. 94, pp. 102–119, 2017.
- [31] Nascimento, H., Mujica, M., and Benoussaad, M., “Collision avoidance interaction between human and a hidden robot based on kinect and robot data fusion,” *IEEE Robot. Autom. Lett.*, vol. 6, no. 1, pp. 88–94, 2021.

- [32] Nikolakis, N., Maratos, V., and Makris, S., “A cyber physical system (cps) approach for safe human-robot collaboration in a shared workplace,” *Robotics Comput. Integ. Manuf.*, vol. 56, pp. 233–243, 2019.
- [33] Polverini, M. P., Zanchettin, A. M., and Rocco, P., “A computationally efficient safety assessment for collaborative robotics applications,” *Robot. Comput. Integr. Manuf.*, vol. 46, pp. 25–37, 2017.
- [34] Liu, Z., Wang, X., Cai, Y., *et al.*, “Dynamic risk assessment and active response strategy for industrial human-robot collaboration,” *Comput. Ind. Eng.*, vol. 141, p. 106302, 2020.
- [35] Ferraguti, F., Landi, C. T., Costi, S., *et al.*, “Safety barrier functions and multi-camera tracking for human–robot shared environment,” *Rob. Auton. Syst.*, vol. 124, p. 103388, 2020.
- [36] Ferraguti, F., Bertuletti, M., Landi, C. T., Bonfè, M., Fantuzzi, C., and Secchi, C., “A control barrier function approach for maximizing performance while fulfilling to iso/ts 15066 regulations,” *IEEE Robot. Autom. Lett.*, vol. 5, no. 4, pp. 5921–5928, 2020.
- [37] Haddadin, S., De Luca, A., and Albu-Schäffer, A., “Robot collisions: A survey on detection, isolation, and identification,” *IEEE Trans. Robot.*, vol. 33, no. 6, pp. 1292–1312, 2017.
- [38] Han, L., Xu, W., Li, B., and Kang, P., “Collision detection and coordinated compliance control for a dual-arm robot without force/torque sensing based on momentum observer,” *IEEE/ASME Trans. Mechatronics*, vol. 24, no. 5, pp. 2261–2272, 2019.
- [39] Ren, T., Dong, Y., Wu, D., and Chen, K., “Collision detection and identification for robot manipulators based on extended state observer,” *Control Eng. Pract.*, vol. 79, pp. 144–153, 2018.
- [40] Heo, Y. J., Kim, D., Lee, W., Kim, H., Park, J., and Chung, W. K., “Collision detection for industrial collaborative robots: A deep learning approach,” *IEEE Robot. Autom. Lett.*, vol. 4, no. 2, pp. 740–746, 2019.
- [41] Park, K. M., Kim, J., Park, J., and Park, F. C., “Learning-based real-time detection of robot collisions without joint torque sensors,” *IEEE Robot. Autom. Lett.*, vol. 6, no. 1, pp. 103–110, 2020.
- [42] Sharkawy, A.-N. and Mostfa, A. A., “Neural networks’ design and training for safe human-robot cooperation,” *Journal of King Saud University-Engineering Sciences*, 2021.
- [43] Lippi, M. and Marino, A., “Enabling physical human-robot collaboration through contact classification and reaction,” in *2020 IEEE Int. Conf. on Robot Hum. Interact. Commun. (RO-MAN)*, IEEE, 2020, pp. 1196–1203.
- [44] Zhang, Z., Qian, K., Schuller, B. W., and Wollherr, D., “An online robot collision detection and identification scheme by supervised learning and bayesian decision theory,” *IEEE Trans. Autom. Sci. Eng.*, 2020.
- [45] Aivaliotis, P., Aivaliotis, S., Gkournelos, C., Kokkalis, K., Michalos, G., and Makris, S., “Power and force limiting on industrial robots for human-robot collaboration,” *Robotics Comput. Integ. Manuf.*, vol. 59, pp. 346–360, 2019.
- [46] Kouris, A., Dimeas, F., and Aspragathos, N., “A frequency domain approach for contact type distinction in human–robot collaboration,” *IEEE Robot. Autom. Lett.*, vol. 3, no. 2, pp. 720–727, 2018. DOI: [10.1109/LRA.2017.2789249](https://doi.org/10.1109/LRA.2017.2789249).
- [47] Mariotti, E., Magrini, E., and De Luca, A., “Admittance control for human-robot interaction using an industrial robot equipped with a f/t sensor,” in *2019 Int. Conf. on Robotics and Automation (ICRA)*, IEEE, 2019, pp. 6130–6136.

- [48] Gaz, C., Magrini, E., and De Luca, A., “A model-based residual approach for human-robot collaboration during manual polishing operations,” *Mechatronics*, vol. 55, pp. 234–247, 2018.
- [49] Magrini, E. and De Luca, A., “Human-robot coexistence and contact handling with redundant robots,” in *2017 IEEE/RSJ Int. Conf. on Intelligent Robots and Systems (IROS)*, IEEE, 2017, pp. 4611–4617.
- [50] Magrini, E., Ferraguti, F., Ronga, A. J., Pini, F., De Luca, A., and Leali, F., “Human-robot coexistence and interaction in open industrial cells,” *Robot. Comput. Integr. Manuf.*, vol. 61, p. 101 846, 2020.
- [51] Labrecque, P. D., Laliberté, T., Foucault, S., Abdallah, M. E., and Gosselin, C., “Uman: A low-impedance manipulator for human–robot cooperation based on underactuated redundancy,” *IEEE/ASME Trans. Mechatronics*, vol. 22, no. 3, pp. 1401–1411, 2017.
- [52] Chan, C.-C. and Tsai, C.-C., “Collision-free speed alteration strategy for human safety in human-robot coexistence environments,” *IEEE Access*, vol. 8, pp. 80 120–80 133, 2020.
- [53] Oleinikov, A., Kuskavletov, S., Shintemirov, A., and Rubagotti, M., “Safety-aware nonlinear model predictive control for physical human-robot interaction,” *IEEE Robot. Autom. Lett.*, 2021.
- [54] Sloth, C. and Petersen, H. G., “Computation of safe path velocity for collaborative robots,” in *2018 IEEE/RSJ Int. Conf. on Intelligent Robots and Systems (IROS)*, 2018, pp. 6142–6148. DOI: [10.1109/IROS.2018.8594217](https://doi.org/10.1109/IROS.2018.8594217).
- [55] Lucci, N., Lacevic, B., Zanchettin, A. M., and Rocco, P., “Combining speed and separation monitoring with power and force limiting for safe collaborative robotics applications,” *IEEE Robot. Autom. Lett.*, vol. 5, no. 4, pp. 6121–6128, 2020.
- [56] Lemmerz, K., Glogowski, P., Kleineberg, P., Hypki, A., and Kuhlenkötter, B., “A hybrid collaborative operation for human-robot interaction supported by machine learning,” in *2019 12th Int. Conf. on Human System Interaction (HSI)*, 2019, pp. 69–75. DOI: [10.1109/HSI47298.2019.8942606](https://doi.org/10.1109/HSI47298.2019.8942606).
- [57] Costanzo, M., De Maria, G., Lettera, G., and Natale, C., “A multimodal approach to human safety in collaborative robotic workcells,” *IEEE Trans. Autom. Sci. Eng.*, pp. 1–15, 2021. DOI: [10.1109/TASE.2020.3043286](https://doi.org/10.1109/TASE.2020.3043286).
- [58] Zanchettin, A. M., Ceriani, N. M., Rocco, P., Ding, H., and Matthias, B., “Safety in human-robot collaborative manufacturing environments: Metrics and control,” *IEEE Trans. Autom. Sci. Eng.*, vol. 13, no. 2, pp. 882–893, 2015.
- [59] Ragaglia, M., Zanchettin, A. M., and Rocco, P., “Trajectory generation algorithm for safe human-robot collaboration based on multiple depth sensor measurements,” *Mechatronics*, vol. 55, pp. 267–281, 2018.
- [60] Palleschi, A., Hamad, M., Abdolshah, S., Garabini, M., Haddadin, S., and Pallotino, L., “Fast and safe trajectory planning: Solving the cobot performance/safety trade-off in human-robot shared environments,” *IEEE Robot. Autom. Lett.*, vol. 6, no. 3, pp. 5445–5452, 2021.
- [61] Zhang, S., Zanchettin, A. M., Villa, R., and Dai, S., “Real-time trajectory planning based on joint-decoupled optimization in human-robot interaction,” *Mech. Mach. Theory*, vol. 144, p. 103 664, 2020.
- [62] Weitschat, R. and Aschemann, H., “Safe and efficient human–robot collaboration part ii: Optimal generalized human-in-the-loop real-time motion generation,” *IEEE Robot. Autom. Lett.*, vol. 3, no. 4, pp. 3781–3788, 2018.
- [63] Casalino, A., Bazzi, D., Zanchettin, A. M., and Rocco, P., “Optimal proactive path planning for collaborative robots in industrial contexts,” in *Int. Conf. on Robotics and Automation (ICRA)*, IEEE, 2019, pp. 6540–6546.

- 
- [64] Kanazawa, A., Kinugawa, J., and Kosuge, K., “Adaptive motion planning for a collaborative robot based on prediction uncertainty to enhance human safety and work efficiency,” *IEEE Trans. Robot.*, vol. 35, no. 4, pp. 817–832, 2019.
- [65] Ducaju, J. M. S., Olofsson, B., Robertsson, A., and Johansson, R., “Joint stiction avoidance with null-space motion in real-time model predictive control for redundant collaborative robots,” in *2021 IEEE Int. Conf. on Robot Hum. Interact. Commun. (RO-MAN)*, IEEE, 2021, pp. 307–314.
- [66] Mainprice, J., Hayne, R., and Berenson, D., “Goal set inverse optimal control and iterative replanning for predicting human reaching motions in shared workspaces,” *IEEE Trans. Robot.*, vol. 32, no. 4, pp. 897–908, 2016.
- [67] Cheng, Y., Sun, L., Liu, C., and Tomizuka, M., “Towards efficient human-robot collaboration with robust plan recognition and trajectory prediction,” *IEEE Robot. Autom. Lett.*, vol. 5, no. 2, pp. 2602–2609, 2020.
- [68] Landi, C. T., Cheng, Y., Ferraguti, F., Bonfè, M., Secchi, C., and Tomizuka, M., “Prediction of human arm target for robot reaching movements,” in *IEEE/RSJ Int. Conf. on Intelligent Robots and Systems (IROS)*, 2019.
- [69] Maric, B., Mutka, A., and Orsag, M., “Collaborative human-robot framework for delicate sanding of complex shape surfaces,” *IEEE Robot. Autom. Lett.*, vol. 5, no. 2, pp. 2848–2855, 2020.
- [70] Zhao, X., Fan, T., Li, Y., Zheng, Y., and Pan, J., “An efficient and responsive robot motion controller for safe human-robot collaboration,” *IEEE Robot. Autom. Lett.*, 2021.
- [71] Chen, J. and Song, K., “Collision-free motion planning for human-robot collaborative safety under cartesian constraint,” in *IEEE Int. Conf. on Robotics and Automation (ICRA)*, 2018, pp. 4348–4354. DOI: [10.1109/ICRA.2018.8460185](https://doi.org/10.1109/ICRA.2018.8460185).
- [72] Ji, Z., Liu, Q., Xu, W., *et al.*, “Towards shared autonomy framework for human-aware motion planning in industrial human-robot collaboration,” in *IEEE 16th Int. Conf. on Automation Science and Engineering (CASE)*, 2020, pp. 411–417. DOI: [10.1109/CASE48305.2020.9217003](https://doi.org/10.1109/CASE48305.2020.9217003).
- [73] He, W., Xue, C., Yu, X., Li, Z., and Yang, C., “Admittance-based controller design for physical human–robot interaction in the constrained task space,” *IEEE Trans. Autom. Sci. Eng.*, vol. 17, no. 4, pp. 1937–1949, 2020.
- [74] Besset, P. and Béarée, R., “Fir filter-based online jerk-constrained trajectory generation,” *Control Eng. Pract.*, vol. 66, pp. 169–180, 2017.
- [75] Cherubini, A., Passama, R., Crosnier, A., Lasnier, A., and Fraisse, P., “Collaborative manufacturing with physical human–robot interaction,” *Robot. Comput. Integr. Manuf.*, vol. 40, pp. 1–13, 2016.
- [76] Roveda, L., Iannacci, N., and Tosatti, L. M., “Discrete-time formulation for optimal impact control in interaction tasks,” *J. Intell. Robot. Syst.*, vol. 90, no. 3, pp. 407–417, 2018.
- [77] Kimmel, M. and Hirche, S., “Invariance control for safe human–robot interaction in dynamic environments,” *IEEE Trans. Robot.*, vol. 33, no. 6, pp. 1327–1342, 2017.
- [78] Bednarczyk, M., Omran, H., and Bayle, B., “Model predictive impedance control,” in *Int. Conf. on Robotics and Automation (ICRA)*, IEEE, 2020, pp. 4702–4708.
- [79] Reyes-Uquillas, D. and Hsiao, T., “Safe and intuitive manual guidance of a robot manipulator using adaptive admittance control towards robot agility,” *Robotics Comput. Integr. Manuf.*, vol. 70, p. 102 127, 2021.
- [80] Xiao, J., Dou, S., Zhao, W., and Liu, H., “Sensorless human-robot collaborative assembly considering load and friction compensation,” *IEEE Robot. Autom. Lett.*, 2021.



- 
- [81] Cherubini, A., Passama, R., Fraisse, P., and Crosnier, A., “A unified multimodal control framework for human–robot interaction,” *Rob. Auton. Syst.*, vol. 70, pp. 106–115, 2015.
- [82] Suzuki, K., Mori, H., and Ogata, T., “Compensation for undefined behaviors during robot task execution by switching controllers depending on embedded dynamics in rnn,” *IEEE Robot. Autom. Lett.*, pp. 1–1, 2021. DOI: [10.1109/LRA.2021.3063702](https://doi.org/10.1109/LRA.2021.3063702).
- [83] Chen, S. and Wen, J. T., “Adaptive neural trajectory tracking control for flexible-joint robots with online learning,” in *Int. Conf. on Robotics and Automation (ICRA)*, IEEE, 2020, pp. 2358–2364.
- [84] Cremer, S., Das, S. K., Wijayasinghe, I. B., Popa, D. O., and Lewis, F. L., “Model-free online neuroadaptive controller with intent estimation for physical human–robot interaction,” *IEEE Trans. Robot.*, vol. 36, no. 1, pp. 240–253, 2019.
- [85] Dimeas, F. and Aspragathos, N., “Online stability in human-robot cooperation with admittance control,” *IEEE Trans. Haptics*, vol. 9, no. 2, pp. 267–278, 2016. DOI: [10.1109/TOH.2016.2518670](https://doi.org/10.1109/TOH.2016.2518670).
- [86] Li, S., Li, J., Li, S.-q., and Huang, Z.-l., “Design and implementation of robot serial integrated rotary joint with safety compliance,” *J. Cent. South Univ.*, vol. 24, no. 6, pp. 1307–1321, 2017.
- [87] Sirintuna, D., Aydin, Y., Caldiran, O., Tokatli, O., Patoglu, V., and Basdogan, C., “A variable-fractional order admittance controller for phri,” in *Int. Conf. on Robotics and Automation (ICRA)*, IEEE, 2020, pp. 10 162–10 168.
- [88] Raiola, G., Cardenas, C. A., Tadele, T. S., De Vries, T., and Stramigioli, S., “Development of a safety-and energy-aware impedance controller for collaborative robots,” *IEEE Robot. Autom. Lett.*, vol. 3, no. 2, pp. 1237–1244, 2018.
- [89] El Makrini, I., Rodriguez-Guerrero, C., Lefeber, D., and Vanderborght, B., “The variable boundary layer sliding mode control: A safe and performant control for compliant joint manipulators,” *IEEE Robot. Autom. Lett.*, vol. 2, no. 1, pp. 187–192, 2016.
- [90] Solanes, J. E., Gracia, L., Munoz-Benavent, P., Miro, J. V., Carmichael, M. G., and Tornero, J., “Human–robot collaboration for safe object transportation using force feedback,” *Rob. Auton. Syst.*, vol. 107, pp. 196–208, 2018.
- [91] Liu, X., Ge, S. S., Zhao, F., and Mei, X., “A dynamic behavior control framework for physical human-robot interaction,” *J. Intell. Robot. Syst.*, vol. 101, no. 1, pp. 1–18, 2021.
- [92] Fu, L. and Zhao, J., “Maxwell-model-based compliance control for human–robot friendly interaction,” *IEEE Trans. Cogn. Devel. Syst.*, vol. 13, no. 1, pp. 118–131, 2021. DOI: [10.1109/TCDS.2020.2992538](https://doi.org/10.1109/TCDS.2020.2992538).
- [93] Maurice, P., Huber, M. E., Hogan, N., and Sternad, D., “Velocity-curvature patterns limit human–robot physical interaction,” *IEEE Robot. Autom. Lett.*, vol. 3, no. 1, pp. 249–256, 2017.
- [94] Raessa, M., Chen, J. C. Y., Wan, W., and Harada, K., “Human-in-the-loop robotic manipulation planning for collaborative assembly,” *IEEE Trans. Autom. Sci. Eng.*, vol. 17, no. 4, pp. 1800–1813, 2020.
- [95] Rojas, R. A., Garcia, M. A. R., Wehrle, E., and Vidoni, R., “A variational approach to minimum-jerk trajectories for psychological safety in collaborative assembly stations,” *IEEE Robot. Autom. Lett.*, vol. 4, no. 2, pp. 823–829, 2019. DOI: [10.1109/LRA.2019.2893018](https://doi.org/10.1109/LRA.2019.2893018).
- [96] Rojas, R. A. and Vidoni, R., “Designing fast and smooth trajectories in collaborative workstations,” *IEEE Robot. Autom. Lett.*, vol. 6, no. 2, pp. 1700–1706, 2021. DOI: [10.1109/LRA.2021.3058916](https://doi.org/10.1109/LRA.2021.3058916).

- 
- [97] Pearce, M., Mutlu, B., Shah, J., and Radwin, R., “Optimizing makespan and ergonomics in integrating collaborative robots into manufacturing processes,” *IEEE Trans. Autom. Sci. Eng.*, vol. 15, no. 4, pp. 1772–1784, 2018.
- [98] Maderna, R., Poggiali, M., Zanchettin, A. M., and Rocco, P., “An online scheduling algorithm for human-robot collaborative kitting,” in *Int. Conf. on Robotics and Automation (ICRA)*, IEEE, 2020, pp. 11 430–11 435.
- [99] Hu, B. and Chen, J., “Optimal task allocation for human–machine collaborative manufacturing systems,” *IEEE Robot. Autom. Lett.*, vol. 2, no. 4, pp. 1933–1940, 2017.
- [100] Faber, M., Mertens, A., and Schlick, C. M., “Cognition-enhanced assembly sequence planning for ergonomic and productive human–robot collaboration in self-optimizing assembly cells,” *Prod. Eng.*, vol. 11, no. 2, pp. 145–154, 2017.
- [101] Rahman, S. M. and Wang, Y., “Mutual trust-based subtask allocation for human–robot collaboration in flexible lightweight assembly in manufacturing,” *Mechatronics*, vol. 54, pp. 94–109, 2018.
- [102] Jiang, L. and Wang, Y., “A personalized computational model for human-like automated decision-making,” *IEEE Trans. Autom. Sci. Eng.*, 2021.
- [103] Medina, J. R., Lorenz, T., and Hirche, S., “Synthesizing anticipatory haptic assistance considering human behavior uncertainty,” *IEEE Trans. Robot.*, vol. 31, no. 1, pp. 180–190, 2015.
- [104] Jaberzadeh Ansari, R. and Karayiannidis, Y., “Task-based role adaptation for human-robot cooperative object handling,” *IEEE Robot. Autom. Lett.*, pp. 1–1, 2021. DOI: [10.1109/LRA.2021.3064498](https://doi.org/10.1109/LRA.2021.3064498).
- [105] Peternel, L., Kim, W., Babič, J., and Ajoudani, A., “Towards ergonomic control of human-robot co-manipulation and handover,” in *Int. Conf. on Humanoid Robotics (Humanoids)*, IEEE, 2017, pp. 55–60.
- [106] Kim, W., Peternel, L., Lorenzini, M., Babič, J., and Ajoudani, A., “A human-robot collaboration framework for improving ergonomics during dexterous operation of power tools,” *Robotics Comput. Integ. Manuf.*, vol. 68, p. 102 084, 2021.
- [107] Sadrfaridpour, B. and Wang, Y., “Collaborative assembly in hybrid manufacturing cells: An integrated framework for human–robot interaction,” *IEEE Trans. Autom. Sci. Eng.*, vol. 15, no. 3, pp. 1178–1192, 2018. DOI: [10.1109/TASE.2017.2748386](https://doi.org/10.1109/TASE.2017.2748386).
- [108] Messeri, C., Masotti, G., Zanchettin, A. M., and Rocco, P., “Human-robot collaboration: Optimizing stress and productivity based on game theory,” *IEEE Robot. Autom. Lett.*, 2021.
- [109] Rahman, S., “Machine learning-based cognitive position and force controls for power-assisted human–robot collaborative manipulation,” *Machines*, vol. 9, no. 2, p. 28, 2021.
- [110] Oliff, H., Liu, Y., Kumar, M., and Williams, M., “Improving human–robot interaction utilizing learning and intelligence: A human factors-based approach,” *IEEE Trans. Autom. Sci. Eng.*, vol. 17, no. 3, pp. 1597–1610, 2020.
- [111] Shen, Z., Elibol, A., and Chong, N. Y., “Understanding nonverbal communication cues of human personality traits in human-robot interaction,” *IEEE/CAA J. Autom. Sin.*, vol. 7, no. 6, pp. 1465–1477, 2020.
- [112] Modares, H., Ranatunga, I., Lewis, F. L., and Popa, D. O., “Optimized assistive human–robot interaction using reinforcement learning,” *IEEE Trans. Cybern.*, vol. 46, no. 3, pp. 655–667, 2015.
- [113] Tang, G. and Webb, P., “The design and evaluation of an ergonomic contactless gesture control system for industrial robots,” *J. Robot.*, vol. 2018, 2018.



- [114] Zanchettin, A. M., Lotano, E., and Rocco, P., “Collaborative robot assistant for the ergonomic manipulation of cumbersome objects,” in *IEEE/RSJ Int. Conf. on Intelligent Robots and Systems (IROS)*, IEEE, 2019, pp. 6729–6734.
- [115] Yao, B., Zhou, Z., Wang, L., Xu, W., Liu, Q., and Liu, A., “Sensorless and adaptive admittance control of industrial robot in physical human-robot interaction,” *Robotics Comput. Integ. Manuf.*, vol. 51, pp. 158–168, 2018.
- [116] Shah, J. A., “Fluid coordination of human-robot teams,” Ph.D. dissertation, Massachusetts Institute of Technology, 2011.
- [117] Stouraitis, T., Chatzinikolaidis, I., Gienger, M., and Vijayakumar, S., “Online hybrid motion planning for dyadic collaborative manipulation via bilevel optimization,” *IEEE Trans. Robot.*, vol. 36, no. 5, pp. 1452–1471, 2020.
- [118] Balatti, P., Fusaro, F., Villa, N., Lamon, E., and Ajoudani, A., “A collaborative robotic approach to autonomous pallet jack transportation and positioning,” *IEEE Access*, vol. 8, pp. 142 191–142 204, 2020.
- [119] Wu, Y., Lamon, E., Zhao, F., Kim, W., and Ajoudani, A., “A unified approach for hybrid motion control of moca based on weighted whole-body cartesian impedance formulation,” *IEEE Robot. Autom. Lett.*, pp. 1–1, 2021. DOI: [10.1109/LRA.2021.3062316](https://doi.org/10.1109/LRA.2021.3062316).
- [120] Li, R., Pham, D. T., Huang, J., *et al.*, “Unfastening of hexagonal headed screws by a collaborative robot,” *IEEE Trans. Autom. Sci. Eng.*, vol. 17, no. 3, pp. 1455–1468, 2020.
- [121] Yu, T., Huang, J., and Chang, Q., “Mastering the working sequence in human-robot collaborative assembly based on reinforcement learning,” *IEEE Access*, vol. 8, pp. 163 868–163 877, 2020.
- [122] Johannsmeier, L. and Haddadin, S., “A hierarchical human-robot interaction-planning framework for task allocation in collaborative industrial assembly processes,” *IEEE Robot. Autom. Lett.*, vol. 2, no. 1, pp. 41–48, 2016.
- [123] Casalino, A., Zanchettin, A. M., Piroddi, L., and Rocco, P., “Optimal scheduling of human-robot collaborative assembly operations with time petri nets,” *IEEE Trans. Autom. Sci. Eng.*, vol. 18, no. 1, pp. 70–84, 2021. DOI: [10.1109/TASE.2019.2932150](https://doi.org/10.1109/TASE.2019.2932150).
- [124] Zanchettin, A. M., “Robust scheduling and dispatching rules for high-mix collaborative manufacturing systems,” *Flex. Serv. Manuf. J.*, pp. 1–24, 2021.
- [125] Michalos, G., Spiliotopoulos, J., Makris, S., and Chryssolouris, G., “A method for planning human robot shared tasks,” *CIRP J. Manuf. Sci. Technol.*, vol. 22, pp. 76–90, 2018.
- [126] Tsarouchi, P., Matthaiakis, A.-S., Makris, S., and Chryssolouris, G., “On a human-robot collaboration in an assembly cell,” *Int. J. Comput. Integr. Manuf.*, vol. 30, no. 6, pp. 580–589, 2017.
- [127] Xu, W., Tang, Q., Liu, J., Liu, Z., Zhou, Z., and Pham, D. T., “Disassembly sequence planning using discrete bees algorithm for human-robot collaboration in remanufacturing,” *Robotics Comput. Integ. Manuf.*, vol. 62, p. 101 860, 2020.
- [128] Cheng, Y., Sun, L., and Tomizuka, M., “Human-aware robot task planning based on a hierarchical task model,” *IEEE Robot. Autom. Lett.*, vol. 6, no. 2, pp. 1136–1143, 2021. DOI: [10.1109/LRA.2021.3056370](https://doi.org/10.1109/LRA.2021.3056370).
- [129] Wang, Q., Jiao, W., Wang, P., and Zhang, Y., “Digital twin for human-robot interactive welding and welder behavior analysis,” *IEEE/CAA J. Autom. Sin.*, vol. 8, no. 2, pp. 334–343, 2020.
- [130] Bilberg, A. and Malik, A. A., “Digital twin driven human-robot collaborative assembly,” *CIRP Annals*, vol. 68, no. 1, pp. 499–502, 2019.
- [131] Lv, Q., Zhang, R., Sun, X., Lu, Y., and Bao, J., “A digital twin-driven human-robot collaborative assembly approach in the wake of covid-19,” *J. Manuf. Syst.*, 2021.

- 
- [132] Aydin, Y., Tokatli, O., Patoglu, V., and Basdogan, C., “A computational multicriteria optimization approach to controller design for physical human-robot interaction,” *IEEE Trans. Robot.*, vol. 36, no. 6, pp. 1791–1804, 2020.
- [133] Li, Z., Liu, J., Huang, Z., Peng, Y., Pu, H., and Ding, L., “Adaptive impedance control of human-robot cooperation using reinforcement learning,” *IEEE Trans. Ind. Electron.*, vol. 64, no. 10, pp. 8013–8022, 2017.
- [134] Darvish, K., Simetti, E., Mastrogiovanni, F., and Casalino, G., “A hierarchical architecture for human-robot cooperation processes,” *IEEE Trans. Robot.*, vol. 37, no. 2, pp. 567–586, 2020.
- [135] Noohi, E., Žefran, M., and Patton, J. L., “A model for human-human collaborative object manipulation and its application to human-robot interaction,” *IEEE Trans. Robot.*, vol. 32, no. 4, pp. 880–896, 2016.
- [136] Zeng, F., Xiao, J., and Liu, H., “Force/torque sensorless compliant control strategy for assembly tasks using a 6-dof collaborative robot,” *IEEE Access*, vol. 7, pp. 108 795–108 805, 2019.
- [137] Roveda, L., Magni, M., Cantoni, M., Piga, D., and Bucca, G., “Human-robot collaboration in sensorless assembly task learning enhanced by uncertainties adaptation via bayesian optimization,” *Rob. Auton. Syst.*, vol. 136, p. 103 711, 2021.
- [138] Polverini, M. P., Zanchettin, A. M., and Rocco, P., “A constraint-based programming approach for robotic assembly skills implementation,” *Robot. Comput. Integr. Manuf.*, vol. 59, pp. 69–81, 2019.
- [139] Lamon, E., Leonori, M., Kim, W., and Ajoudani, A., “Towards an intelligent collaborative robotic system for mixed case palletizing,” in *IEEE Int. Conf. on Robotics and Automation (ICRA)*, 2020, pp. 9128–9134. DOI: [10.1109/ICRA40945.2020.9196850](https://doi.org/10.1109/ICRA40945.2020.9196850).
- [140] Al-Yacoub, A., Zhao, Y., Eaton, W., Goh, Y., and Lohse, N., “Improving human robot collaboration through force/torque based learning for object manipulation,” *Robot. Comput. Integr. Manuf.*, vol. 69, p. 102 111, 2021.
- [141] Ghadirzadeh, A., Chen, X., Yin, W., Yi, Z., Bjorkman, M., and Kragic, D., “Human-centered collaborative robots with deep reinforcement learning,” *IEEE Robot. Autom. Lett.*, 2020.
- [142] Whitsell, B. and Artemiadis, P., “Physical human-robot interaction (phri) in 6 dof with asymmetric cooperation,” *IEEE Access*, vol. 5, pp. 10 834–10 845, 2017.
- [143] *ABB Robotics website*, <https://new.abb.com/products/robotics>, Accessed: 2021-07-29.
- [144] *Universal Robots Support website*, <https://www.universal-robots.com/articles/>, Accessed: 2021-12-01.
- [145] *Rethink Robotics website*, <https://www.rethinkrobotics.com/>, Accessed: 2021-07-29.
- [146] *Omron website*, <https://automation.omron.com/en/us/>, Accessed: 2021-07-29.

## Chapter 3

# A Multi-objective Optimization Approach for Trajectory Planning in a Safe and Ergonomic Human-Robot Collaboration



### Abstract

The demand for safe and ergonomic workplaces is rapidly growing in modern industrial scenarios, especially for companies that intensely rely on *human-robot collaboration* (HRC). This work focuses on optimizing the trajectory of the end-effector of a cobot arm in a collaborative industrial environment, ensuring the maximization of the operator's safety and ergonomics without sacrificing production efficiency requirements. Hence, a multi-objective optimization strategy for trajectory planning in a safe and ergonomic HRC is defined. This approach aims at finding the best trade-off between the total traversal time of the cobot's end-effector trajectory and ergonomics for the human worker, while respecting in the kinematic constraint of the optimization problem the ISO safety requirements through the well-known *speed and separation monitoring* (SSM) methodology. Guaranteeing an ergonomic HRC means reducing musculoskeletal disorders linked to risky and highly repetitive activities. The three main phases of the proposed technique are described as follows. First, a manikin designed using a dedicated software is employed to evaluate the *rapid upper limb assessment* (RULA) ergonomic index in the working area. Next, a second-order cone programming problem is defined to represent a time-optimal safety compliant trajectory planning problem. Finally, the trajectory that ensures the best compromise between these two opposing goals –minimizing the task's traversal time and maintaining a high level of ergonomics for the human worker– is computed by defining and solving a multi-objective control problem. The method is tested on an experimental case study in reference to an assembly task and the obtained results are discussed, showing the effectiveness of the proposed approach.

### 3.1 Introduction

*Human-robot collaboration* (HRC) is widely recognized as the essential enabling technology of the fourth industrial revolution, also known as Industry 4.0, and as one of the foundation stones of the upcoming Industry 5.0. HRC can improve manufacturing processes, increasing productivity and profitability and, then, leading to prominent positions in the current hyper-competitive industrial scenario.

The goal of the latest collaborative robots, the so-called cobots, is to allow humans and robots to work together in the same industrial environment without compromising the health and safety of workers [1]–[3]. In the cobot's design, safety is guaranteed by a large number of proprioceptive and exteroceptive sensors positioned ad hoc to control all movements relative to both internal and external states and by limitations on speed and force that are taken into consideration by the International Standards Organization (ISO) requirements –i.e., *speed and separation monitoring* (SSM) and *power and force limiting* (PFL). In the industrial setting, physical and cognitive ergonomics are additional crucial factors to be considered in order to prevent injuries, associated with highly repetitive and dangerous tasks, and to minimize mental stress and psychological discomfort, which could be experienced by operators sharing their working space with cobots.

**Table 3.1:** Summary of works related to the trajectory planning optimization problem.

Publication	Optimization target	Resolution method
Industrial robot applications		
[9]	time	direct transcription
[10]	time	indirect
[11]	time	indirect
[12]	time	dynamic programming
[13]	time	dynamic programming
[14]	time	direct transcription
[15]	time	direct transcription
[16]	time	direct transcription
[17]	time-energy	direct transcription
Cobot applications		
[18]	time-safety	direct transcription
[19]	safety-ergonomics	not specified
proposed approach	time-safety-ergonomics	direct transcription

The implementation of comprehensive analyses to evaluate risk factors for human operators and the development of consequent risk reduction strategies are nowadays necessary, due to the rapid increase of work-related musculoskeletal disorders, which are affecting approximately 50% of human workers in industrialized countries. As an example, the HRC designs can incorporate the evaluation of the well-known *rapid upper limb assessment* (RULA) [4], [5] and *rapid entire body assessment* (REBA) [6] indices to determine the exposure of employees to ergonomic risk factors.

A key factor for an efficient and ergonomic HRC is the development of a systematic procedure that allows the simultaneous optimization of the human worker’s well-being and industrial process productivity. Therefore, the aim of this work is to deal with the three pivotal goals of the trajectory planning for a cobot arm in a manufacturing environment, i.e., safety, ergonomics, and efficiency [7], [8]. In particular, the objective is to ensure the best compromise between the traversal time of the trajectory for the cobot and ergonomics for the human worker, while guaranteeing the SSM ISO safety requirement.

The remainder of this chapter is structured as follows. Section 3.2 sheds light on the main contributions of this work, positioning them with respect to the related literature. Section 3.3 delineates the structure of the optimization problem, and in particular the procedure for evaluating the operator’s ergonomic posture (Section 3.3.1), the speed and separation monitoring requirement (Section 3.3.2), and the time-optimal trajectory planning along a predefined path while ensuring ISO safety requirements (Section 3.3.3), and the mathematical formulation of the multi-objective optimization (MOO) approach (Section 3.3.4). The case study with the experimental setup and results are discussed in Section 3.4. Finally, concluding remarks and future developments are reported in Section 3.5.

## 3.2 Related Works and Contributions

Despite the growing amount of papers on HRC, comprehensive literature reviews on the related feedback control problems [8], [20], [21] highlight that only a small percentage of works aims at simultaneously optimizing multiple control targets, such as time, energy, and efficiency. Furthermore, to the best of the authors’ knowledge, all scientific contributions addressing the trajectory planning problem for collaborative robots do not aim at simultaneously fulfilling time, safety, and ergonomics requirements, as summarized in Table 3.1. Therefore, the goal and innovation of this work is to develop a novel approach to fill this gap in the HRC control field.

In the scientific and industrial sectors the trajectory planning of robot arms is a well-known and largely discussed topic. Due to the advantages it provides, as well as its issues with the simultaneous optimization of the time interval required to complete the task and of the smoothness of the trajectory execution by the manipulator, time-optimal trajectory planning emerges as an ongoing and complicated research challenge [9]. From the analysis of the related works in the literature, it emerges that the problem of planning a time-optimal motion along a predefined path is mainly performed for

traditional industrial robots (see Table 3.1). The time-optimal trajectory planning is eventually extended to a multi-objective optimization problem by combining time and energy optimization. Still, the majority of works are related to industrial robots, whose main aim is to remove humans from hazardous, hard and dirty jobs in industry. In this context, the available contributions can be classified into three categories, based on the programming methodology used to solve the optimization problem, i.e., indirect methods, dynamic programming methods, and direct transcription methods (see Table 3.1 - column III). The indirect methods [10], [11] are more precise than the other two methods, but they are difficult to implement, since they find the numerical solution through a procedure based on “forward” and “backward” integrations and require the implementation of a certain number of steps, which need the choice of tolerance and stop criteria. An alternative approach is represented by dynamic programming methods [12], [13], based on the principle of the mathematician Richard Bellman, that simplifies a trajectory planning problem by decomposing it into simpler sub-problems in a recursive manner. The third category consists of the direct transcription methods, used in [9], [14]–[18], that are even less precise, but are easier to implement, being based on the resolution of non linear systems, which can be solved by ad hoc "solvers" that compute the solution to the problem in a short time and efficiently.

Only recently, due to the advances in industrial automation introduced by the Industry 4.0 key enabling technologies [22], [23], the scientific community has focused on collaborative robotics and dedicated efforts to the related trajectory planning problem. However, although time and safety are critical HRC requirements, to the best of our knowledge, only one work [18] proposes a trajectory planning algorithm to plan fast and safe motions for cobots. In particular, in [18], the time-optimal planning is combined with a safety evaluation module for collaborative robots in shared environments.

Finally, also ergonomics is barely considered in HRC control targets. Indeed, one of the few works considering safety and ergonomics but not time for industrial co-manipulators is the article [19] by Ferraguti *et al.*, as the control architecture incorporates two working modes, an ergonomic planner and an admittance controller that can be initialized in a mutually exclusive manner.

With the aim of filling the discussed gaps, this work, which comes as an extension of the article [24], proposes a novel methodology for the trajectory planning of a cobot arm that aims at simultaneously optimizing time and ergonomics, while guaranteeing safety for the human worker through the SSM ISO requirement. First, we propose a time-optimal trajectory planning problem that integrates the SSM safety requirements in accordance with the ISO/TS 15066 standards [25]. Unlike our previous work [24], the proposed approach integrates the SSM into the kinematic constraint of the optimization problem, limiting the speed of the robot’s end-effector. This innovation, along with the technical limits on joint speed and acceleration described in [24], allows reducing the risk of injury as specified in the ISO technical specification for collaborative robots. Consequently, our approach enhances the overall operator safety and improves the capabilities of the control system. The time-optimal trajectory planning task is then solved using a direct transcription method, transforming the initial non linear and non convex optimal control problem into a convex optimization problem in *second-order cone programming* (SOCP) form [16]. This ensures the existence and uniqueness of a solution to the problem. Additionally, to ensure ergonomic collaboration, reduce operator fatigue, increase comfort, and boost productivity, we define a systematic procedure for evaluating the RULA index in the whole collaborative working space [4], [5]. Finally, by solving a multi-objective control problem, we determine a trajectory that strikes the best balance between minimizing task traversal time and maintaining a high level of ergonomics for the human operator. Differently from [24], we perform a sensitivity analysis to assess the uncertainty associated with the non-optimal positioning of the cobot’s end-effector, using the results obtained from the *multi-objective optimization* (MOO) problem. We remark that, to the best of our knowledge, there is no paper in the literature that simultaneously addresses the trajectory planning problem considering efficiency and safety while also ensuring a comfortable and ergonomic working environment for human operators.

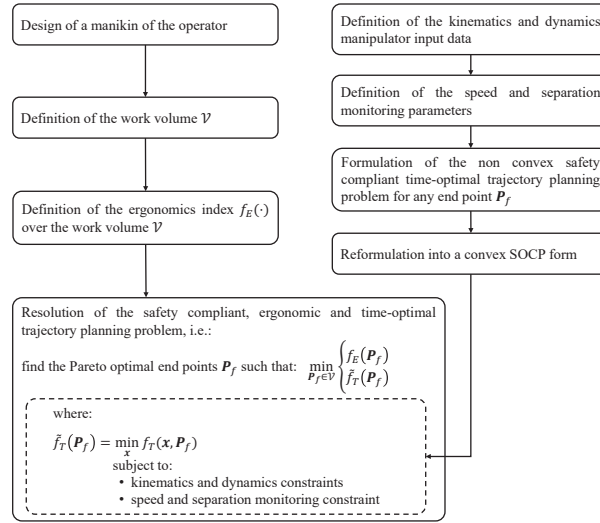


Figure 3.1: Overview diagram of the proposed methodology.

The method proposed in this work has a number of potential applications in the context of Industry 4.0. In particular, the approach can be employed in tasks where high precision is needed, ranging from pick and place to accurate assembly (e.g., screw driving, nut driving, part fitting), material removal, or any other specific application that can be associated with the “3D” (Dull, Dirty, Dangerous). An experimental case study is analyzed to verify the effectiveness of the suggested approach in one of the aforementioned industrial scenarios.

### 3.3 Proposed Methodology

The main objective of this work is to ergonomically optimize the posture for the operator and satisfy the SSM ISO safety requirement during the trajectory planning of the task to be performed by the cobot in the shortest possible time.

In particular, the considered industrial scenario examines the collaboration in a shared workspace between a human operator and a cobot that moves with its end-effector a work-piece on which the human is expected to complete some operations. All the tasks performed by the cobot must take into account the safety of the human operator. The cobot follows a trajectory that minimizes the time required to move the object from a fixed starting point to an end point that is ergonomically optimal for the operator, with the aim of reducing the musculoskeletal disorders that may arise, especially in highly repetitive tasks.

Figure 3.1 summarizes all the steps of the proposed methodology. The formulation of the multi-objective control problem (bottom of the diagram) – aimed at finding the best compromise between the ergonomics for the human worker and the traversal time of the trajectory for the cobot, while guaranteeing the SSM ISO safety requirement inside the kinematic constraint (see Section 3.3.4) and thus, at allowing the offline solution of the trajectory planning problem – relies on some preliminary steps related to the evaluation of ergonomics, and to the formulation of the time-optimal safety compliant trajectory planning along a predefined path. On the one hand, a three-step systematic procedure (described in the three blocks on the top-left of the diagram) is conducted with the aim of determining the level of ergonomics in terms of RULA index (denoted as  $f_E(\mathbf{P}_f)$  as detailed in the sequel) for a set of potential end points (denoted as  $\mathbf{P}_f$  as detailed in the sequel) of the planned cobot’s trajectory (see Section 3.3.1). On the other hand, for any end point, the time-optimal safety compliant trajectory planning problem is converted into a SOCP problem following the steps illustrated in the top-right of the diagram. The first preliminary step consists in generating the path and defining



the kinematics and dynamics manipulator input data, i.e., the starting and ending pose, the Denavit-Hartenberg parameters, and the kinematic and dynamics indicators. In the second step, the speed and separation monitoring parameters (see Section 3.3.2) are defined in order to be included in the kinematic constraint. Then, the non convex time-optimal safety compliant trajectory planning problem is formulated by defining the objective function and the kinematic and dynamic constraints. Finally, by performing the convex relaxation, such problem is discretized and transformed into a convex optimization problem in SOCP form (see Section 3.3.3), whose resolution consists in optimizing one of the objective functions (denoted as  $\tilde{f}_T(\mathbf{P}_f)$  as detailed in the sequel) of the MOO problem (dashed block at the bottom of the diagram).

### 3.3.1 Evaluation of Ergonomics in HRC

In this section, we present the specific procedure to determine the ergonomics' level. This novel procedure is based on three steps and employs the RULA index to classify the set of potential end points of the planned cobot's trajectory.

Different criteria, including the RULA, *rapid entire body assessment* (REBA), *postural loading on the upper body assessment* (LUBA), and *occupational repetitive action* (OCRA) are nowadays employed in the related literature to estimate the ergonomics of a given posture [26]. We employ the RULA index as a means of assessing the ergonomic posture of the operator as we are interested in reducing upper limb disorders in the investigated industrial setting. Nevertheless, the procedure described in the sequel is still valid replacing the RULA with other evaluation indicators.

The RULA index is calculated by analyzing postures, repetitiveness of movements, applied strength, and static musculoskeletal activity. To this aim, each of the main body areas —arm, forearm, wrist, neck, and trunk— receives a score. Each RULA score corresponds to a degree of risk exposure ranging from 0 (representing a minimal risk requiring no special countermeasure) to 6 (corresponding to high risk). Note that one RULA test can only measure the effort made by the right or left side of the body.

Ad hoc computer-aided design and engineering software, such as CATIA [27] or Process Simulate (Siemens) [28], can be used to evaluate ergonomics of human operators in generic workspaces. With the help of these tools, it is possible to easily design virtual manikins that represent the operator and consequently simulate any possible working condition in a given work volume.

The first step of the proposed systematic procedure is therefore the design of a virtual manikin in the selected tool to assess the operator's ergonomic posture. During this phase, a number of different features can be given in the manikin configuration, such as gender, percentile applied to the stature (height), weight, and any other anthropometric factors determined in accordance with the selected reference population. Note that during the characterization of the manikin it is convenient to place its initial reference point between its feet.

The second step of the procedure is the definition of a work volume  $\mathcal{V} \subseteq \mathbb{R}^3$ , whose dimensions depend on the characteristics of the manikin generated in the previous phase. The work volume is made of a set of points  $\mathbf{P}_f \in \mathcal{V}$  that the manikin arm is able to reach and that coincides with all the endpoints of the trajectory that the end-effector can follow.

Then, in the third step of the procedure the ergonomics function  $f_E(\mathbf{P}_f)$ , i.e., the function that estimates ergonomics in terms of RULA for each candidate point  $\mathbf{P}_f \in \mathcal{V}$ , is determined with a *design of experiments* (DOE). For each candidate point, the RULA is estimated considering that the manikin simulates an operator standing and handling a tool in a posture that allows to reach the candidate point.

As previously mentioned, the RULA index allows the evaluation of the ergonomic posture with regard to just one side of the body. Hence, for a right-handed person, the RULA analysis must be carried out on the right side, and for a left-handed person, on the left side. It is important to note that the previously defined work volume will be mirrored around the mid-sagittal plane of the body for a left-handed person. Additionally, the frequency at which the operation is performed as well as the load of the manipulated



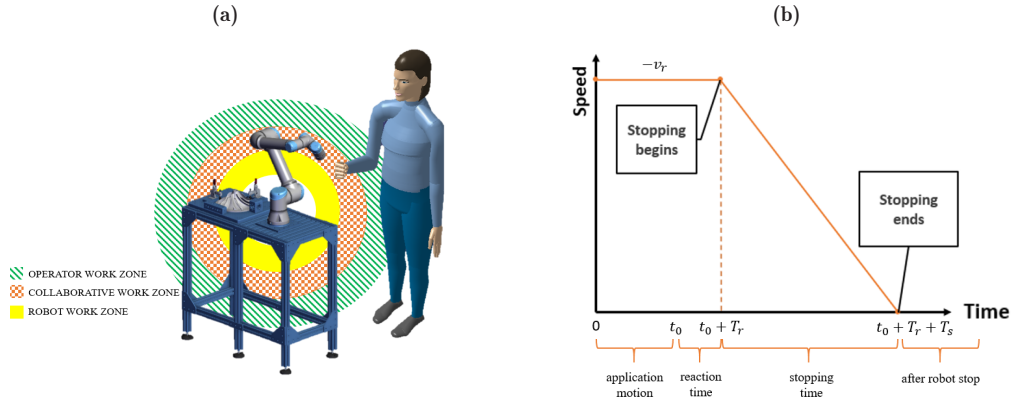


**Figure 3.2:** Scheme of the SSM criterion with the operator (green), collaborative (orange), and robot (yellow) working zones (a). Profile of the robot speed during the task execution (b).

item must be specified during the evaluation of the RULA index. It is evident that the RULA score grows when task repetition and load increase.

### 3.3.2 Speed and Separation Monitoring Requirement

HRC is leaving behind the traditional paradigm of robots living in separate safety cages, allowing human operators to work side-by-side with “fenceless” robots for completing an increasing number of complex industrial tasks. Consequently, the safety of human operators is nowadays understood as a fundamental requirement in collaborative robotic applications.

In the related literature, several control algorithms have been implemented to safely guide a robot during the execution of its tasks. These approaches avoid dangerous situations by defining safety regions, that the robot cannot access, or by dynamically tracking the separation distance between the robot and other obstacles, such as human operators [8].

According to the ISO/TS 15066 standards, safety can be guaranteed by limiting the maximum permissible forces or torques and consequently the energy transfer on potential direct physical contact between the operator and the robot, i.e., PFL, or by prescribing that the speed must be related to a certain separation distance between the human and the robot, i.e., SSM. In the current work, we assume that no undesired contact must happen between the operator and the cobot arm. Thus, during the collaboration, the SSM ISO safety requirement is chosen to help safeguard the operator by allowing the robot actuation system to have the deceleration capability necessary to achieve a complete stop before eventually coming in contact with the operator [29], [30].

With the aim of preserving a safe separation distance between the operator and the cobot arm, the SSM method monitors the regions surrounding the robot, and issues a command to slow or stop the robot as the human operator approaches. This method is based on the continuous measurement of the distance between the robot and a detected operator (i.e., the human-robot separation distance), which is compared with the so-called authorized (operator protective) distance [31], [32]. Hence, when the separation distance is lower than the authorized distance, and consequently when the cobot arm enters the collaborative working zone (Fig. 3.2a), the SSM system decreases the robot’s speed, initiating a safety-rated controlled stop to avoid an impact with the operator (Fig. 3.2b). The robot may then resume its motion once the separation distance is greater than the authorized distance.

More in detail, the minimum allowable human-robot distance  $S$  at a given time  $t_0$  is computed by using the equation prescribed in ISO/TS 15066 [25], that is:

$$S(t_0) = S_h + S_r + S_s + C + Z_d + Z_r \quad (3.1)$$

where  $S_h$  and  $S_r$  indicate the operator's and robot's change in location, respectively, and  $S_s$  is the maximum stopping distance of the robot. The remaining terms of (3.1) capture the uncertainty of measurements, being  $C$  an intrusion distance safety margin based on the expected human reach and  $Z_d + Z_r$  the position uncertainty for both the robot and operator.

Equation (3.1) can be reformulated under static conditions, i.e., assuming a constant speed of the robot, as follows:

$$S(t_0) = (v_h(t_0)T_r + v_h(t_0)T_s) + v_r T_r + B + C + Z_d + Z_r \quad (3.2)$$

where  $v_h(t_0)$  indicates the speed of the operator (i.e., the rate of the operator's motion toward the robot),  $v_r$  is the speed of the robot directed towards the operator in the collaborative work zone,  $T_r$  represents the time for the robot system to respond to the operator's presence, including the time required to detect the position of the operator, process this signal, and activate the robot's stop, and finally  $T_s$  is the time to safely stop the motion of the robot. Note that  $T_s$  is a function of the robotic system configuration, planned movement, speed, and load, while parameter  $B$  denotes the braking distance traveled by the cobot arm.

In particular, since in our work the operator is in a fixed standing position,  $v_h$  is equal to zero as well as parameter  $C$  and uncertainties  $Z_d + Z_r$ . Hence, given our assumptions, (3.2) may be rewritten as:

$$S(t_0) = v_r T_r + B \quad (3.3)$$

where parameter  $B$  is computed as  $v_r^2/2a_r$  with  $a_r$  being the worst-case deceleration value of the robot during the stopping procedure. In Fig. 3.2b, we report the profile of the robot's speed  $v_r$  as a function of time, which drops abruptly once the robot enters into the collaborative work zone.

With the aim of controlling the robot's speed, the SSM criterion is applied in the kinematic constraint of the time-optimal safety compliant trajectory planning along a predefined path problem (see Section 3.3.3). In particular, being the human-robot distance  $S(t_0)$  known at each given time, in (3.3) the allowed speed  $v_r$  is treated as an unknown. From the resolution of the second degree equation (3.3) with respect to  $v_r$  we get two speed values, one of which is positive and one negative. Among these two solutions, we disregard the negative one having no physical meaning while we employ the positive speed value  $\bar{v}_r$  as the upper limit of the kinematic constraint as follows:

$$v_r \leq \bar{v}_r. \quad (3.4)$$

### 3.3.3 Time-Optimal Safety Compliant Trajectory Planning along a Predefined Path

In this section we formulate the problem of planning the trajectory of the cobot, aiming at minimizing the traversal time, from a fixed starting point  $\mathbf{P}_i \in \mathbb{R}^3$  to a given ergonomically optimal end point  $\mathbf{P}_f \in \mathcal{V} \subseteq \mathbb{R}^3$ . We specifically assume that the end-effector of the cobot must follow a geometrical rectilinear path between these two points while satisfying the SSM requirement inside the kinematic constraint and the imposed kinematic and dynamic joint's limits.

Without loss of generality, we assume that the trajectory starts at time  $t = 0$  in  $\mathbf{P}_i$  and ends at time  $t = T$  in  $\mathbf{P}_f$ . Hence, by defining the time-dependent scalar path coordinate  $s(t)$ , we have that  $s(0) = 0 \leq s(t) \leq 1 = s(T)$ . For the sake of notation clarity, we omit the time dependency of  $s$  and its derivatives in the rest of this manuscript.

As the aforementioned geometric path is given in the operational spatial coordinates, let us employ the kinematic inversion to obtain the path in joint space coordinates. More in detail, we consider a generic  $n$ -DOF (degree of freedom) robotic manipulator, that can be represented by its configuration, i.e., the angular position of its  $n$  joints  $\mathbf{q} \in \mathbb{R}^n$ . The goal of the inverse kinematic is therefore to define a map that, given the scalar time

dependent path coordinate  $s(t)$ , calculates the related path in joint space coordinates  $\mathbf{q}(s) \in \mathbb{R}^n$ .

By following the procedures outlined in [17], the joint velocities and accelerations for the given path  $\mathbf{q}(s)$  can be expressed using the chain rule as follows:

$$\dot{\mathbf{q}} = \mathbf{q}'(s)\dot{s} \quad (3.5)$$

$$\ddot{\mathbf{q}} = \mathbf{q}'(s)\ddot{s} + \mathbf{q}''(s)\dot{s}^2 \quad (3.6)$$

where  $\mathbf{q}'(s) = \frac{\delta \mathbf{q}(s)}{\delta s}$  and  $\mathbf{q}''(s) = \frac{\delta^2 \mathbf{q}(s)}{\delta s^2}$  represent the first and second partial derivatives of the geometric path  $\mathbf{q}(s)$  with respect to parameter  $s$ , whereas  $\dot{s} = \frac{\delta s}{\delta t}$  and  $\ddot{s} = \frac{\delta^2 s}{\delta t^2}$  represent the pseudo-speed and pseudo-acceleration along the path, respectively. We remark that  $s$  is a monotonically increasing parameter, and thus it holds  $\dot{s} > 0$ .

Let us express the dynamical equation of motion for the robotic manipulator as a function of the applied torques  $\boldsymbol{\tau} \in \mathbb{R}^n$  in each joint:

$$\mathbf{M}(\mathbf{q})\ddot{\mathbf{q}} + \mathbf{C}(\mathbf{q}, \dot{\mathbf{q}})\dot{\mathbf{q}} + \mathbf{F}_v\dot{\mathbf{q}} + \mathbf{F}_s \operatorname{sgn}(\dot{\mathbf{q}}) + \mathbf{g}(\mathbf{q}) = \boldsymbol{\tau} \quad (3.7)$$

where we define  $\mathbf{M}(\mathbf{q}) \in \mathbb{R}^{n \times n}$  as a positive definite mass matrix,  $\mathbf{C}(\mathbf{q}, \dot{\mathbf{q}}) \in \mathbb{R}^{n \times n}$  as a matrix taking into account the Coriolis and centrifugal factors,  $\mathbf{g}(\mathbf{q}) \in \mathbb{R}^n$  as the vector denoting the gravitational torques, and lastly  $\mathbf{F}_v, \mathbf{F}_s \in \mathbb{R}^{n \times n}$  as diagonal matrices that represent the coefficients of viscous and Coulomb friction, respectively.

By replacing (3.5) and (3.6) in (3.7), and neglecting the impact of viscous and Coulomb frictions  $\mathbf{F}_v\dot{\mathbf{q}} + \mathbf{F}_s \operatorname{sgn}(\dot{\mathbf{q}})$ , we obtain the following dynamic equation:

$$\mathbf{a}_1(s)a(s) + \mathbf{a}_2(s)b(s) + \mathbf{a}_3(s) = \boldsymbol{\tau}(s) \quad (3.8)$$

where  $\mathbf{a}_i(s) \in \mathbb{R}^n, i = 1, 2, 3$  are defined as:

$$\mathbf{a}_1(s) = \mathbf{M}(\mathbf{q}(s))\mathbf{q}'(s) \quad (3.9)$$

$$\mathbf{a}_2(s) = \mathbf{M}(\mathbf{q}(s))\mathbf{q}''(s) + \mathbf{C}(\mathbf{q}(s), \mathbf{q}'(s))\mathbf{q}'(s) \quad (3.10)$$

$$\mathbf{a}_3(s) = \mathbf{g}(\mathbf{q}(s)) \quad (3.11)$$

and:

$$a(s) = \ddot{s} \quad (3.12)$$

$$b(s) = \dot{s}^2 \quad (3.13)$$

are optimization variables introduced to allow a convexification of the trajectory planning problem [16]. Furthermore, to solve the time-optimal trajectory planning problem, the following linear differential equality constraint must be included:

$$b'(s) = 2a(s) \quad (3.14)$$

which follows from the fact that:

$$\dot{b}(s) = b'(s)\dot{s} = 2\dot{s}\ddot{s} \leftrightarrow b'(s) = 2a(s) \text{ if } \dot{s} > 0. \quad (3.15)$$

Having defined the dynamical equations of the manipulator, let us now represent a number of technical constraints that must be included in the trajectory planning problem.

First, we include the torque limit constraints as follows:

$$\underline{\boldsymbol{\tau}}(s) \leq \boldsymbol{\tau}(s) \leq \bar{\boldsymbol{\tau}}(s) \quad (3.16)$$

where we define  $\underline{\boldsymbol{\tau}}(s) \in \mathbb{R}^n$  and  $\bar{\boldsymbol{\tau}}(s) \in \mathbb{R}^n$ , with  $\underline{\boldsymbol{\tau}}(s) = -\bar{\boldsymbol{\tau}}(s)$ , as the lower and upper limits on joints torques that are a function of  $s$ . Note that (3.16) is necessary to obtain a solution for the trajectory planning problem that guarantees a positive traversal time, i.e.,  $T > 0$ .

In addition to the above constraints on torques, let us now describe in detail the constraints on the kinematic variables. These constraints must be included in order to satisfy the technical limitations imposed by the HRC task and to guarantee the SSM requirements and thus, safety of the human operator.

On the one hand, the speed limits are defined as:

$$\underline{\dot{\mathbf{q}}}(s) \leq \dot{\mathbf{q}}(s) \leq \bar{\dot{\mathbf{q}}}(s) \quad (3.17)$$

where  $\underline{\dot{\mathbf{q}}}(s) \in \mathbb{R}^n$  and  $\bar{\dot{\mathbf{q}}}(s) \in \mathbb{R}^n$ , with  $\underline{\dot{\mathbf{q}}}(s) = -\bar{\dot{\mathbf{q}}}(s)$ , are the lower and upper limits of the robot's speed. More specifically,  $\underline{\dot{q}}_i(s)$  and  $\bar{\dot{q}}_i(s)$  with  $i = 1, \dots, n-1$  represent the technical limits of the robot's joints, whereas  $\underline{\dot{q}}_n(s)$  and  $\bar{\dot{q}}_n(s)$  represent the limits of the robot's end-effector. In particular,  $\bar{\dot{q}}_n(s)$  is set equal to  $\bar{v}_r$  in compliance with the SSM ISO safety requirement for the operator (i.e., inequality (3.4)). Note that the SSM criterion is applied to limit the speed of the robot's end-effector which will then affect the slowdown of the entire kinematic chain. Inequality (3.17) can be conveniently reformulated as:

$$(\mathbf{q}'(s) \odot \mathbf{q}'(s))b(s) \leq \bar{\dot{\mathbf{q}}}^2(s) \quad (3.18)$$

due to the fact that  $\underline{\dot{\mathbf{q}}}(s) \leq \dot{\mathbf{q}}(s) \leq \bar{\dot{\mathbf{q}}}(s) \leftrightarrow \dot{\mathbf{q}}(s)^2 = (\mathbf{q}'(s)\dot{s})^2 = (\mathbf{q}'(s) \odot \mathbf{q}'(s))b(s) \leq \bar{\dot{\mathbf{q}}}^2(s)$ .

On the other hand, the acceleration limits are:

$$\underline{\ddot{\mathbf{q}}}(s) \leq \ddot{\mathbf{q}}(s) \leq \bar{\ddot{\mathbf{q}}}(s) \quad (3.19)$$

where  $\underline{\ddot{\mathbf{q}}}(s) \in \mathbb{R}^n$  and  $\bar{\ddot{\mathbf{q}}}(s) \in \mathbb{R}^n$ , with  $\underline{\ddot{\mathbf{q}}}(s) = -\bar{\ddot{\mathbf{q}}}(s)$ , represent the lower and upper limits of the acceleration, respectively. Similarly to the velocity, also in this case we can rewrite (3.19) as:

$$\underline{\ddot{\mathbf{q}}}(s) \leq \mathbf{q}''(s)b(s) + \mathbf{q}'(s)a(s) \leq \bar{\ddot{\mathbf{q}}}(s). \quad (3.20)$$

Clearly, by adding the limits on speed and acceleration, the total traversal time  $T$  will not be the optimal one, but rather a compromise between safety for the human operator and efficiency of the task.

By changing the integration variable from  $t$  to  $s$  after completing the aforementioned preceding stages, it is straightforward to formulate the objective function of the time-optimal trajectory planning problem. The goal is to minimize the total traversal time, defined as:

$$T = \int_0^T dt = \int_0^1 \left( \frac{ds}{dt} \right)^{-1} ds = \int_0^1 \frac{1}{\dot{s}} ds. \quad (3.21)$$

In addition, by defining:

$$c(s) = \sqrt{b(s)} = \dot{s} \quad (3.22)$$

and since  $b(s), c(s) \geq 0$  during the trajectory, we can rewrite the objective function (3.21) as follows:

$$T = \int_0^1 \frac{1}{\dot{s}} ds = \int_0^1 \frac{1}{\sqrt{b(s)}} ds = \int_0^1 \frac{1}{c(s)} ds. \quad (3.23)$$

Note that the integral in (3.23) is defined in the interval  $[0^+, 1^-]$ , as the objective function has no upper bound when the initial and final pseudo-speeds are zero.

Summing up, let us formulate the time-optimal trajectory planning problem as:

$$\begin{aligned}
 & \underset{a(s), b(s), c(s), \boldsymbol{\tau}(s)}{\text{minimize}} && \int_{0^+}^{1^-} \frac{1}{c(s)} ds \\
 & \text{subject to} && \\
 & b(0) = \dot{s}_0^2, b(1) = \dot{s}_T^2, && \\
 & c(0) = \dot{s}_0, c(1) = \dot{s}_T, && \\
 & \boldsymbol{\tau}(s) = \mathbf{a}_1(s)a(s) + \mathbf{a}_2(s)b(s) + \mathbf{a}_3(s), && \\
 & \underline{\boldsymbol{\tau}} \leq \boldsymbol{\tau}(s) \leq \bar{\boldsymbol{\tau}}, && \\
 & \forall s \in [0, 1], && (3.24) \\
 & b'(s) = 2a(s), && \\
 & c(s) = \sqrt{b(s)}, && \\
 & (\mathbf{q}'(s) \odot \mathbf{q}'(s))b(s) \leq \bar{\mathbf{q}}^2(s), && \\
 & \underline{\mathbf{q}}(s) \leq \mathbf{q}''(s)b(s) + \mathbf{q}'(s)a(s) \leq \bar{\mathbf{q}}(s), && \\
 & b(s), c(s) \geq 0, && \\
 & \forall s \in [0^+, 1^-]. &&
 \end{aligned}$$

Let us gather the decision variables in one decision vector:

$$\mathbf{x} = (a(s), b(s), c(s), \boldsymbol{\tau}(s)^\top)^\top \quad (3.25)$$

and then, let us rewrite the above problem in a compact form by defining  $f_T(\cdot)$  as the function expressing the total traversal time with respect to the end point  $\mathbf{P}_f$  and trajectory parameters  $\mathbf{x}$  in (3.25):

$$\begin{aligned}
 & \underset{\mathbf{x}}{\text{minimize}} && f_T(\mathbf{x}, \mathbf{P}_f) \\
 & \text{subject to} && (3.26) \\
 & \text{constraints} && (3.24).
 \end{aligned}$$

There are a variety of approaches (such as indirect methods, dynamic programming methods, and direct transcription methods) that are commonly used to address problem (3.26), however, for the sake of simplicity and computational speed, we opted for the methodology suggested by [16]. In particular, we perform the "convex relaxation" by transforming the unique non linear equality constraint  $c(s) = \sqrt{b(s)}$  with the equivalent expression  $\frac{1}{\sqrt{b(s)}} \leq \frac{1}{c(s)}$ , and then we convert the optimal control problem (3.24) into a convex optimization problem in SOCP form using the direct transcription technique and the relation  $d(s) \geq \frac{1}{c(s)}$ . The resulting convex optimization problem can be solved by one of several tools available for convex programming and is formally defined as follows:

$$\begin{aligned}
 & \underset{a_k, b_k, c_k, d_k, \boldsymbol{\tau}_k}{\text{minimize}} && \frac{1}{2}[(1 - \alpha)\Delta s_1(d(0^+) + d_2) + \\
 & && \sum_{k=2}^{N-2} \Delta s_k(d_k + d_{k+1}) + \\
 & && (1 - \alpha)\Delta s_{N-1}(d_{N-1} + d(1^-))] \\
 & \text{subject to} && \\
 & b_1 = \dot{s}_0^2, b_N = \dot{s}_T^2, && \\
 & c_1 = \dot{s}_0, c_N = \dot{s}_T, && \\
 & \boldsymbol{\tau}_k = \mathbf{a}_1(s_k)a_k + \mathbf{a}_2(s_k)b_k + \mathbf{a}_3(s_k), && (3.27) \\
 & \underline{\boldsymbol{\tau}} \leq \boldsymbol{\tau}(s_k) \leq \bar{\boldsymbol{\tau}}, && \\
 & \left\| \begin{bmatrix} 2c_k \\ b_k - 1 \end{bmatrix} \right\|_2 \leq b_k + 1, &&
 \end{aligned}$$

$$\begin{aligned}
& (\mathbf{q}'(s_k) \odot \mathbf{q}'(s_k))b(s_k) \leq \bar{\mathbf{q}}^2(s_k), \\
& \ddot{\mathbf{q}}(s_k) \leq \mathbf{q}''(s_k)b(s_k) + \mathbf{q}'(s_k)a(s_k) \leq \bar{\mathbf{q}}(s_k), \\
& \text{for } k = 1, \dots, N, \\
& b_{j+1} - b_j = \Delta s_j(a_{j+1} + a_j) \text{ for } j = 1, \dots, N - 1, \\
& b_l > 0, \quad c_l > 0, \\
& \left\| \begin{bmatrix} 2 \\ c_l - d_l \end{bmatrix} \right\|_2 \leq c_l + d_l \text{ for } l = 2, \dots, N - 1, \\
& \left\| \begin{bmatrix} 2 \\ c(0^+) - d(0^+) \end{bmatrix} \right\|_2 \leq c(0^+) + d(0^+), \\
& \left\| \begin{bmatrix} 2 \\ c(1^-) - d(1^-) \end{bmatrix} \right\|_2 \leq c(1^-) + d(1^-)
\end{aligned}$$

where parameter  $\Delta s_j = s_{j+1} - s_j, j = 1, 2, \dots, N - 1$  is a discretization interval while  $\alpha > 0$  is a technical parameter that can be adjusted based on the applicative scenario. The solution of problem (3.27), i.e.,  $a^*(s), b^*(s), c^*(s), d^*(s)$ , and  $\tau^*(s)$ , is computed at the sampling points  $s_1 = 0 < s_2 < \dots < s_N = 1$ . Clearly, it is possible to derive  $\mathbf{q}_d^*(t), \dot{\mathbf{q}}_d^*(t), \ddot{\mathbf{q}}_d^*(t)$ , and  $\tau_d^*(t)$  as we remark that a one-to-one correspondence between  $s$  and  $t$  is enforced. Hence, the last step is to compute time  $t$  with the inverse relation shown below:

$$t(s) = t(0^+) + \int_{0^+}^s \frac{1}{c(u)} du \quad (3.28)$$

that can be expressed as a function of the previously discretized  $k$ -th parameter  $1/c(s) = d(s)$  as follows:

$$\begin{aligned}
t(s_k) &= t(s_{k-1}) + \int_{s_{k-1}}^{s_k} d(u) du = \\
& t(s_{k-1}) + \frac{1}{2} \Delta s_{k-1} (d_{k-1} + d_k)
\end{aligned} \quad (3.29)$$

for  $k = 1, \dots, N$ . The value corresponding to  $t_N$  is therefore the total traversal time  $T$  of the planned trajectory.

Note that the problem (3.27) is a convex optimization problem. As, it is well known, convexity in optimization problems guarantees the existence and uniqueness of a solution and ensures the convergence of the solver [33]. The convexity of the trajectory planning problem provides strong theoretical assurances regarding the effectiveness and reliability of our approach. It ensures that the optimization algorithm will converge to an optimal solution that satisfies both the time optimization objective and the safety constraint, further strengthening the practical applicability and effectiveness of our methodology.

### 3.3.4 Formulation of the Multi-Objective Optimization Problem

This section is devoted to the description of the MOO problem that determines the optimal cobot trajectory by seeking a trade-off solution between two different needs. In detail, the MOO approach aims at efficiently operating the robot, that is minimizing the traversal time with the constrained trajectory planning optimal control problem in Section 3.3.3, and maximizing the ergonomics level for the human worker in Section 3.3.1, while respecting the SSM ISO safety requirement in Section 3.3.2.

More in detail, for a given starting point  $\mathbf{P}_i$ , the MOO problem seeks to choose the best end point  $\mathbf{P}_f \in \mathcal{V}$  such that the corresponding RULA ergonomics index is minimized and the associated trajectory parameters  $\mathbf{x}$  defined in (3.25) correspond to a traversal time that can be safely attained by the end-effector of the cobot in the shortest time.

The MOO problem can be formally defined as follows:

$$\begin{aligned}
& \min_{\mathbf{x}, \mathbf{P}_f} \begin{cases} f_E(\mathbf{P}_f) \\ f_T(\mathbf{x}, \mathbf{P}_f) \end{cases} \\
& \text{subject to} \\
& \text{constraints (3.24) and} \\
& \mathbf{P}_f \in \mathcal{V}
\end{aligned} \tag{3.30}$$

where we recall that  $f_E(\mathbf{P}_f)$  indicates the evaluation of the RULA index for the end point  $\mathbf{P}_f$  varying over the work volume  $\mathcal{V}$  while  $f_T(\mathbf{x}, \mathbf{P}_f)$  denotes the total traversal time along the rectilinear path connecting the fixed initial point  $\mathbf{P}_i$  and the end point  $\mathbf{P}_f$  given the trajectory parameters  $\mathbf{x}$ .

By leveraging the parametric optimization properties (i.e.,  $\min_{y,z} f(y,z) = \min_y(\min_z f(y,z)) = \min_y \tilde{f}(y)$  where  $\tilde{f}(y) = \min_z f(y,z)$ ) [34], we can define the parametric optimization function  $\tilde{f}_T(\mathbf{P}_f)$  as:

$$\begin{aligned}
\tilde{f}_T(\mathbf{P}_f) &= \min_{\mathbf{x}} f_T(\mathbf{x}, \mathbf{P}_f) \\
& \text{subject to} \\
& \text{constraints (3.24)}
\end{aligned} \tag{3.31}$$

and thus we can transform the MOO problem (3.30) in the following equivalent form:

$$\begin{aligned}
& \min_{\mathbf{P}_f} \begin{cases} f_E(\mathbf{P}_f) \\ \tilde{f}_T(\mathbf{P}_f) \end{cases} \\
& \text{subject to} \\
& \mathbf{P}_f \in \mathcal{V}.
\end{aligned} \tag{3.32}$$

The MOO problem in (3.32) has, in general, a number of (possibly infinite) solutions. Nevertheless, there may not exist a single solution that simultaneously optimizes the two above-mentioned objectives, which are therefore said to be conflicting. Informally speaking, a solution for the MOO problem in (3.32) is called Pareto optimal if none of the two conflicting objectives functions, i.e.,  $\tilde{f}_T$  and  $f_E$ , can be improved without degrading the other one. Hence, we can identify different Pareto optimal points  $\mathbf{P}_f \in \mathcal{V}$ , corresponding to solutions with minimum RULA index, shorter traversal time, and intermediate trade-offs between time and ergonomics. The choice of the final solution for (3.32) depends on the prioritization given by the HRC targets, in fact, without additional preferences, all the Pareto optimal solutions are considered equally good [35]–[38].

## 3.4 Case Study

### 3.4.1 Experimental Setup

In this section we describe the experimental setup of the proposed MOO trajectory planning approach for a safe and ergonomic HRC. The goal of our case study is to safely and ergonomically perform an assembly task in an industrial scenario where an operator works closely with a cobot. In detail, we assume that a cam organ is moved and oriented by the cobot's end-effector in such a way as to allow its assembly inside the engine head where the operator inserts the screws as efficiently and ergonomically as possible (Fig. 3.3).

All the experiments are conducted on a laptop with a 2.5 GHz Intel Core i5-7200U CPU and 8 GB RAM using the CAD software CATIA V5 [27] and MATLAB.

The main focus is the time optimization along the desired trajectory followed by the cobot from a fixed starting point  $\mathbf{P}_i = (P_{x_i}, P_{y_i}, P_{z_i})^\top = (0.6, -0.1, 1.7)^\top$  (coordinates in meters) to an ergonomically optimal end point  $\mathbf{P}_f = (P_{x_f}, P_{y_f}, P_{z_f})^\top$  for the operator. The end points should be comprised in the work volume  $\mathcal{V}$ , comprehending all candidate



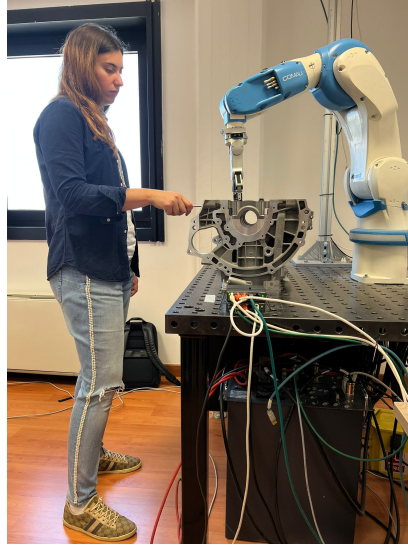


**Figure 3.3:** The assembly task performed in a safe and ergonomic HRC.

**Table 3.2:** Denavit Hartenberg parameters for Comau Racer5-0.80.

Joint	$q_i$ [rad]	$d_i$ [m]	$\alpha_i$ [rad]	$a_i$ [m]
Base	$q_1$	0.365	-1.571	0.05
Shoulder	$q_2$	0	0	0.37
Elbow	$q_3$	0	-1.571	0.05
Wrist 1	$q_4$	0.386	1.571	0
Wrist 2	$q_5$	0	-1.571	0
Wrist 3	$q_6$	0.08	0	0

points where the cobots and the operator may interact, that is designed as a rectangular cuboid with the subsequent bounding dimensions (in meters):  $P_{x_f, min} = 0.2$ ,  $P_{x_f, max} = 0.5$ ,  $P_{y_f, min} = -0.5$ ,  $P_{y_f, max} = 0.1$ ,  $P_{z_f, min} = 1$ ,  $P_{z_f, max} = 1.5$ .

In order to perform the collaborative assembly, we design a human operator on the CAD software CATIA. In particular, we consider a real right-handed female operator with height and weight percentile equal to 95 and 80, respectively. The initial referential point of the manikin is chosen between the feet for the evaluation of the operator's ergonomic posture.

Subsequently, a DOE is performed in order to identify the ergonomics function  $f_E(\mathbf{P}_f)$ , i.e., the function that quantifies ergonomics in terms of RULA for each candidate point  $\mathbf{P}_f \in \mathcal{V}$ . To this aim, we divide the given work volume  $\mathcal{V}$  into  $u$  rectangular cuboids  $\mathcal{V}_u \subseteq \mathcal{V}$  of equal size and we assume that the ergonomics function is constant within these volumes. i.e.,  $f_E(\mathbf{P}_f)$  is constant for all  $\mathbf{P}_f \in \mathcal{V}_u$ . Note that this assumption allows fast identification of the ergonomics function and, for a sufficiently high number of cuboids, also an accurate computation of ergonomics for each candidate point. For the presented scenario we assume a number of cuboids equal to  $u = 225$  with sizes (in meters) of 0.06, 0.12 and 0.05 along the X, Y, and Z axis, respectively. Then, we compute the RULA index for the centroid  $C_u$  of each of these cuboids  $\mathcal{V}_u$  and we assign this value to all the points belonging to it,  $f_E(\mathbf{P}_f) = f_E(C_u)$  for all  $\mathbf{P}_f \in \mathcal{V}_u$ . Lastly, we save the value of this function in a look-up table, in which all the RULA indices are collected.

As a cobot, we employ the Racer5-0.80, an adaptable and flexible collaborative arm by the Italian corporation Comau [39]. The *Denavit Hartenberg* (DH) parameters and the dynamic parameters of the cobot are fed into the developed framework including the MATLAB Peter Corke Robotic Toolbox [40]. Table 3.2 shows the Racer5-0.80 DH characteristics, while Table 3.3 collects data related to mass ( $m$ ), center of mass ( $\mathbf{r}_{mi}$ ) of each link, and inertia matrices ( $\mathbf{I}$ ). The motor inertia ( $J_m$ ) and transmission ratio ( $G$ ) of each link are available on the manufacturer's website [39]. It should be noted that the center of mass is determined with respect to the  $i$ -th link reference frame, and link inertia matrices

**Table 3.3:** Dynamics Parameters for the Comau Racer5-0.80.

Link	$m$ [Kg]	$r_{mi}$ [m]	$I$ [kg m <sup>2</sup> ]
1	9.843	[0.002929, -0.000097, 0.153701]	[0.266 0 -0.005; 0 0.285 0; -0.005 0 0.042]
2	5.131	[0.040000, -0.320000, -0.018000]	[0.564 0.069 0.004; 0.069 0.038 -0.030; 0.004 -0.030 0.560]
3	8.242	[0.222000, -0.009000, -0.013000]	[0.235 0.029 0.029; 0.029 0.432 -0.009; 0.029 -0.009 0.415]
4	3.320	[0.022000, -0.002000, 0.000300]	[0.008 0 -0.002; 0 0.011 0; -0.002 0 0.008]
5	5.230	[-0.016000, 0.229000, -0.002000]	[0.316 0.002 0; 0.002 0.009 0.002; 0 0.002 0.373]
6	0.979	[0, 0, 0.039000]	[0.002 0 0; 0 0.002 0; 0 0 0]

**Table 3.4:** Lower and upper Kinematic Limits for the Comau Racer5-0.80.

Link	$q$ [rad]	$\dot{q}$ [rad/s]	$\ddot{q}$ [rad/s <sup>2</sup> ]
1	$\pm 3.142$	$\pm 6.283$	$\pm 15.708$
2	$\pm 3.142$	$\pm 5.236$	$\pm 8.055$
3	$\pm 3.142$	$\pm 5.760$	$\pm 14.399$
4	$\pm 3.142$	$\pm 8.727$	$\pm 17.453$
5	$\pm 3.142$	$\pm 8.727$	$\pm 17.453$
6	$\pm 3.142$	$\pm v$	$\pm 27.890$

associated with the  $i$ -th link reference frame are calculated with good approximation by characterizing each link as a cylinder with different densities [41]. Additionally, the Racer5-0.80 base is set up in the workbench location  $\mathbf{P}_w = (x_w, y_w, z_w)^\top = (0.15, -0.10, 1.00)^\top$  (coordinates in meters).

The starting and end points of the geometric rectilinear path are related to the orientation of the cobot's end-effector in Euler's angles (in radians) as follows:  $\Phi_i = (\phi_i, \theta_i, \psi_i)^\top = (1.396, 0.262, 2.007)^\top$  and  $\Phi_f = (\phi_f, \theta_f, \psi_f)^\top$  where  $\phi_f = 1.396, \theta_f = 0.367, \psi_f = 1.571$  if  $\mathbf{P}_f \in \{(P_{x_f}, P_{y_f}, P_{z_f})^\top \in \mathcal{V} \mid 0.2 \leq P_{x_f} \leq 0.5, -0.5 \leq P_{y_f} \leq 0.1, 1 \leq P_{z_f} < 1.437\}$ , and  $\phi_f = 1.571, \theta_f = 0, \psi_f = 1.222$  if  $\mathbf{P}_f \in \{(P_{x_f}, P_{y_f}, P_{z_f})^\top \in \mathcal{V} \mid P_{z_f} \geq 1.435\}$ .

Then, we select the parametric optimization function  $\tilde{f}_T(\mathbf{P}_f)$ , which is the function that identifies the traversal time to bring the work-piece from the starting point to each end point of the work volume. The value  $\tilde{f}_T(\mathbf{P}_f)$  is the solution of the time-optimal trajectory planning problem (3.31).

In order to solve problem (3.31), a set of technical parameters must be carefully determined. For the speed (ineq. 3.18), and acceleration (ineq. 3.20) constraints, we specifically refer to the lower and upper Racer5-0.80 kinematic limits reported in Table 3.4, and to the torque limits (ineq. (3.16)) in [39]. The discretization interval  $\Delta s$  and parameter  $\alpha$  are both equal to 0.1. Note that the end-effector's speed is limited by the values  $v$  obtained in the simulation through the SSM criterion.

Next, we solve the overall MOO control problem (3.32). Note that the mathematical formulation in (3.32) is nontrivial as it comprehends the minimization of two functions with different natures:  $\tilde{f}_T$  in (3.31) is computed by solving the convex optimization problem formulated in (3.27), whereas  $f_E$  is calculated using the look-up table in which all the RULA indices are collected for each point of the work volume  $\mathcal{V}$ .

Due to the extremely non linear structure of the proposed optimization problem, we solve it employing a genetic algorithm. These solution algorithms are widely recognized as efficient and powerful global methods to handle non linear optimization problems [42]. In detail, we implement the problem in MATLAB using the *gamultiobj* function of the Global Optimization Toolbox with a tolerance parameter, i.e., *FunctionTolerance*, equal to  $10^{-6}$ .

As regards the integration of the objective functions in the genetic algorithm, on the one hand,  $f_E(\mathbf{P}_f)$  is computed with the built look-up table; on the other hand, for each point  $\mathbf{P}_f \in \mathcal{V}$ ,  $\tilde{f}_T(\mathbf{P}_f)$  is coded using the CVX Toolbox in MATLAB, an efficient solver for convex optimization problem in SOCP form [43], which is interfaced with the genetic algorithm.

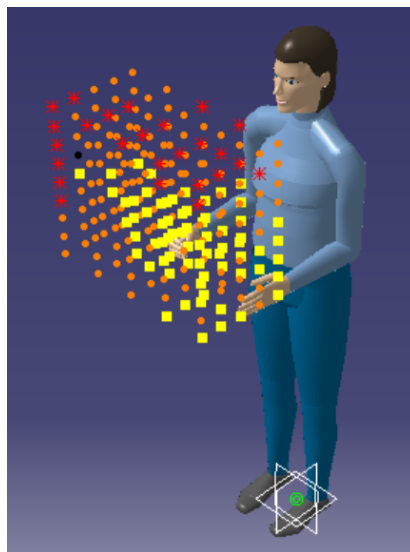


**Figure 3.4:** Virtual manikin and work volume. We indicate the centroid  $C_u$  of each of these cuboids  $\mathcal{V}_u$  with different shapes and colors: yellow squares (RULA 3), orange spots (RULA 4), and red stars (RULA 5).

### 3.4.2 Experimental Results

In order to evaluate the efficiency of the approach presented in this work, we analyze the results that are presented and discussed in detail in the current subsection.

The problem presented in Section 3.3.4 consists in finding an ergonomic point in the volume  $\mathcal{V}$  (see Fig. 3.4), defined in Section 3.3.1, that is the end point of the time-optimal trajectory taken by the end-effector of the Racer5-0.80.

As already mentioned in the previous sections, a RULA index is associated with the centroid of each sub-volume where ergonomics is assumed constant, as depicted in Fig. 3.4 with a color scale varying from yellow (for the minimum RULA index) passing through orange to red (for the highest RULA index). Hence, in our case study, the RULA index can have a score ranging from 3 (negligible risk) to 5 (medium risk that requires further investigation and must be changed soon) within volume  $\mathcal{V}$ .

As a result of the optimization problem (3.32), using the genetic algorithm (*gamultiobj*), we obtain three solutions on the Pareto front associated with the three RULA indices (Table 3.5). It is clear from Table 5.2 that the two optimization goals are in competition with each other. The traversal time decreases together with the distance covered by the robot: indeed, the longest traversal time is associated with the lowest RULA index equal to 3, whereas the lowest time corresponds to the highest RULA index equal to 5. The smallest RULA region corresponds to points closer to the operator in the work volume  $\mathcal{V}$  (Fig. 3.4), thus it is obvious that time is greater for these points. Therefore, the solution having a RULA index equal to 4 is a good trade-off between ergonomics and task efficiency. Nevertheless, we remark that the definitive choice of the end point of the robot's trajectory must be conducted by the decision maker. As mentioned above, the MOO problem is solved offline; thus, the computation time does not pose a significant issue to consider for a practical application. In our setting, the computation time is approximately three hours, thus making the methodology implementable for any collaborative robotic system.

Uncertainty in robot components modeling and sensor measurements may result in a non-optimal positioning of the end-effector. This leads to a possible deviation from the optimum in the ergonomics and efficiency performance of the end point associated to the actually executed trajectory. Hence, it is important to evaluate the sensitivity of the results obtained by the MOO approach with respect to small spatial deviations of the end point from the optimum due to uncertainty. We analyze this effect by exploring two grids of  $5 \times 5$  additional end points in the x-y and y-z planes centered in each of

**Table 3.5:** Solutions of the multi-objective optimization problem.

$P_f^z$	Coordinates [m]	RULA	Time [s]
$P_f^a$	[0.4250, -0.0500, 1.3125]	3	4.3847
$P_f^b$	[0.3500, -0.3500, 1.4375]	4	1.7875
$P_f^c$	[0.3500, -0.3500, 1.5000]	5	1.6964

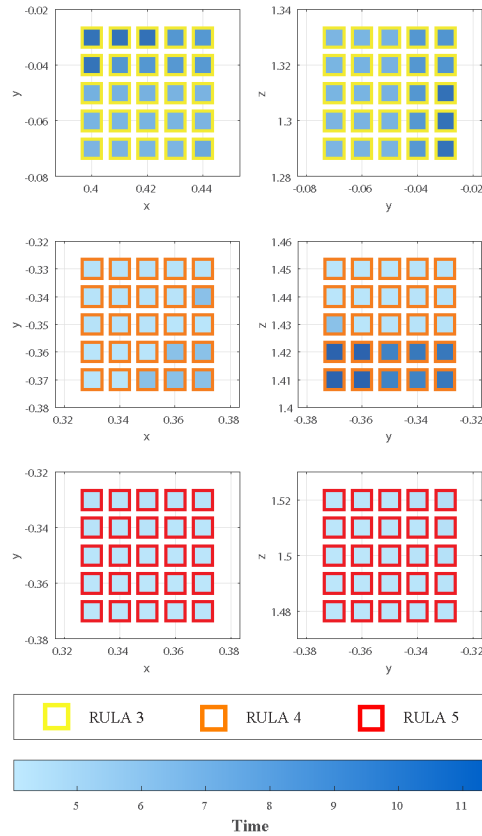


**Figure 3.5:** Results of the sensitivity analysis on Pareto solutions obtained by the proposed method: the plots show the variation of the RULA index and traversal time induced by moving the end-effector position in the x-y and y-z planes. For the analyzed end points, the RULA index is represented by different edge colors (yellow, orange, and red for RULA equal to 3, 4, and 5, respectively), whilst the traversal time is denoted in accordance with a blue colormap (higher the time, higher the color intensity).

the above-mentioned Pareto frontier points as shown in Fig. 3.5. In particular, for each analyzed point, we represent the value of the RULA index with different colors (yellow, orange, and red for RULA equal to 3, 4, and 5, respectively), whilst the traversal time is denoted in accordance with a blue colormap (the higher the time, the higher the color intensity). From the figure, it is clear that the points with a RULA index equal to 5 (which have a lower traversal time than the former ones, as expected) do not show significant variation in the traversal time. Conversely, by analyzing both the points with a RULA index equal to 3 and the ones with a RULA index equal to 4, it is interesting to note that the traversal time has a non negligible variation, even if the spatial deviation of the end point is small, and this effect could thus be taken into account as a criterion in the choice of the Pareto solution.

### 3.5 Conclusions

Trajectory planning is one of the major challenges addressed in the robotics and cobotics literature. Indeed, speeding up a task in real experiments and/or industrial applications, can increase profitability for industrial players.

In this chapter, we propose a novel multi-objective optimization approach for time-optimal trajectory planning in a safe and ergonomic HRC scenario with the aim of guaranteeing the best compromise between ergonomics for the human worker and time efficiency for the cobot, while adhering to the Speed and Separation Monitoring ISO safety regulations. The effectiveness of the proposed technique is verified through an experimental case study on the Comau Racer5-0.80, while the manikin replicating the operator is developed in the CATIA software and the optimization problem is solved by a genetic algorithm in the MATLAB environment.

Future works will focus on enhancing the safe and ergonomic HRC architecture by accounting for unpredictable human behaviors and thus by replanning online the trajectory taking into account large variations in the position and eventually physical features of the operators that collaborate with the robot. In this perspective, our proposed technique should be extended and integrated with other ad-hoc methodologies. For instance, a future development could consist in the offline definition, with the proposed approach, of a proper database of trajectories that considers the most varied positions of several types of operators with different characteristics (i.e., gender, height, weight). The database could provide the appropriate trajectory and control actions depending on the considered scenario (i.e., the features of the operator and the monitored and/or predicted dynamics of the operator). Finally, it may be convenient to evaluate the RULA index on a more advanced manikin that is able to emulate reality more accurately.

## References

- [1] Cardoso, A., Colim, A., Bicho, E., Braga, A. C., Menozzi, M., and Arezes, P., “Ergonomics and human factors as a requirement to implement safer collaborative robotic workstations: A literature review,” *Safety*, vol. 7, no. 4, p. 71, 2021.
- [2] Li, H., Wang, X., Huang, X., Ma, Y., and Jiang, Z., “Multi-joint active collision avoidance for robot based on depth visual perception,” *IEEE/CAA J. Autom.*, vol. 9, no. 12, pp. 2186–2189, 2022.
- [3] Ren, X., Li, Z., Zhou, M., and Hu, Y., “Human intention-aware motion planning and adaptive fuzzy control for a collaborative robot with flexible joints,” *IEEE Trans Fuzzy Syst*, 2022.
- [4] McAtamney, L. and Corlett, E. N., “Rula: A survey method for the investigation of work-related upper limb disorders,” *Appl. Ergon.*, vol. 24, no. 2, pp. 91–99, 1993.
- [5] Manghisi, V. M., Uva, A. E., Fiorentino, M., Bevilacqua, V., Trotta, G. F., and Monno, G., “Real time rula assessment using kinect v2 sensor,” *Appl. Ergon.*, vol. 65, pp. 481–491, 2017.
- [6] Zanchettin, A. M., Lotano, E., and Rocco, P., “Collaborative robot assistant for the ergonomic manipulation of cumbersome objects,” in *IEEE/RSJ Int. Conf. on Intelligent Robots and Systems (IROS)*, IEEE, 2019, pp. 6729–6734.
- [7] Proia, S., Carli, R., Cavone, G., and Dotoli, M., “A literature review on control techniques for collaborative robotics in industrial applications,” in *2021 IEEE 17th International Conference on Automation Science and Engineering (CASE)*, Lyon, France, 2021, pp. 591–596. DOI: [10.1109/CASE49439.2021.9551600](https://doi.org/10.1109/CASE49439.2021.9551600).
- [8] Proia, S., Carli, R., Cavone, G., and Dotoli, M., “Control techniques for safe, ergonomic, and efficient human-robot collaboration in the digital industry: A survey,” *IEEE Transactions on Automation Science and Engineering*, vol. 19, no. 3, pp. 1798–1819, 2022. DOI: [10.1109/TASE.2021.3131011](https://doi.org/10.1109/TASE.2021.3131011).
- [9] Palleschi, A., Mengacci, R., Angelini, F., *et al.*, “Time-optimal trajectory planning for flexible joint robots,” *IEEE Robot. Autom. Lett.*, vol. 5, no. 2, pp. 938–945, 2020.

- 
- [10] Shin, K. and McKay, N., “Minimum-time control of robotic manipulators with geometric path constraints,” *IEEE Trans. Automat. Contr.*, vol. 30, no. 6, pp. 531–541, 1985.
- [11] Bobrow, J. E., Dubowsky, S., and Gibson, J. S., “Time-optimal control of robotic manipulators along specified paths,” *Int. J. Robot. Res.*, vol. 4, no. 3, pp. 3–17, 1985.
- [12] Shin, K. and McKay, N., “A dynamic programming approach to trajectory planning of robotic manipulators,” *IEEE Trans. Automat. Contr.*, vol. 31, no. 6, pp. 491–500, 1986.
- [13] Singh, S. and Leu, M.-C., “Optimal trajectory generation for robotic manipulators using dynamic programming,” *Trans. Am. Soc. Mech. Eng.*, 1987.
- [14] Betts, J. T. and Huffman, W. P., “Path-constrained trajectory optimization using sparse sequential quadratic programming,” *J. Guid. Control Dyn.*, vol. 16, no. 1, pp. 59–68, 1993.
- [15] Constantinescu, D. and Croft, E. A., “Smooth and time-optimal trajectory planning for industrial manipulators along specified paths,” *J. Robot. Syst.*, vol. 17, no. 5, pp. 233–249, 2000.
- [16] Mora, P. R., *On the Time-optimal Trajectory Planning along Predetermined Geometric Paths and Optimal Control Synthesis for Trajectory Tracking of Robot Manipulators*. University of Berkeley, 2013.
- [17] Verscheure, D., Demeulenaere, B., Swevers, J., De Schutter, J., and Diehl, M., “Practical time-optimal trajectory planning for robots: A convex optimization approach,” *IEEE Trans. Automat. Contr.*, 2008.
- [18] Palleschi, A., Hamad, M., Abdolshah, S., Garabini, M., Haddadin, S., and Pallotino, L., “Fast and safe trajectory planning: Solving the cobot performance/safety trade-off in human-robot shared environments,” *IEEE Robot. Autom. Lett.*, vol. 6, no. 3, pp. 5445–5452, 2021.
- [19] Ferraguti, F., Villa, R., Landi, C. T., Zanchettin, A. M., Rocco, P., and Secchi, C., “A unified architecture for physical and ergonomic human–robot collaboration,” *Robotica*, vol. 38, no. 4, pp. 669–683, 2020.
- [20] Gualtieri, L., Rauch, E., and Vidoni, R., “Emerging research fields in safety and ergonomics in industrial collaborative robotics: A systematic literature review,” *Robot. Comput. Integr. Manuf.*, vol. 67, p. 101998, 2021.
- [21] Hentout, A., Aouache, M., Maoudj, A., and Akli, I., “Human–robot interaction in industrial collaborative robotics: A literature review of the decade 2008–2017,” *Adv. Robot.*, vol. 33, no. 15-16, pp. 764–799, 2019.
- [22] Tresca, G., Cavone, G., Carli, R., Cerviotti, A., and Dotoli, M., “Automating bin packing: A layer building matheuristics for cost effective logistics,” *IEEE Transactions on Automation Science and Engineering*, vol. 19, no. 3, pp. 1599–1613, 2022.
- [23] Cavone, G., Bozza, A., Carli, R., and Dotoli, M., “MPC-based process control of deep drawing: An industry 4.0 case study in automotive,” *IEEE Transactions on Automation Science and Engineering*, vol. 19, no. 3, pp. 1586–1598, 2022.
- [24] Proia, S., Cavone, G., Carli, R., and Dotoli, M., “A multi-objective optimization approach for trajectory planning in a safe and ergonomic human-robot collaboration,” in *2022 IEEE 18th International Conference on Automation Science and Engineering (CASE)*, Mexico City, Mexico, 2022, pp. 2068–2073. DOI: [10.1109/CASE49997.2022.9926513](https://doi.org/10.1109/CASE49997.2022.9926513).
- [25] *International Organization for Standardization, ISO/TS 15066 (2016), Robots and Robotic Devices - Collaborative Robots*.



- [26] Colombini, D., Grieco, A., and Occhipinti, E., “Occupational musculo-skeletal disorders of the upper limbs due to mechanical overload,” *Ergonomics*, vol. 41, no. 9, 1998.
- [27] Qutubuddin, S., Pallavi, R., Sambrani, A., Padashetty, D., *et al.*, “Analysis of working postures in a small-scale fastener industry by rapid upper limb assessment (rula) using catia software,” in *Technology Enabled Ergonomic Design*, Springer, 2022, pp. 75–85.
- [28] Baskaran, S., Niaki, F. A., Tomaszewski, M., *et al.*, “Digital human and robot simulation in automotive assembly using siemens process simulate: A feasibility study,” *Procedia Manuf.*, vol. 34, pp. 986–994, 2019.
- [29] Byner, C., Matthias, B., and Ding, H., “Dynamic speed and separation monitoring for collaborative robot applications—concepts and performance,” *Robot. Comput.-Integr. Manuf.*, vol. 58, pp. 239–252, 2019.
- [30] Lucci, N., Lacevic, B., Zanchettin, A. M., and Rocco, P., “Combining speed and separation monitoring with power and force limiting for safe collaborative robotics applications,” *IEEE Robot. Autom. Lett.*, vol. 5, no. 4, pp. 6121–6128, 2020.
- [31] Marvel, J. A. and Norcross, R., “Implementing speed and separation monitoring in collaborative robot workcells,” *Robot Comput-Integr Manuf.*, vol. 44, pp. 144–155, 2017.
- [32] Belingardi, G., Heydaryan, S., and Chiabert, P., “Application of speed and separation monitoring method in human-robot collaboration: Industrial case study,” in *17th International Scientific Conference on Industrial Systems*, 2017.
- [33] Boyd, S. and Vandenberghe, L., *Convex Optimization*. Cambridge University Press, 2004. DOI: [10.1017/CBO9780511804441](https://doi.org/10.1017/CBO9780511804441).
- [34] Boyd, S. P. and Vandenberghe, L., *Convex optimization*. Cambridge university press, 2004.
- [35] Zhao, Z., Liu, S., Zhou, M., and Abusorrah, A., “Dual-objective mixed integer linear program and memetic algorithm for an industrial group scheduling problem,” *IEEE/CAA Journal of Automatica Sinica*, vol. 8, no. 6, pp. 1199–1209, 2020.
- [36] Li, H., Wang, B., Yuan, Y., Zhou, M., Fan, Y., and Xia, Y., “Scoring and dynamic hierarchy-based nsga-ii for multiobjective workflow scheduling in the cloud,” *IEEE Transactions on Automation Science and Engineering*, vol. 19, no. 2, pp. 982–993, 2021.
- [37] Ning, Z., Sun, S., Zhou, M., *et al.*, “Online scheduling and route planning for shared buses in urban traffic networks,” *IEEE trans Intell Transp Sys*, vol. 23, no. 4, pp. 3430–3444, 2021.
- [38] Guo, X., Fan, C., Zhou, M., *et al.*, “Human–robot collaborative disassembly line balancing problem with stochastic operation time and a solution via multi-objective shuffled frog leaping algorithm,” *IEEE Trans. Autom. Sci. Eng.*, 2023.
- [39] *Comau website*, <https://www.comau.com/it/competencies/robotics-automation/collaborative-robotics/racer-5-0-80-cobot/>, Accessed: 2021-04-01.
- [40] *Peter Corke Toolbox website*, <https://petercorke.com/toolboxes/robotics-toolbox/>, Accessed: 2021-12-01.
- [41] Kufieta, K., “Force estimation in robotic manipulators: Modeling,” *Simulation and Experiments, NTNU Norwegian University of Science and Technology*, 2014.
- [42] Gallagher, K. and Sambridge, M., “Genetic algorithms: A powerful tool for large-scale nonlinear optimization problems,” *Computers & Geosciences*, vol. 20, no. 7-8, pp. 1229–1236, 1994.
- [43] *CVX Toolbox website*, <http://cvxr.com/cvx/>, Accessed: 2021-12-01.

## Chapter 4

# A Safe and Ergonomic Collaboration between Human and Drone in Warehouses

### Abstract

Recently, collaboration between human and drone is gaining momentum for indoor environments applications, with a notable focus on the enhancement of automation in industrial processes. In particular, drones have shown high potential for warehousing operations in three areas: inventory management, intra-logistics, and inspection & surveillance. In this work, we propose an application of human collaboration with drone to warehouses 4.0 devoted to one pick and place operation in the intra-logistics sector, with the aim of improving the operators' safety and well-being, while augmenting efficiency and reducing production costs. The *speed and separation monitoring* (SSM) criterion is applied for the first time to collaboration between human and drone, in analogy to the *human-robot collaboration* (HRC) ISO safety requirements, for safeguarding the operator in the collaborative task. In addition, we employ the *rapid upper limb assessment* (RULA) method for evaluating the operator's ergonomic posture during the collaboration with the drone. In order to validate the proposed approach in a realistic industrial scenario, a quadrotor is controlled to perform a pick and place task along a desired trajectory, from the picking bay to the palletizing area, where the operator is located, avoiding collisions with shelves and eventual other drones in motion inside the warehouse. The control strategy implements the *artificial potential field* (APF) technique for trajectory planning and the *linear quadratic regulator* (LQR) and iterative LQR algorithms for trajectory tracking. The obtained results of the human-drone framework simulations are presented and discussed in detail, proving the effectiveness of the proposed method for a safe and ergonomic collaboration.

### 4.1 Introduction

*Unmanned Aerial Vehicles* (UAVs), commonly known as drones, represent a key enabling technology of Industry 4.0 [1], thanks to their functionality and versatility in several industrial sectors. In particular, drones are having a great impact on smart warehouse management, due to their ability to fly and hover autonomously, avoid obstacles in different warehouse layouts, navigate indoor, land precisely, and operate in fleets [2].

Nowadays, warehouse areas are typically not completely automated, so that significant margins are available to improve the industrial process. In this context, indoor drones play a fundamental role for taking further steps in the complete automation of modern warehouses (warehouses 4.0). The use of drones can definitely lead to a reduction of production downtime and of labor turnover, and to a rise in warehouse flexibility and productivity, as well as in the efficiency of storage processes. Beyond the advantages mentioned above [3], the main benefit of using drones in warehouses is the improvement of the operator's safety in the industrial three-D –dull, dirty, dangerous– operations. However, as drone involvement in human working activities grows, it is increasingly crucial to achieve a natural, efficient, and effective collaboration between human and drone.

Not surprisingly, human collaboration with drone is emerging as a research field with high potential [4]. Until recently, attention has mostly been devoted to human-drone systems in the outdoor context [5] (e.g., photography, structural inspections, and

sports applications), while few contributions focus on human-drone indoor industrial applications. As the most promising areas of indoor drone use cases in warehouses are inventory management, intra-logistics, as well as inspection and surveillance [2], in the current work, a safe and ergonomic human collaboration with drone is addressed in reference to the pick and place task in the intra-logistics sector.

As highlighted by the extensive literature review [6] proposed in Chapter 2, safety is the primary need in human-robot collaboration applications, followed by efficiency and ergonomics targets. More specifically, in collaborative robotics safety is the fundamental requirement that allows operators to work side-by-side with “fenceless” manipulators in compliance with the technical specification ISO/TS 15066, i.e., *speed and separation monitoring* (SSM) and *power and force limiting* (PFL) [7], [8]. In addition, the evaluation of the operator’s ergonomic posture is necessary to prevent injuries associated with repetitive and dangerous tasks and to design workplaces appropriately, whereas efficiency is considered as the improvement of the entire industrial process, and thus as the enhancement of profitability and productivity of companies.

Therefore, in accordance with the aforementioned targets, the aim of this chapter is to define a novel trajectory planning and tracking control algorithm for a quadrotor transporting items and supporting the operator inside a warehouse, while respecting the ISO safety requirements and physical ergonomics in approaching the operator during the human collaboration with drone phase.

The remainder of this chapter is structured as follows. Section 4.2 sheds light on the main contributions of this work, positioning them with respect to the related literature. Section 4.3 delineates the quadrotor model, and in particular the dynamics, operating modes, and task phases. In Section 4.4 the ascent and descent control problem is presented, whereas in Section 4.5 the free flight control problem, which includes collision free trajectory planning and tracking, is formulated. In Section 4.6 the descent for human collaboration with drone control problem is presented by describing the procedure for the evaluation of the operator’s ergonomic posture and the SSM methodology. The experimental setup and results are discussed in Section 4.7. Finally, some concluding remarks are reported in Section 4.8.

## 4.2 Related Works and Contributions

One of the major trends in the era of the industrial digitalization and technologization is the automation of physical and informational processes in logistics and supply chain management [9]. In this context automation means partial or full replacement or support of/to an operator-performed physical or informational process by intelligent machines and robots. All the tasks that concern planning, control, and execution of physical flow of items, as well as the correlated informational and financial flows within companies and with supply chain partners, are included in the logistics and supply chain automation processes [9].

Since warehouses are undoubtedly essential elements in logistics and supply chains, it becomes important to define and develop new advanced control technologies to enhance their level of automation. Fully automated warehouses imply the direct control of handling equipment, inducing movement and storage of loads without the need for operators or drivers [10]. This affects all the warehouses technologies, which can be divided into devices that assist the movement of goods and those that improve their handling [11], [12]. The former class groups *automated guided vehicles* (AGVs), which move cases and pallets, automated storage and retrieval systems, which store goods in huge racks with robotic shuttle systems, conveyorised sortation systems, and innovative swarm robots, like the famous Amazon’s Kiva robots. The latter class includes devices for autonomous pick and place, sorting, and palletizing of items. Pick and place operations are the most expensive and labor-intensive tasks for warehouses, thus their improvement is considered a top priority for companies worldwide, since it directly affects customer satisfaction, business reputation, and profitability of the entire industrial process. In general, the automated

pick and place system includes a robotic arm equipped with sensors and actuators to detect and measure the shape of the objects to be grasped. Moreover, the robotic arm is generally devoted to the movement of huge loads and, for safety reasons, it operates in areas delimited by metallic cages, where mainly automated machines can have access to provide and collect products to/from the robotized area. In particular, the movement of goods by AGVs, forklifts, and pallet jacks is employed. However, the exclusive use of robotic arms for pick and place operations still has technical limitations, and the intervention of operators, particularly for palletizing activities, is still fundamental.

In fact, another tendency of flexible autonomous warehousing is the adoption of robots that are designed to work alongside human operators [6], [13]. The reason for this crucial shift in the global robotics industry is related to the large benefits provided, from maximization of asset utilization to easy programmability, which are ideal for dynamic warehousing operations. Collaborative robots (cobots) are largely employed in manufacturing, warehousing, and logistics sectors since they are lightweight, moveable, and easy to integrate into existing infrastructure and at the same time they make human workers more efficient, helping to sustain labor gaps and facilitate the graceful running of facilities to fill short-run peaks in demand. Their goal is also the improvement of accuracy and reduction of human mistakes that can be expensive for warehouses and the enhancement of the productivity level with the reduction of unnecessary walks between functional sectors during the pick and place process and so the mitigation of fatigue and boost of employees' satisfaction.

With the advent of cobots and the elimination of robots' protection cages, regulations have been introduced to ensure the operators' safety in the work environment and ergonomic indices like the *rapid upper limb assessment* (RULA) [14] and the *rapid entire body assessment* (REBA)[15] have been integrated as assessment tools in *human-robot collaboration* (HRC) architectures to evaluate the exposure of workers to risk factors.

HRC is by now playing a central role in repetitive monotonous tasks, jobs requiring heavy workloads, or tasks in dangerous environments for the operators. In this chapter, since drones are also key emerging technologies especially for inventory management systems in indoor environments [11], [16], [17], we focus on the arising field of human collaboration with drone, extending to this area the key requirements of HRC. In fact, although there are notable differences between both fixed and mobile cobots and drones, since the latter have the ability to fly in the three-dimensional (3D) space, there are similarities in the definition of HRC and human collaboration with drone. As discussed in [4], HRC can be defined as a field of study dedicated to understanding, designing, and evaluating robotic systems for use by or with humans; analogously, human collaboration with drone can be defined as a research field focused on understanding, designing, and evaluating drone systems for use by or with human users. Therefore, by analogy with cobots, in this chapter, we apply in an integrated way the well-known *speed and separation monitoring* (SSM) approach [7], to guarantee a safe collaboration between human and drone, and the RULA index, to ensure an ergonomic posture of the operator during the human collaboration with drone phase. It has to be highlighted that the SSM approach is more appropriate for collision avoidance, which is the aim of our approach, while the PFL one is more appropriate for collision detection.

Differently from the state of the art, where the usage of drones for pick and place in intra-logistics is lacking behind, in this work an indoor quadrotor or quadropter is chosen to transport items inside a warehouse 4.0 from the picking bay to the palletizing area, where the collaboration with the operator takes place. Note that quadrotors are a type of drones that have currently received increased attention in robotics for their straightforward dynamics and widespread use in the industrial sector [18], [19]. Due to the novelty of drone applications in indoor manufacturing environments, there are only few articles in the literature related to operation management [3]. For instance, in [20] Kloetzer *et al.* propose a type of vehicle routing problem specifically for drones' goods gathering and deployment scenarios. In [21] Cristiani *et al.* present an architecture for inventory management within large-scale warehouses through mini-drones. A platform for controlling and monitoring connected drones in indoor environments is proposed in [22]

by using indoor flight plans defined by users in a web application. Given the challenges proposed by the new line of research of human collaboration with drone, there is a great need to develop control techniques for drones in indoor environments.

Hence, one of the purposes of this chapter is to develop a control algorithm with the aim of finding a collision free shortest path for the quadrotor inside the warehouse. As discussed in [23], two approaches named deliberative and reactive paradigm can be employed for collision avoidance planning. On the one hand, in the former, which is an open-loop planning, the coordinated trajectories are globally pre-computed for all agents, sharing the workspace from their initial to goal configuration. On the other hand, in the latter, which is a closed loop planning, collisions are locally resolved by an agent observing the immediate surroundings and re-planning the instantaneous locally relevant trajectory. Although there are some heuristic approaches including prioritised planning [24] that can handle dynamic and uncertain domains, it may be impractical for several real-world applications to know a priori the entire environment. Therefore, reactive collision avoidance techniques, such as methods that utilize the concept of velocity obstacles and *artificial potential field* (APF) introduced in [25] and in [26] respectively, are widely preferred in the related literature. Due to its conceptual simplicity and favourable characteristics for collision avoidance in the continuous space, in the current work we implement the APF technique.

In order to follow the planned collision free shortest path, a trajectory tracking algorithm is needed. Among the classic control techniques, we must certainly mention the *proportional-integral-derivative* (PID) control [27], the *linear quadratic regulator* (LQR) [28] with the iterative LQR (iLQR) control, and the *model predictive control* (MPC) [29]. Although PID control is the simplest and easiest algorithm to implement, it requires its parameters' re-tuning every time the system changes, to guarantee robustness and stability. On the other hand, MPC is very popular in industrial process engineering, since it handles system constraints and non-linearities and it presents a high tracking performance. However, given the high computational cost that increases as the non-linearity of the dynamics rises, also MPC is sometimes not adequate. Hence, in this work, we employ the LQR and iLQR control approaches, which present a good trade off in terms of tracking performance, simplicity of implementation and computational cost.

Summarizing, the main contribution of this work is the design of a safe and ergonomic collaboration between human and drone control framework for enhancing automation in warehouses 4.0 by assisting the movement of items with a quadrotor. In particular, the efficiency of the pick and place task is improved by planning, with the APF algorithm, and tracking, with the iLQR controller, the shortest path for the quadrotor to reach the operator in the palletizing area, while avoiding collisions with shelves and other drones circulating in the warehouse.

### 4.3 Quadrotor Model and Tasks

This section describes the dynamic model of the quadrotor (Section 4.3.1) and explains in detail its operating modes (Section 4.3.2).

Note that throughout the chapter the North-East-Down (NED) inertial frame is considered as the Reference Coordinate System (RCS) used by drones.

#### 4.3.1 Quadrotor Dynamics

The quadrotor or quadcopter belongs to the family of UAVs, and it consists of two pairs of counter-rotating rotors and propellers, located at the vertex of a square frame.

The space motion that can be described through six *degrees of freedom* (DOF) consists of three barycenter movements and three angular movements, namely, three translation motions with respect to  $x$ - $y$ - $z$  axes of the NED RCS (i.e., forward and backward, lateral, and vertical motions) and three rotation motions along the three drone principal axes (i.e., roll, pitch, and yaw motions), which can be controlled by changing the rotational speeds of the four motors.

Since the quadrotor is an underactuated non-linear complex system with four inputs and six outputs, we model the quadrotor as a rigid body, with a symmetric structure and without ground effect, following the model proposed in [30]. Assuming small angles of movement [31], the quadrotor's dynamic model can be simplified and the state's vector can be defined as:

$$\mathbf{s} = [\mathbf{p}^\top, \dot{\mathbf{p}}^\top, \boldsymbol{\zeta}^\top, \dot{\boldsymbol{\zeta}}^\top]^\top \in \mathbb{R}^{12} \quad (4.1)$$

where  $\mathbf{p} = [x, y, z]^\top$  and  $\boldsymbol{\zeta} = [\psi, \theta, \phi]^\top$  represent respectively the linear and angular positions along the x-y-z axes, whereas the vectors  $\dot{\mathbf{p}} = [\dot{x}, \dot{y}, \dot{z}]^\top$  and  $\dot{\boldsymbol{\zeta}} = [\dot{\psi}, \dot{\theta}, \dot{\phi}]^\top$  constitute respectively the linear and angular velocities.

As a consequence, by using the state vector  $\mathbf{s}$ , the non-linear equations of the quadrotor's dynamics are written in the state space form as:

$$\dot{\mathbf{s}} = \mathbf{f}(\mathbf{s}) + \sum_{i=1}^4 \mathbf{g}_i(\mathbf{s})u_i. \quad (4.2)$$

Note that in (4.2) the control inputs  $u_1, u_2, u_3, u_4$  are the four actuators (one for the vertical thrust  $f_t$  taken upwards and one for each of the angular motions  $\tau_x, \tau_y, \tau_z$ ) collected in the control input vector  $\mathbf{u} = [f_t, \tau_x, \tau_y, \tau_z]^\top \in \mathbb{R}^4$ , while vectors  $\mathbf{f}, \mathbf{g}_i$  ( $i = 1, \dots, 4$ ) are defined as:

$$\mathbf{f}(\mathbf{s}) = \begin{bmatrix} \dot{x} \\ \dot{y} \\ \dot{z} \\ \dot{\theta} \frac{\sin(\phi)}{\cos(\theta)} + \dot{\phi} \frac{\cos(\phi)}{\cos(\theta)} \\ \dot{\theta}[\cos(\phi)] - \dot{\phi}[\sin(\phi)] \\ \dot{\psi} + \dot{\theta}[\sin(\phi)\tan(\theta)] + \dot{\phi}[\cos(\phi)\tan(\theta)] \\ 0 \\ 0 \\ \mathbf{g} \\ \frac{I_{yy} - I_{zz}}{I_{xx}} \dot{\theta} \dot{\phi} \\ \frac{I_{zz} - I_{xx}}{I_{yy}} \dot{\psi} \dot{\phi} \\ \frac{I_{xx} - I_{yy}}{I_{zz}} \dot{\psi} \dot{\theta} \end{bmatrix}$$

$$\mathbf{g}_1(\mathbf{s}) = [0 \ 0 \ 0 \ 0 \ 0 \ 0 \ 0 \ g_1^7 \ g_1^8 \ g_1^9 \ 0 \ 0 \ 0]^\top$$

$$\mathbf{g}_2(\mathbf{s}) = [0 \ 0 \ 0 \ 0 \ 0 \ 0 \ 0 \ 0 \ 0 \ 0 \ \frac{1}{I_{xx}} \ 0 \ 0]^\top$$

$$\mathbf{g}_3(\mathbf{s}) = [0 \ 0 \ 0 \ 0 \ 0 \ 0 \ 0 \ 0 \ 0 \ 0 \ 0 \ \frac{1}{I_{yy}} \ 0]^\top$$

$$\mathbf{g}_4(\mathbf{s}) = [0 \ 0 \ 0 \ 0 \ 0 \ 0 \ 0 \ 0 \ 0 \ 0 \ 0 \ 0 \ \frac{1}{I_{zz}}]^\top$$

where  $\mathbf{g}$  is the gravitational acceleration,  $I_{xx}, I_{yy}, I_{zz}$  are the components of the diagonal inertia matrix  $\mathbf{I} = \text{diag}(I_{xx}, I_{yy}, I_{zz})$ , and:

$$g_1^7 = -\frac{1}{m}[\sin(\phi)\sin(\psi) + \cos(\phi)\cos(\psi)\sin(\theta)]$$

$$g_1^8 = -\frac{1}{m}[\cos(\psi)\sin(\phi) - \cos(\phi)\sin(\psi)\sin(\theta)]$$

$$g_1^9 = -\frac{1}{m}[\cos(\phi)\cos(\theta)]$$

with  $m$  the total mass of the quadrotor. Note that  $m$  varies according to the presence of the payload: in particular,  $m = m_0$  without payload and  $m = m_0 + M$  with a payload of mass  $M$  equal to the weight of the transported item.



Starting from the non-linear quadrotor's dynamics in (4.2), the discretized and linearized version of the model is often considered for control purposes. As for the discretization procedure, a given sampling time  $\Delta t$  is considered, while the discrete time index is denoted by  $n$  and is used as a subscript of vectors and variables. Moreover, in order to apply the LQR in the ascent and descent mode (see Section 4.4) and the iLQR in the free flight and descent for human collaboration with drone modes (see Sections 4.5 and 4.6), the system is linearized around the equilibrium point  $(\mathbf{s}_e, \mathbf{u}_e)$  defined as:

- a constant nominal point  $\mathbf{s}_e = \mathbf{s}^*$  and a given control input  $\mathbf{u}_e = \mathbf{u}^*$  in the case of LQR,
- a sequence of points over the nominal trajectory  $\mathbf{s}_e = \mathbf{s}_n^*$  and a sequence of given control inputs  $\mathbf{u}_e = \mathbf{u}_n^*$  in the case of iLQR.

The linearized model is the following:

$$\bar{\mathbf{s}}_{n+1} = \mathbf{A}\bar{\mathbf{s}}_n + \mathbf{B}\bar{\mathbf{u}}_n \quad (4.3)$$

where:

$$\mathbf{A} = \begin{bmatrix} 1 & 0 & 0 & 0 & 0 & 0 & \Delta t & 0 & 0 & 0 & 0 & 0 \\ 0 & 1 & 0 & 0 & 0 & 0 & 0 & \Delta t & 0 & 0 & 0 & 0 \\ 0 & 0 & 1 & 0 & 0 & 0 & 0 & 0 & \Delta t & 0 & 0 & 0 \\ 0 & 0 & 0 & 1 & 0 & 0 & 0 & 0 & 0 & 0 & 0 & \Delta t \\ 0 & 0 & 0 & 0 & 1 & 0 & 0 & 0 & 0 & 0 & \Delta t & 0 \\ 0 & 0 & 0 & 0 & 0 & 1 & 0 & 0 & 0 & \Delta t & 0 & 0 \\ 0 & 0 & 0 & 0 & -\Delta t g & 0 & 1 & 0 & 0 & 0 & 0 & 0 \\ 0 & 0 & 0 & 0 & 0 & -\Delta t g & 0 & 1 & 0 & 0 & 0 & 0 \\ 0 & 0 & 0 & 0 & 0 & 0 & 0 & 0 & 1 & 0 & 0 & 0 \\ 0 & 0 & 0 & 0 & 0 & 0 & 0 & 0 & 0 & 1 & 0 & 0 \\ 0 & 0 & 0 & 0 & 0 & 0 & 0 & 0 & 0 & 0 & 1 & 0 \\ 0 & 0 & 0 & 0 & 0 & 0 & 0 & 0 & 0 & 0 & 0 & 1 \end{bmatrix}_{\mathbf{s}=\mathbf{s}_e, \mathbf{u}=\mathbf{u}_e}$$

$$\mathbf{B} = \begin{bmatrix} 0 & 0 & 0 & 0 \\ 0 & 0 & 0 & 0 \\ 0 & 0 & 0 & 0 \\ 0 & 0 & 0 & 0 \\ 0 & 0 & 0 & 0 \\ 0 & 0 & 0 & 0 \\ 0 & 0 & 0 & 0 \\ 0 & 0 & 0 & 0 \\ 0 & 0 & 0 & 0 \\ -\frac{\Delta t}{m} & 0 & 0 & 0 \\ 0 & \frac{\Delta t}{I_{xx}} & 0 & 0 \\ 0 & 0 & \frac{\Delta t}{I_{yy}} & 0 \\ 0 & 0 & 0 & \frac{\Delta t}{I_{zz}} \end{bmatrix}_{\mathbf{s}=\mathbf{s}_e, \mathbf{u}=\mathbf{u}_e}$$

with  $\bar{\mathbf{s}}_n = \mathbf{s}_n - \mathbf{s}_e$  and  $\bar{\mathbf{u}}_n = \mathbf{u}_n - \mathbf{u}_e$ .

### 4.3.2 Quadrotor Operating Modes

For the development of our quadrotor automation, we consider three operating modes that are described as follows.

**1) Ascent and descent mode:** Ascent and descent are performed along a vertical axis. In particular, for the ascent the quadrotor starts from a base raised from the ground and reaches a certain altitude where it begins to hover, while for the descent the opposite occurs. Since the current operating mode is quite simple, an LQR controller is implemented for the computation of the gains to be applied to the front and back motors.

**II) Free flight mode:** In this operating mode, the quadrotor is in free flight and there is no contact with the warehouse floor. First, the shortest path that avoids collisions with the shelves and any possible moving drones is found with the APF algorithm. Then, an iterative LQR controller is implemented to ensure tracking of the desired planned trajectory.

**III) Descent for human collaboration with drone mode:** Starting from a certain altitude with a non-zero velocity, the quadrotor descends along a vertical axis with a gradually decreasing velocity as it approaches the operator. In order to have greater control over the quadrotor's velocity, an iLQR is implemented instead of a simple LQR controller.

## 4.4 Ascent and Descent Control Problem

For the ascent and descent operating modes, solved as a go to goal task along a vertical trajectory, an LQR controller is implemented on the quadrotor. Given a control horizon whose length is  $N$ , the objective of the LQR is to find the  $\mathbf{u}_0^{LQR}, \dots, \mathbf{u}_{N-1}^{LQR}$  that minimize the following quadratic cost function subject to the model in (4.3) [32]:

$$\begin{aligned} J^{A,D} &= (\mathbf{s}_N - \mathbf{s}^*)^\top \mathbf{Q}_N^{A,D} (\mathbf{s}_N - \mathbf{s}^*) \\ &+ \sum_{n=0}^{N-1} [(\mathbf{s}_n - \mathbf{s}^*)^\top \mathbf{Q}_n^{A,D} (\mathbf{s}_n - \mathbf{s}^*) \\ &+ (\mathbf{u}_n - \mathbf{u}^*)^\top \mathbf{R}_n^{A,D} (\mathbf{u}_n - \mathbf{u}^*)] \end{aligned} \quad (4.4)$$

where  $\mathbf{Q}_n^{A,D} \in \mathbb{R}^{12 \times 12}$ ,  $\mathbf{Q}_N^{A,D} \in \mathbb{R}^{12 \times 12}$ , and  $\mathbf{R}_n^{A,D} \in \mathbb{R}^{4 \times 4}$  are the state cost, final cost, and input cost diagonal matrices to be tuned. Note that the three terms in (4.4) present the final state deviation, state deviation, and input size, respectively.

By solving the minimization problem with the objective function  $J^{A,D}$ , the state constraint (4.3), and the initial state  $\mathbf{s}_0$ , we obtain the optimal control law:

$$\mathbf{u}_n^{LQR} = \mathbf{K}_n^{A,D} (\mathbf{s}_n - \mathbf{s}^*) + \mathbf{u}^*, \forall n = 0, \dots, N-1 \quad (4.5)$$

where the feedback gain  $\mathbf{K}_n^{A,D} \in \mathbb{R}^{12 \times 12}$  is obtained through the following well-known Riccati equations [33] that are solved recursively backwards:

$$\begin{aligned} \mathbf{K}_n^{A,D} &= -(\mathbf{R}_n^{A,D} + \mathbf{B}^\top \mathbf{P}_{n+1}^{A,D} \mathbf{B})^{-1} \mathbf{B}^\top \mathbf{P}_{n+1}^{A,D} \mathbf{A}, \\ \mathbf{P}_n^{A,D} &= \mathbf{Q}_n^{A,D} + \mathbf{A}^\top \mathbf{P}_{n+1}^{A,D} \mathbf{A} + \mathbf{A}^\top \mathbf{P}_{n+1}^{A,D} \mathbf{B} \mathbf{K}_n^{A,D}, \\ \forall n &= 0, \dots, N-1 \end{aligned} \quad (4.6)$$

being  $\mathbf{P}_n^{A,D} \in \mathbb{R}^{12 \times 12}$  the parameter matrix and initializing  $\mathbf{P}_N^{A,D} = \mathbf{Q}_N^{A,D}$ .

## 4.5 Free Flight Control Problem

### 4.5.1 Trajectory Planning

In order to perform the pick and place task efficiently, we need to compute the collision free shortest path for the drone from the charging area (where it is located awaiting the start of the activity) to the picking bay (in case of free flight without payload) and from the picking bay to the palletizing area (in case of free flight with payload), where the operator waits for the delivery of the load by the drone.

Since the warehouse is a dynamic environment, where several missions and tasks can be performed simultaneously, it is important to consider different drones conducting multiple human-drone tasks. Hence, we suppose that in total  $H_D + 1$  drones executing a pick and place task are included in the operating scenario. Unlike warehouse's shelves that are fixed obstacles within the collision free shortest path planning, for a given drone

all the others  $H_D$  UAVs performing their task simultaneously act as mobile obstacles. Thanks to sensors mounted on board drones', their positioning is available in real time. To simplify the discussion, in this chapter we assume that each drone receives the position along the  $x$ - $y$ - $z$  axes of the other drones via the control station, in accordance with the sampling step  $\Delta t$ . Through this assumption, for each drone the collision with the shelves and other drones can be avoided at any instant by implementing the APF-based path planning algorithm. The APF technique is a straightforward and well-known real-time path planning algorithm mostly implemented for mobile robots and also for UAVs, e.g., in [34], where a modified Khatib's potential field algorithm is proposed for a quadrotor, and in [35], where a novel dynamic APF path planning technique is developed for multirotor UAVs that follow ground moving targets. The optimal path planning through the potential field principle for UAVs is also the objective of [36], where a dynamic environment is investigated.

According to the APF approach, denoting the position of the drone at time step  $n$  by  $\mathbf{p}_n$ , the total potential  $U_{APF}(\mathbf{p}_n)$  in the configuration space ( $\mathcal{C}$ ) representing the warehouse is the sum of the attractive potential field  $U_{att}(\mathbf{p}_n)$  to the goal and the repulsive potential field  $U_{rep}(\mathbf{p}_n)$  from the  $\mathcal{C}$ -obstacles region ( $\mathcal{CO}$ ):

$$U_{APF}(\mathbf{p}_n) = U_{att}(\mathbf{p}_n) + U_{rep}(\mathbf{p}_n). \quad (4.7)$$

The most promising direction of local motion is given by the artificial potential force  $\mathbf{f}_{APF} = -\nabla U_{APF}(\mathbf{p}_n)$ .

By employing a paraboloidal potential, the attractive potential field  $U_{att}$  is given by:

$$U_{att}(\mathbf{p}_n) = \frac{1}{2}k_a \mathbf{e}(\mathbf{p}_n)^\top \mathbf{e}(\mathbf{p}_n) = \frac{1}{2}k_a \|\mathbf{e}(\mathbf{p}_n)\|^2 \quad (4.8)$$

where  $k_a > 0$  is the potential attractive constant and  $\mathbf{e}(\mathbf{p}_n) = \mathbf{p}_{goal} - \mathbf{p}_n$  with  $\mathbf{p}_{goal}$  the end point of the first free flight without payload (i.e., picking bay) and of the second free flight with payload (i.e., palletizing area). The resulting attractive force is linear in  $\mathbf{e}(\mathbf{p}_n)$  and is equal to:

$$\mathbf{f}_{att}(\mathbf{p}_n) = -\nabla U_{att}(\mathbf{p}_n) = k_a \mathbf{e}(\mathbf{p}_n) \quad (4.9)$$

With respect to the generic drone, we consider the set of fixed  $\mathcal{H}_S = \{1, \dots, H_S\}$  and mobile  $\mathcal{H}_D = \{1, \dots, H_D\}$  obstacles, which coincide with the  $H_S = |\mathcal{H}_S|$  shelves and the  $H_D = |\mathcal{H}_D|$  other possible drones circulating in the operating scenario. Hence, the  $\mathcal{C}$ -obstacles region is given by the union of all the convex regions representing the fixed ( $\mathcal{CO}_h, h \in \mathcal{H}_S$ ) and mobile ( $\mathcal{CO}_h, h \in \mathcal{H}_D$ ) obstacles:

$$\mathcal{CO} = \bigcup_{h \in \mathcal{H}_S} \mathcal{CO}_h \cup \bigcup_{h \in \mathcal{H}_D} \mathcal{CO}_h. \quad (4.10)$$

As for the repulsive potential field, it is determined by the superimposition of the repulsive potential fields induced individually by all the obstacles. The equation of the repulsive potentials  $U_{rep,h}$  that keep the quadrotor away from  $\mathcal{CO}_h$  is the following:

$$U_{rep,h}(\mathbf{p}_n) = \begin{cases} \frac{k_{r,h}}{\gamma} \left( \frac{1}{\eta_h(\mathbf{p}_n)} - \frac{1}{\eta_{0,h}} \right)^\gamma & \text{if } \eta_h(\mathbf{p}_n) \leq \eta_{0,h} \\ 0 & \text{if } \eta_h(\mathbf{p}_n) > \eta_{0,h} \end{cases} \quad (4.11)$$

where  $k_{r,h} > 0$  is the potential repulsive constant, and  $\gamma = 2, 3, \dots, \eta_{0,h}$  is the range of influence of  $\mathcal{CO}_h$ . Note that  $\eta_h(\mathbf{p}_n)$  represents the distance of the drone position  $\mathbf{p}_n$  from  $\mathcal{CO}_h$ :

$$\eta_h(\mathbf{p}_n) = \begin{cases} \min_{\mathbf{p}' \in \mathcal{CO}_h} \|\mathbf{p}_n - \mathbf{p}'\| & \text{if } h \in \mathcal{H}_S \\ \|\mathbf{p}_n - \mathbf{p}_n^{(h)}\| & \text{if } h \in \mathcal{H}_D \end{cases} \quad (4.12)$$

where  $\mathbf{p}_n^{(h)}$  denotes the position of the other drone  $h \in \mathcal{H}_D$  circulating in the operating scenario.

The resulting repulsive force is equal to:

$$\begin{aligned} \mathbf{f}_{rep,h}(\mathbf{p}_n) &= -\nabla U_{rep,h}(\mathbf{p}_n) = \\ &= \begin{cases} \frac{k_{r,h}}{\eta_h^2(\mathbf{p}_n)} \left( \frac{1}{\eta_h(\mathbf{p}_n)} - \frac{1}{\eta_{0,h}} \right)^{\gamma-1} \nabla \eta_h(\mathbf{p}_n) & \text{if } \eta_h(\mathbf{p}_n) \leq \eta_{0,h} \\ 0 & \text{if } \eta_h(\mathbf{p}_n) > \eta_{0,h}. \end{cases} \end{aligned} \quad (4.13)$$

In particular,  $\mathbf{f}_{rep,h}(\mathbf{p}_n)$  is orthogonal to the equipotential contour, passes through  $\mathbf{p}_n$  and points away from the obstacle and is continuous everywhere thanks to the convex decomposition of  $\mathcal{CO}$ .

Summing up, combining (4.9) and (4.13), the overall force is the following:

$$\mathbf{f}_{APF}(\mathbf{p}_n) = \mathbf{f}_{att}(\mathbf{p}_n) + \sum_{h \in \mathcal{H}_S \cup \mathcal{H}_D} \mathbf{f}_{rep,h}(\mathbf{p}_n). \quad (4.14)$$

Finally, relying on the expression of the overall force in (4.14), the planned trajectory is computed by integrating the drone model at each sampling step  $\Delta t$  through, for instance, the Euler method or similar.

### 4.5.2 Trajectory Tracking

After finding the shortest path through the warehouse's shelves while avoiding collisions with other drones with the APF trajectory planning algorithm, the goal is to obtain the optimal tracking of the desired trajectory.

Since the quadrotor has a nonlinear nature and an under-actuated configuration, which makes it a great research platform for control systems [37]–[39], several algorithms for trajectory tracking have been implemented in the literature, from an unconstrained MPC problem using *sequential linear quadratic* (SLQ) control in [40] to a combination of *sliding mode control* (SMC) and LQR in [41]. A SLQ and iterative linear quadratic gaussian controllers are also presented by de Crousaz *et al.* in [18], [28] to achieve stability with aggressive maneuvers for a quadrotor with slung load. Stabilization of a quadrotor and tracking of a pre-defined flight path in the presence of external disturbances and model uncertainties are the objectives of [42], where Nekoukar *et al.* propose a new robust flight control system that consists of an adaptive fuzzy terminal sliding mode controller, and two proportional-derivative controllers. Given the high computational cost resulting from the nonlinear nature of the quadrotor employed in this work, the iLQR results a good compromise in terms of tracking performance, simplicity of implementation, and computational cost.

With the aim of optimizing the overall performance of the human-drone warehouse framework, we consider the iLQR algorithm that iteratively computes a state evolution of the system, linearizes it along the simulated trajectory, and then minimizes a quadratic cost function using the finite-time discrete LQR of the trajectory. This approach allows us to overcome the inaccuracies of the single operating point of the LQR algorithm while also designing a feedforward control action to better adapt to a changing trajectory [18], [40].

In order to implement and initialize the iLQR algorithm, a stable control law is required to generate a first sequence of states of the system. Even if the algorithm is designed to work with any initial stable law, aiming at increasing its performance, a standard LQR is first applied to obtain the initial state and control action guess required by the algorithm. In particular, the input-state trajectory optimized through LQR is used as a starting point to linearize the system at each state-control pair with the matrices  $\mathbf{A}_n$  and  $\mathbf{B}_n$  that, differently from the ascent and descent control problem, are time-variant.

At each iteration step, the system is linearized around the nominal trajectory  $(\mathbf{s}_n^*, \mathbf{u}_n^*)$  and a quadratic approximation of the cost function is minimized.

Given a control horizon whose length is  $N$ , analogously to Section 4, the optimal control vectors  $\mathbf{u}_0^{iLQR}, \dots, \mathbf{u}_{N-1}^{iLQR}$  are found by minimizing the following cost function [32] subject to the model in (4.3):

$$\begin{aligned}
 J^{FF} &= (\mathbf{s}_N - \mathbf{s}_N^*)^\top \mathbf{Q}_N^{FF} (\mathbf{s}_N - \mathbf{s}_N^*) \\
 &+ \sum_{n=0}^{N-1} [(\mathbf{s}_n - \mathbf{s}_n^*)^\top \mathbf{Q}_n^{FF} (\mathbf{s}_n - \mathbf{s}_n^*) \\
 &\quad + (\mathbf{u}_n - \mathbf{u}_n^*)^\top \mathbf{R}_n^{FF} (\mathbf{u}_n - \mathbf{u}_n^*)]
 \end{aligned} \tag{4.15}$$

where  $\mathbf{Q}_n^{FF} \in \mathbb{R}^{12 \times 12}$ ,  $\mathbf{Q}_N^{FF} \in \mathbb{R}^{12 \times 12}$ , and  $\mathbf{R}_n^{FF} \in \mathbb{R}^{4 \times 4}$  are the state cost, final cost, and input cost diagonal matrices to be tuned. Note that the three terms in (4.15) present the final state deviation, state deviation, and input size, respectively.

By solving the minimization problem with the objective function  $J^{FF}$ , the state constraint (4.3), and the initial state  $\mathbf{s}_0$ , we obtain the optimal control law:

$$\mathbf{u}_n^{iLQR} = \mathbf{K}_n^{FF} (\mathbf{s}_n - \mathbf{s}_n^*) + \mathbf{u}_n^* + \alpha_n \boldsymbol{\kappa}_n^{FF}, \forall n = 0, \dots, N-1 \tag{4.16}$$

where  $0 < \alpha_n \leq 1$  is the backtracking stepsize, whilst the feedback gain  $\mathbf{K}_n^{FF} \in \mathbb{R}^{12 \times 12}$  and the feedforward gain  $\boldsymbol{\kappa}_n^{FF} \in \mathbb{R}^4$  are obtained through the following well-known Riccati equations [33] that are solved recursively backwards:

$$\begin{aligned}
 \mathbf{K}_n^{FF} &= -(\mathbf{R}_n^{FF} + \mathbf{B}_n^\top \mathbf{P}_{n+1}^{FF} \mathbf{B}_n)^{-1} \mathbf{B}_n^\top \mathbf{P}_{n+1}^{FF} \mathbf{A}_n, \\
 \mathbf{P}_n^{FF} &= \mathbf{Q}_n^{FF} + \mathbf{A}_n^\top \mathbf{P}_{n+1}^{FF} \mathbf{A}_n + \mathbf{A}_n^\top \mathbf{P}_{n+1}^{FF} \mathbf{B}_n \mathbf{K}_n^{FF}, \\
 \boldsymbol{\kappa}_n^{FF} &= -(\mathbf{R}_n^{FF} + \mathbf{B}_n^\top \mathbf{P}_{n+1}^{FF} \mathbf{B}_n)^{-1} (\mathbf{B}_n^\top \boldsymbol{\pi}_{n+1}^{FF} + \mathbf{r}_n^{FF}), \\
 \boldsymbol{\pi}_n^{FF} &= \mathbf{q}_n^{FF} + \mathbf{A}_n^\top \boldsymbol{\pi}_{n+1}^{FF} + \mathbf{A}_n^\top \mathbf{P}_{n+1}^{FF} \mathbf{B}_n \boldsymbol{\kappa}_n^{FF}, \\
 &\forall n = 0, \dots, N-1
 \end{aligned} \tag{4.17}$$

being  $\mathbf{P}_n^{FF}$  and  $\boldsymbol{\pi}_n^{FF}$  the parameter matrices,  $\mathbf{q}_n^{FF} = -\mathbf{Q}_n^{FF} \mathbf{s}_n^*$  and  $\mathbf{r}_n^{FF} = -\mathbf{R}_n^{FF} \mathbf{u}_n^*$ , and initializing  $\mathbf{P}_N^{FF} = \mathbf{Q}_N^{FF}$  and  $\boldsymbol{\pi}_N^{FF} = \mathbf{q}_N^{FF}$ .

We remark that since the iLQR solves a linearized system along a certain trajectory,  $\boldsymbol{\kappa}_n$  may not be optimal or even not stable for the non-linear system. Thus, with the aim of minimizing the cost function and avoiding that the system stumbles into a local optimum, we perform a line search to find the backtracking parameter  $\alpha_n$  [43]. To test the series of the feedforward term, the system is simulated with a diminishing stepsize until finding the increment that minimizes the cost function.

## 4.6 Descent for Human Collaboration with Drone Control Problem

In this section, the crucial phase of the human collaboration with drone is described. Once the quadrotor has reached the palletizing area at a certain altitude, it begins to approach the collaboration between human and drone point along a vertical trajectory. The release of the payload by the drone must occur at an ergonomically optimal position for the operator, which is evaluated through the RULA index (see Section 4.6.1). Since in the human collaboration with drone it is fundamental to ensure the operator's safety, we control the quadrotor's speed in proximity of the operator applying the SSM approach (see Section 4.6.2).

### 4.6.1 Evaluation of the Operator's Ergonomic Posture

In this work, the evaluation of the operator's ergonomic posture is integrated in the human-drone framework with the aim of reducing the work-related musculoskeletal disorders, which affect workers in repetitive and dangerous tasks, such as the pick and place task under consideration.

Several criteria for evaluating ergonomics of a given posture, e.g., RULA, REBA, postural *postural loading on the upper body assessment* (LUBA), and *occupational repetitive action* (OCRA) are illustrated in the related literature. Since we are interested in evaluating the exposure of workers to risk factors associated with the upper limbs of the body, the RULA index is chosen as an ergonomic tool for assessing the posture of the operator.

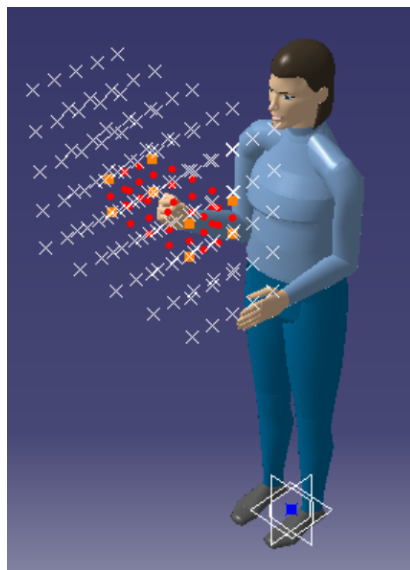


**Figure 4.1:** Virtual manikin with the work volume consisting of sampling points identified by the white cross markers and the rectangular cuboid with the optimal RULA index highlighted by the red spots.

In the RULA methodology, a score ranging from 0 (negligible risk that requires no specific countermeasure) to 6+ (high risk) can be assigned to arm, forearm, wrist, neck, and trunk [14]. Since only the effort made by the right or left part of the body can be assessed with a single RULA test, in this work the simulation is performed only for a right-handed woman.

Specifically, following the systematic procedure [44] reported in Chapter 3, a design of experiments approach is performed to determine the ergonomic operator's posture. The first phase of this procedure consists in designing a virtual manikin that simulates the operator in a fixed standing position with the use of ad hoc computer-aided design and engineering software, such as CATIA [45] or Process Simulate [46]. Note that it is convenient to choose the initial referential point of the manikin between its feet for this procedure. Then, a work volume, whose dimensions depend on the characteristics of the manikin generated in the previous phase, is defined in the work zone. It consists of equidistant points reachable by the manikin's arm, for which the RULA index is evaluated and collected in a look-up table. Finally, for the sake of identifying the region in which the collaboration between human and drone point must be located, it is necessary to subdivide the work volume into rectangular cuboids of equal size, in which we assume that the ergonomics RULA index is constant, after which we choose the region with minimum value (Fig. 4.1).

#### 4.6.2 Speed and Separation Monitoring Control Problem

After identifying the rectangular cuboid of the work volume with minimum RULA index in which the quadrotor must arrive and hover in position, the operator is ready to receive the item in an ergonomically optimal posture. In addition to the evaluation of ergonomics in the human-drone framework proposed in this work, another goal is to respect the ISO safety requirements for the operator during the collaboration [47].

The concept of safety is the fundamental requirement in HRC applications since it allows operators to work side-by-side with "fenceless" robots in compliance with ISO/TS 15066 standards. According to these requirements, safety can be guaranteed by limiting the maximum permissible forces or torques, i.e., by a PFL approach, or by prescribing that the speed must be related to a certain separation distance between the human and the robot, i.e., by a SSM approach (see Chapter 3). For this work, we assume that no undesired contact must happen between quadrotor and human. Therefore, the SSM



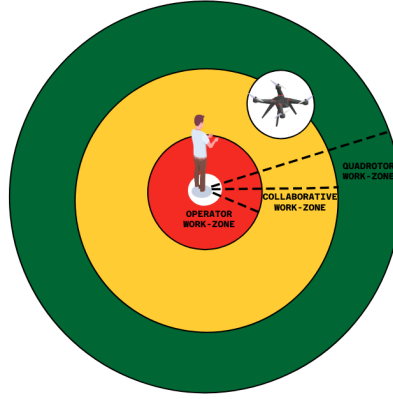


Figure 4.2: SSM scheme in the human collaboration with drone framework.

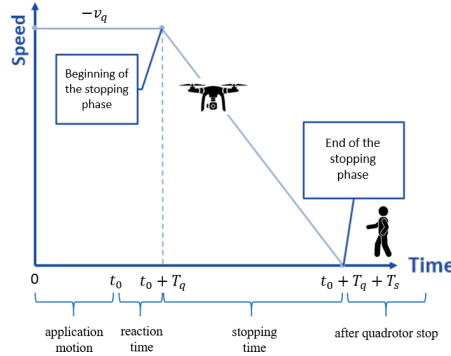


Figure 4.3: Quadrotor speed profile in the SSM criterion.

strategy is chosen to help safeguarding the operator in this collaborative application, by allowing the quadrotor actuation system to have the required deceleration capability to achieve a complete stop before eventually coming in contact with the operator [7], [8].

With the aim of preserving a safe separation distance between the operator and the quadrotor flying around the collaborative work zone, the SSM method measures the human-quadrotor separation distance, which is compared with the so called authorized (operator protective) distance [48], [49]. In particular, it can be assumed that the operator is safe when the quadrotor is moving outside a sphere of a certain radius, with the human worker in the center of such a sphere (Fig. 4.2). Since the collaboration occurs in the descent mode and we know the exact ergonomically optimal position of the operator in the  $x$ - $y$  plane, we are interested in controlling only the quadrotor velocity along the  $z$  axis (i.e., the vertical axis), whose increase is extremely dangerous for the operator. Using the SSM method, when the separation distance tends to reduce below the authorized distance, and so when the quadrotor enters the collaborative work zone (Fig. 4.2), the quadrotor must strongly decrease its linear velocity until it stops (Fig. 4.3).

The above-described SSM method is implemented as follows. The minimum allowable quadrotor-human distance  $S(t_0)$  is computed by using the following equation in ISO/TS 15066 [47]:

$$S(t_0) = S_q + S_h + S_s + C + Z_d + Z_r \quad (4.18)$$

where,  $t_0$  is the initial time of the human collaboration with drone phase,  $S_q$  and  $S_h$  indicate the quadrotor's and operator's change in location respectively,  $S_s$  is the quadrotor's stopping distance,  $C$  is an intrusion distance safety margin based on the expected human reach, and  $Z_d + Z_r$  designates the position uncertainty for both the quadrotor and operator.

For our case study, in which the operator is located in the center of the sphere and the quadrotor flies around the work zone (Fig. 4.2), by assuming a constant speed of

the quadrotor, we can now reformulate eq. (4.18) under static conditions, considering  $S_q = v_q T_q + v_q T_s$ ,  $S_h = v_h T_s$ ,  $S_s = B$ , thus obtaining:

$$S(t_0) = (v_q T_q + v_q T_s) + v_h T_s + B + C + Z_d + Z_r \quad (4.19)$$

where  $v_q$  is the quadrotor's speed in the collaborative work zone (i.e., the rate of the quadrotor's motion toward the operator)  $v_h$  indicates the speed of the operator,  $T_q$  is the quadrotor responding time in case of operator's presence, and  $T_s$  is the time to stop the quadrotor motion. Parameter  $B$  is computed as  $v_q^2/2a$  and  $T_s$  as  $v_q/a$ , with  $v_q = \dot{z}$  being the maximum scalar velocity of the quadrotor along the z axis and  $a$  the worst-case deceleration value of the quadrotor during the stopping procedure.

In particular, since here the operator is in a fixed standing position,  $v_h$  is equal to zero as well as parameter  $C$  and uncertainties  $Z_d + Z_r$ . Hence, given our assumptions, the eq. (4.19) is rewritten as:

$$S(t_0) = (v_q T_q + v_q T_s) + B + C. \quad (4.20)$$

In Fig. 4.3 we report the trend of the quadrotor's velocity  $v_q$  as a function of time that drops abruptly once the quadrotor enters the collaborative work zone.

With the aim of controlling the quadrotor's velocity during the descent for human collaboration with drone mode, the SSM criterion is applied inside the iLQR algorithm described in Section 4.5.2. A standard LQR (described in Section 4.4) is first applied to obtain the initial control law guess required by the algorithm and to compute the instant the quadrotor enters the collaborative work zone and violates the authorized distance. Then, the four Riccati equations in (4.17) and the line search procedure (described in Section 4.5.2) are implemented to follow the vertical trajectory and reach the collaboration between human and drone point with a gradually decreasing velocity.

## 4.7 Case Study

In this section, we describe the experimental setup and the results of the proposed safe and ergonomic human-drone framework. In particular, the quadrotor's control system is implemented on a Jupyter Notebook, whereas the manikin that simulates the operator is designed and subject to the RULA analysis on the CAD software CATIA V5.

### 4.7.1 Experimental Setup

The goal of our numerical experiment is to efficiently and ergonomically perform a pick and place task in a warehouse 4.0, by employing a quadrotor that, after leaving the charging area, transports an item from the picking bay to the palletizing area where the collaboration with the operator takes place.

More specifically, with the use of the three quadrotor's operating modes listed in Section 4.3.2, it is possible to deliver items within the warehouse 4.0 through six phases, as detailed below.

1) **Ascent without payload:** In this phase, the quadrotor ascends from its charging base, where it is placed before the beginning of the pick and place task, and reaches a specific altitude along a vertical axis. Then, the quadrotor hovers in this position until the next phase starts.

2) **Free flight without payload:** Starting from the hovering position reached in the previous phase, the quadrotor flies freely in the warehouse towards the picking bay, following the shortest and collision free planned trajectory.

3) **Descent approaching the picking point:** In this phase, the quadrotor descends along a vertical axis to the picking bay, where it picks up the load.

4) **Ascent with payload:** In this phase, the quadrotor ascends again, now carrying its load approaching a specific hovering point.

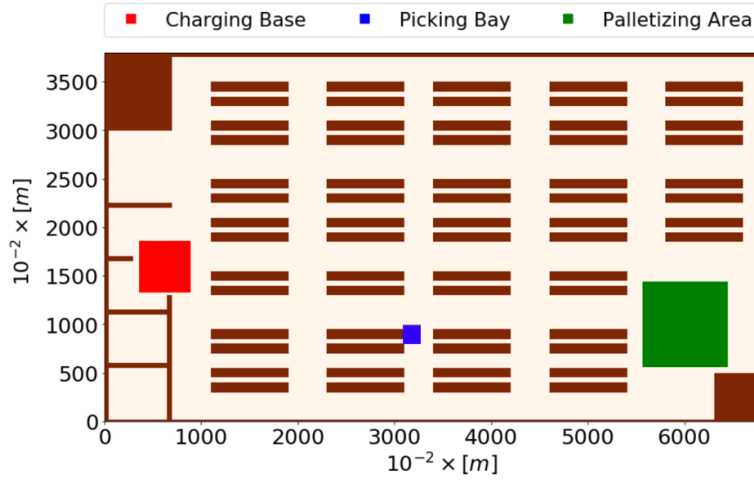


**Figure 4.4:** Warehouse map detailing the layout of shelves and position of the charging base, the palletizing area, and the considered picking bay.

**Table 4.1:** Quadrotor dynamics parameters.

Phase	$m$ [kg]	$I$ [kg m <sup>2</sup> ]
Ascent without payload	1.38	diag(0.0037,0.0037,0.0073)
Free flight without payload		
Descent approaching the picking point		
Ascent with payload	2.18	diag(0.0087,0.0087,0.0123)
Free flight with payload		
Descent approaching the HDI point		

5) **Free flight with payload:** Starting from the hovering point reached in the previous phase, the quadrotor freely flights with the load in the warehouse towards the palletizing area following the shortest and collision free planned trajectory.

6) **Descent approaching the human collaboration with drone point:** Once the palletizing area is reached, the quadrotor begins to approach the operator with a gradually decreasing velocity by respecting the SSM ISO safety requirements. When the ergonomically perfect height for the operator is reached, the quadrotor releases the object to the operator who has a posture with a minimum RULA index.

The realistic scenario addressed in this chapter is shown in Fig. 4.4, which reproduces an Amazon-like warehouse map of horizontal size  $68 \times 38$  m<sup>2</sup>, where we consider that each shelf is equipped with a dedicated automated shuttle system. The shuttle is used to pick the necessary item and place it at the corresponding picking bay, which is located on one of the short sides of the shelf. The warehouse is 6 m high and is equipped with 64 4 m high shelves. Two drones can work simultaneously within the indoor environment. Then, for each drone the sets of fixed and mobile obstacles (i.e.,  $\mathcal{H}_S$  and  $\mathcal{H}_D$ ) are respectively composed of  $H_S = 64$  shelves and  $H_D = 1$  drone.

The experiment is conducted on the well-known DJI Phantom 4 Pro [50] drones, which have a maximum speed of 72 km/h and a flight autonomy of about 30 minutes. In particular, the quadrotor that performs the pick and place task is modeled in accordance with the dynamic parameters in Table 4.1, where  $m$  and  $I$  indicate the total mass of the quadrotor and the diagonal inertia matrix, respectively. The load of mass  $M$  carried by the vacuum gripper attached to the quadrotor base is equal to 0.8 kg. Instead, the drone control input vector is defined as  $\mathbf{u} = [mg, 0, 0, 0]$  with the gravitational acceleration  $g$  set to 9.81 m/s<sup>2</sup>.

As for the definition of the operator posture, several properties are preliminarily defined in the manikin configuration designed on CATIA in terms of gender and percentile, applied to the stature (height) as well as weight and all other anthropometric variables estimated according to the chosen population. In particular, the considered manikin is a right-

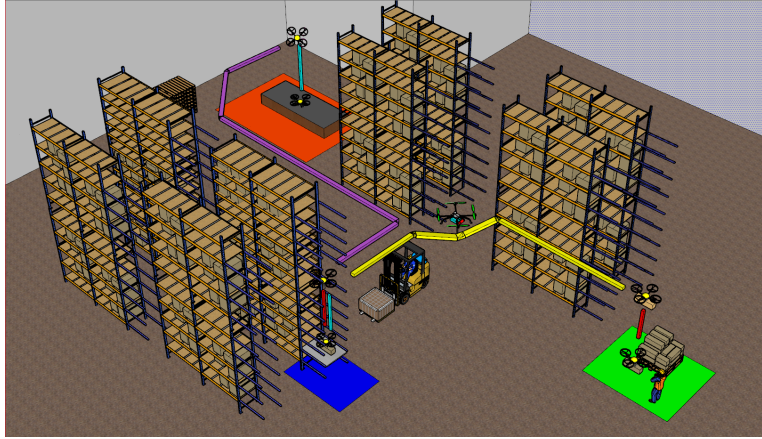


**Figure 4.5:** 3D reconstruction of the warehouse environment where the quadrotor supports the operator in performing a pick and place task.

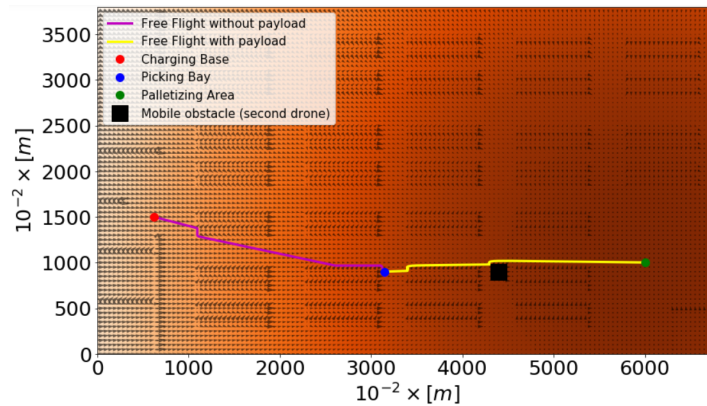


**Figure 4.6:** Top view of the quadrotor planned trajectory: the background represents the value of potential considered by the APF algorithm.

handed woman belonging to the American population with stature and weight percentile both equal to 50. The initial referential point of the manikin is chosen between the feet of the manikin for the evaluation of the operator's ergonomic posture.

The RULA analysis is executed with a payload equal to 0.8 kg for each equidistant point belonging to the work volume  $\mathcal{V}$  with bounding dimensions (in meters) measured in the manikin reference frame:  $X_{min} = 0.2, X_{max} = 0.5, Y_{min} = -0.5, Y_{max} = 0.1, Z_{min} = 1, Z_{max} = 1.5$ . From the performed DOE, it emerges that the human collaboration with drone point must be located in the region  $\mathcal{V}^*$  with minimum RULA index equal to 3, which is delimited by the following bounding dimensions (in meters):  $X_{min}^* = 0.35, X_{max}^* = 0.5, Y_{min}^* = -0.2, Y_{max}^* = 0.1, Z_{min}^* = 1.25, Z_{max}^* = 1.35$ .

To conclude the experimental setup, we set the sampling step  $\Delta t = 0.01$  s and the following values for the application of the SSM criterion to our case study:  $v_q = 4.5$  m/s,  $a = 10$  m/s<sup>2</sup>,  $T_q = 0.2$  s,  $T_s = 0.45$  s, and  $C = 0.3$  m.

## 4.7.2 Results

In our work, the quadrotor aims at reaching the operator in the palletizing area by finding the shortest path and avoiding collisions with the shelves and with another drone moving inside the warehouse 4.0. The whole pick and place task performed by the quadrotor with the corresponding actual trajectory is represented in Fig. 4.5, where a zoomed portion of the warehouse 4.0 in Fig. 4.4 is recreated in a 3D view to help the reader imagine the real industrial scenario.

**Table 4.2:** Tuning parameters in the quadrotor’s trajectory tracking control.

Phase	Control technique	Height at the beginning and end point [m]	$N$	$\Delta t$ [s]	$Q$	$R$	RMSE
Ascent without payload	LQR	[0,5;5]	501	0.01	$10 \mathbf{I}_{12}$	$2 \mathbf{I}_4$	0.0001
Free flight without payload	iLQR	[5;5]	28800	0.01	$\text{diag}(50 \mathbf{I}_3, 100 \mathbf{I}_9)$	$2000 \mathbf{I}_4$	12
Descent approaching the picking point	LQR	[5;1]	2000	0.01	$\text{diag}(200 \mathbf{I}_3, 900 \mathbf{I}_9)$	$100 \mathbf{I}_4$	0.3
Ascent with payload	LQR	[1;5]	501	0.01	$10 \mathbf{I}_{12}$	$2 \mathbf{I}_4$	0.02
Free flight with payload	iLQR	[5;5]	28200	0.01	$\text{diag}(100 \mathbf{I}_3, 1000 \mathbf{I}_9)$	$2000 \mathbf{I}_4$	25.5
Descent approaching the HDI point	iLQR	[5;1.3]	2000	0.01	$\text{diag}(200 \mathbf{I}_3, 900 \mathbf{I}_9)$	$100 \mathbf{I}_4$	0.0001

The result of the trajectory planning achieved by using the APF technique (described in Section 4.5.1) is represented in Fig. 4.6. In particular, it is possible to observe the planned path in the x–y plane in the first and second free flight on a background with a color gradient determined by the attractive and repulsive potential field. As can be seen from Fig. 4.6, the quadrotor manages to avoid the other moving drone, represented as a square in the middle of the shelves, during the second free flight.

The planned trajectory is followed by the quadrotor with ad hoc controllers for each phase as summarized in Table 4.2 (I and II columns). More specifically, all the following parameters are included in Table 4.2: the height, i.e., position of the quadrotor along the z axis, of the beginning and end of each phase (III column), horizon length  $N$  (IV column), iteration step which is the same for all missions (V column), the diagonal matrices  $Q$  (VI column) and  $R$  (VII column).

With the aim of evaluating the effectiveness of the controllers employed in the considered human-drone application, we compute the root-mean-square error (RMSE) between the planned and the actual trajectory (reported in column VIII of Table 4.2) and the minimum distance, that the quadrotor keeps from the shelves and from the other moving drone at each  $\Delta t$ , which are equal to about 0.52 m and 0.4 m, respectively. We remark that the operator’s safety is guaranteed by the protective distance computed by (4.20), which is equal to 4.2 m. Finally, the effectiveness of the ergonomics procedure is highlighted noting that the drone reaches the human collaboration with drone point in the region  $\mathcal{V}^*$ , as indicated in the set up, at a height of 1.3 m with an RMSE less than 0.0001 m.

## 4.8 Conclusions

This chapter presents an industrial application of collaboration between human and drone where a pick and place task is performed by a quadrotor inside a warehouse 4.0. In particular, the quadrotor is used to transport an item from the picking bay to the palletizing area where the collaboration with the operator takes place in a safe and ergonomic way. On the one hand, the ergonomic posture and the human collaboration with drone point are identified through the rapid upper limb assessment method; on the other hand, the safety distance between the operator and the quadrotor within the collaborative work zone is computed using the speed and separation monitoring methodology.

Future works will focus on enhancing the human-drone framework by considering the operator in motion instead of being stationary and forecasting the human movement inside the warehouse 4.0, including collision avoidance with human workers and/or any kind of object in the ascent and descent phases, as well as analyzing the quadrotor model with a retractable gripper under more complex tasks.

## References

- [1] Xu, L. D., Xu, E. L., and Li, L., “Industry 4.0: State of the art and future trends,” *Int. J. Prod. Res.*, vol. 56, no. 8, pp. 2941–2962, 2018.
- [2] Wawrla, L., Maghazei, O., and Netland, T., “Applications of drones in warehouse operations,” *Whitepaper. ETH Zurich, D-MTEC*, 2019.



- [3] Maghazei, O. and Netland, T., “Drones in manufacturing: Exploring opportunities for research and practice,” *Journal of Manufacturing Technology Management*, 2019.
- [4] Tezza, D. and Andujar, M., “The state-of-the-art of human–drone interaction: A survey,” *IEEE Access*, vol. 7, pp. 167 438–167 454, 2019.
- [5] Mirri, S., Prandi, C., and Salomoni, P., “Human-drone interaction: State of the art, open issues and challenges,” in *Proceedings of the ACM SIGCOMM 2019 Workshop on Mobile AirGround Edge Computing, Systems, Networks, and Applications*, 2019, pp. 43–48.
- [6] Proia, S., Carli, R., Cavone, G., and Dotoli, M., “Control techniques for safe, ergonomic, and efficient human-robot collaboration in the digital industry: A survey,” *IEEE Transactions on Automation Science and Engineering*, vol. 19, no. 3, pp. 1798–1819, 2022. DOI: [10.1109/TASE.2021.3131011](https://doi.org/10.1109/TASE.2021.3131011).
- [7] Byner, C., Matthias, B., and Ding, H., “Dynamic speed and separation monitoring for collaborative robot applications—concepts and performance,” *Robot. Comput.-Integr. Manuf.*, vol. 58, pp. 239–252, 2019.
- [8] Lucci, N., Lacevic, B., Zanchettin, A. M., and Rocco, P., “Combining speed and separation monitoring with power and force limiting for safe collaborative robotics applications,” *IEEE Robot. Autom. Lett.*, vol. 5, no. 4, pp. 6121–6128, 2020.
- [9] Nitsche, B., Straube, F., and Wirth, M., “Application areas and antecedents of automation in logistics and supply chain management: A conceptual framework,” in *Supply Chain Forum: An International Journal*, Taylor & Francis, vol. 22, 2021, pp. 223–239.
- [10] Rowley, J., *The principles of warehouse design*. Institute of Logistics and Transport, 2000.
- [11] Dekhne, A., Hastings, G., Murnane, J., and Neuhaus, F., “Automation in logistics: Big opportunity, bigger uncertainty,” *McKinsey Q*, pp. 1–12, 2019.
- [12] Baker, P. and Halim, Z., “An exploration of warehouse automation implementations: Cost, service and flexibility issues,” *Supply Chain Management: An International Journal*, 2007.
- [13] Proia, S., Carli, R., Cavone, G., and Dotoli, M., “A literature review on control techniques for collaborative robotics in industrial applications,” in *2021 IEEE 17th International Conference on Automation Science and Engineering (CASE)*, Lyon, France, 2021, pp. 591–596. DOI: [10.1109/CASE49439.2021.9551600](https://doi.org/10.1109/CASE49439.2021.9551600).
- [14] McAtamney, L. and Corlett, E. N., “Rula: A survey method for the investigation of work-related upper limb disorders,” *Appl. Ergon.*, vol. 24, no. 2, pp. 91–99, 1993.
- [15] Zanchettin, A. M., Lotano, E., and Rocco, P., “Collaborative robot assistant for the ergonomic manipulation of cumbersome objects,” in *IEEE/RSJ Int. Conf. on Intelligent Robots and Systems (IROS)*, IEEE, 2019, pp. 6729–6734.
- [16] Rejeb, A., Rejeb, K., Simske, S. J., and Treiblmaier, H., “Drones for supply chain management and logistics: A review and research agenda,” *International Journal of Logistics Research and Applications*, pp. 1–24, 2021.
- [17] Szalanczi-Orban, V. and Vaczi, D., “Use of drones in logistics: Options in inventory control systems,” *Interdisciplinary Description of Complex Systems: INDECS*, vol. 20, no. 3, pp. 295–303, 2022.
- [18] De Crousaz, C., Farshidian, F., Neunert, M., and Buchli, J., “Unified motion control for dynamic quadrotor maneuvers demonstrated on slung load and rotor failure tasks,” in *2015 IEEE International Conference on Robotics and Automation (ICRA)*, IEEE, 2015, pp. 2223–2229.
- [19] Pounds, P., Mahony, R., and Corke, P., “Modelling and control of a large quadrotor robot,” *Control Engineering Practice*, vol. 18, no. 7, pp. 691–699, 2010.



- 
- [20] Kloetzer, M., Burlacu, A., Enescu, G., Caraiman, S., and Mahulea, C., “Optimal indoor goods delivery using drones,” in *2019 24th IEEE Conference on Emerging Technologies & Factory Automation (ETFA)*, IEEE, 2019, pp. 1579–1582.
- [21] Cristiani, D., Bottonelli, F., Trotta, A., and Di Felice, M., “Inventory management through mini-drones: Architecture and proof-of-concept implementation,” in *2020 IEEE 21st International Symposium on “A World of Wireless, Mobile and Multimedia Networks” (WoWMoM)*, IEEE, 2020, pp. 317–322.
- [22] Pereira, A. A., Espada, J. P., Crespo, R. G., and Aguilar, S. R., “Platform for controlling and getting data from network connected drones in indoor environments,” *Future Generation Computer Systems*, vol. 92, pp. 656–662, 2019.
- [23] Čáp, M., Gregoire, J., and Frazzoli, E., “Provably safe and deadlock-free execution of multi-robot plans under delaying disturbances,” in *2016 IEEE/RSJ International Conference on Intelligent Robots and Systems (IROS)*, IEEE, 2016, pp. 5113–5118.
- [24] Čáp, M., Novák, P., Kleiner, A., and Selecký, M., “Prioritized planning algorithms for trajectory coordination of multiple mobile robots,” *IEEE transactions on automation science and engineering*, vol. 12, no. 3, pp. 835–849, 2015.
- [25] Fiorini, P. and Shiller, Z., “Motion planning in dynamic environments using velocity obstacles,” *The international journal of robotics research*, vol. 17, no. 7, pp. 760–772, 1998.
- [26] Khatib, O., “Real-time obstacle avoidance for manipulators and mobile robots,” in *Proceedings. 1985 IEEE International Conference on Robotics and Automation*, IEEE, vol. 2, 1985, pp. 500–505.
- [27] Pounds, P. E., Bersak, D. R., and Dollar, A. M., “Stability of small-scale uav helicopters and quadrotors with added payload mass under pid control,” *Autonomous Robots*, vol. 33, no. 1, pp. 129–142, 2012.
- [28] De Crousaz, C., Farshidian, F., and Buchli, J., “Aggressive optimal control for agile flight with a slung load,” in *IROS 2014 Workshop on machine learning in planning and control of robot motion*, 2014, p. 7.
- [29] Kunz, K., Huck, S. M., and Summers, T. H., “Fast model predictive control of miniature helicopters,” in *2013 European Control Conference (ECC)*, IEEE, 2013, pp. 1377–1382.
- [30] Sabatino, F., *Quadrotor control: Modeling, nonlinear control design, and simulation*, 2015.
- [31] Das, A., Subbarao, K., and Lewis, F., “Dynamic inversion with zero-dynamics stabilisation for quadrotor control,” *IET control theory & applications*, vol. 3, no. 3, pp. 303–314, 2009.
- [32] Bemporad, A., Morari, M., Dua, V., and Pistikopoulos, E. N., “The explicit linear quadratic regulator for constrained systems,” *Automatica*, vol. 38, no. 1, pp. 3–20, 2002.
- [33] Bittanti, S., Laub, A. J., and Willems, J. C., *The Riccati Equation*. Springer Science & Business Media, 2012.
- [34] Iswanto, I., Ma’arif, A., Wahyunggoro, O., and Imam, A., “Artificial potential field algorithm implementation for quadrotor path planning,” *International Journal of Advanced Computer Science and Applications*, vol. 10, no. 8, pp. 575–585, 2019.
- [35] Jayaweera, H. M. and Hanoun, S., “A dynamic artificial potential field (d-apf) uav path planning technique for following ground moving targets,” *IEEE Access*, vol. 8, pp. 192 760–192 776, 2020.
- [36] Budiyanto, A., Cahyadi, A., Adji, T. B., and Wahyunggoro, O., “Uav obstacle avoidance using potential field under dynamic environment,” in *2015 International Conference on Control, Electronics, Renewable Energy and Communications (ICCEREC)*, IEEE, 2015, pp. 187–192.

- 
- [37] Bertsekas, D., *Dynamic programming and optimal control: Volume I*. Athena scientific, 2012, vol. 1.
- [38] Tedrake, R., “Underactuated robotics: Learning, planning, and control for efficient and agile machines course notes for mit 6.832,” *Working draft edition*, vol. 3, 2009.
- [39] Zulu, A. and John, S., “A review of control algorithms for autonomous quadrotors,” *arXiv preprint arXiv:1602.02622*, 2016.
- [40] Neunert, M., De Crousaz, C., Furrer, F., *et al.*, “Fast nonlinear model predictive control for unified trajectory optimization and tracking,” in *2016 International Conference on Robotics and Automation (ICRA)*, IEEE, 2016, pp. 1398–1404.
- [41] Ghamry, K. A. and Zhang, Y., “Formation control of multiple quadrotors based on leader-follower method,” in *2015 International Conference on Unmanned Aircraft Systems (ICUAS)*, IEEE, 2015, pp. 1037–1042.
- [42] Nekoukar, V. and Dehkordi, N. M., “Robust path tracking of a quadrotor using adaptive fuzzy terminal sliding mode control,” *Control Engineering Practice*, vol. 110, p. 104 763, 2021.
- [43] Tassa, Y., Erez, T., and Todorov, E., “Synthesis and stabilization of complex behaviors through online trajectory optimization,” in *2012 IEEE/RSJ International Conference on Intelligent Robots and Systems*, IEEE, 2012, pp. 4906–4913.
- [44] Proia, S., Cavone, G., Carli, R., and Dotoli, M., “A multi-objective optimization approach for trajectory planning in a safe and ergonomic human-robot collaboration,” in *2022 IEEE 18th International Conference on Automation Science and Engineering (CASE)*, Mexico City, Mexico, 2022, pp. 2068–2073. DOI: [10.1109/CASE49997.2022.9926513](https://doi.org/10.1109/CASE49997.2022.9926513).
- [45] Qutubuddin, S., Pallavi, R., Sambrani, A., Padashetty, D., *et al.*, “Analysis of working postures in a small-scale fastener industry by rapid upper limb assessment (rula) using catia software,” in *Technology Enabled Ergonomic Design*, Springer, 2022, pp. 75–85.
- [46] Baskaran, S., Niaki, F. A., Tomaszewski, M., *et al.*, “Digital human and robot simulation in automotive assembly using siemens process simulate: A feasibility study,” *Procedia Manuf.*, vol. 34, pp. 986–994, 2019.
- [47] *International Organization for Standardization, ISO/TS 15066 (2016), Robots and Robotic Devices - Collaborative Robots.*
- [48] Marvel, J. A. and Norcross, R., “Implementing speed and separation monitoring in collaborative robot workcells,” *Robot Comput-Integr Manuf.*, vol. 44, pp. 144–155, 2017.
- [49] Belingardi, G., Heydaryan, S., and Chiabert, P., “Application of speed and separation monitoring method in human-robot collaboration: Industrial case study,” in *17th International Scientific Conference on Industrial Systems*, 2017.
- [50] *Phantom 4 Pro*, <https://www.dji.com/it/phantom-4-pro/info>, Accessed: 2022-09-01.

**Part 2**  
**Cooperative Robotic Systems:**  
**Aerial - Ground Mobile Robotic**  
**Systems Cooperation**

Cooperation between a fleet of drones or a single drone and a ground mobile robotic system (e.g., train, truck) involves these two entities working together in a coordinated manner to achieve specific objectives or tasks. The cooperation typically requires communication, data sharing, and synchronized actions between drones and mobile robotic systems. This type of cooperation can be applied in various fields, such as railway diagnostics and last-mile delivery, to enhance efficiency and capabilities.

Drones designed to perform landings on a moving platform are often referred to as "land-on-the-move" drones. These specialized drones are equipped with advanced control systems and sensors to facilitate safe and precise landings on platforms that are in motion, such as moving vehicles or trains. This technology is particularly valuable in applications like surveillance, data collection, and inspections where it is necessary to access a mobile platform for various tasks. To the best of our knowledge, the landing on a moving platform approach suitable for quadrotors, where the moving platform is a diagnostic train or a truck, is developed in a different way both in terms of application and control perspective, in comparison to the limited number of articles found in the related literature. Hence, this thesis places particular emphasis on the critical phase of drones returning to and landing on a moving train or truck. This phase occurs either after the railway inspection mission has concluded or during the final stages of last-mile delivery.

The employment of drones is being increasingly investigated in different inspection scenarios including the evaluation of civil engineering structures and infrastructure health. However, their full potential remains untapped in the realm of automated railway surveillance and inspection, as evidenced by the limited number of articles in the existing literature. Thus, the goal of **Chapter 5** is to develop a hybrid movable railway diagnostic architecture based on the use of a diagnostic train and a fleet of drones for the identification and evaluation of anomalies in railway lines and surrounding areas. To manage the fleet of drones, a combination of consensus algorithm in the leader-following mode and the use of *linear quadratic regulator* (LQR) control is applied. This combination is utilized for the flight formation phase and the landing phase onto the mobile base platform, which is the diagnostic train. The landing phase encompasses both vertical and oblique descent using a go to goal approach, as well as oblique descent following a predefined path. The outcomes of simulations within the railway diagnostic architecture are presented and thoroughly discussed.

Existing scientific literature predominantly addresses the strategic aspects of hybrid truck-drone delivery system design and the offline planning of tasks for both trucks and drones. However, there is a noticeable absence of articles that specifically delve into the real-time control of drone missions within a hybrid truck-drone delivery system. Therefore, **Chapter 6** defines a novel control technique for the last-mile delivery problem, where a drone and a truck are able to autonomously cooperate in order to improve the efficiency of the delivery. The reference scenario involves a smart city where the drone within the hybrid delivery framework handles three distinct pick-up and delivery missions: truck to point (collecting from the truck and delivering to the customer), point to point (delivering to one customer and collecting from the next), and point to truck (returning from a customer to the truck). From a control perspective, the drone is optimally guided through various operational modes, including ascent and descent to/from the truck, free flight modes with or without payload, and descent for pick-up/delivery operations. This guidance is achieved using a receding horizon LQR capable of dynamically managing the drone's landing on the mobile truck and adjusting the landing point in real-time. This chapter includes comprehensive simulation results of the truck-drone delivery system, which are presented and thoroughly analyzed, showcasing the effectiveness of the proposed approach.

## Chapter 5

# Optimal Control of Drones for a Train-Drone Railway Diagnostic System

### Abstract

The inspection of railway systems with traditional wayside detectors allows mainly the detection of wheels and axle bearings defects and can be time-demanding, unsafe, and heavily dependent on humans. To overcome these issues and then optimize and automate the rail and track diagnosis process, drones can be an excellent solution thanks to their onboard state-of-the-art cameras and sensors. Thus, with the aim of rapidly collecting highly accurate data, an innovative hybrid movable railway diagnostic architecture, consisting of a diagnostic train and a fleet of drones, is defined in this chapter. From the control point of view, the main interest is in optimally managing the crucial phase of drones returning to and landing on the moving train when the railway inspection mission is completed. To control the fleet of drones, a combination of consensus algorithm in the leader-following mode and *linear quadratic regulator* (LQR) is implemented for the flight formation phase and the landing phase on the moving base platform (i.e., the diagnostic train), respectively. The landing phase is performed both as vertical or oblique descent through a go to goal and as oblique descent along a predefined path. The obtained results of the railway diagnostic architecture simulations are presented and discussed in detail. In particular, they show that the vertical and oblique descent performed as go to goal are certainly faster than the oblique descent along a predefined path.

### 5.1 Introduction

The deterioration of the railway infrastructure is a global problem that needs to be solved. However, the inspection process is typically conducted every year or each several months and it may take too long to detect faults in the track that can cause collapses [1], [2]. Thus, the railway industry needs to improve track diagnostics to ensure the timely detection of structural degradation. Consequently, a predictive maintenance regime can be implemented guaranteeing a more cost-effective management of the railway infrastructure with respect to more traditional tools.

Railway systems employed in infrastructure diagnostic applications include several devices and vehicles classified according to two main categories that are wayside (track-based) detectors and movable detectors [3]. The formers are equipped with sensors, attached to the track or positioned at a certain distance from the track, which are capable of measuring, among other key parameters, strain, displacement, acceleration, temperature, humidity, and defects. They are mainly employed for the inspection of defects related to wheels and axle bearings and present several drawbacks (i.e., limited performance, sensitivity, and accuracy, strong dependence on operators for supervision and periodic maintenance, and presence of health and safety concerns). Conversely, the latter are categorized into trolleys, hi-rail vehicles, condition monitoring systems, track recording vehicles, drones, and smartphones which can inspect rail and track conditions while the train is moving. Each of these movable technologies is developed in line with the recent advances in the related sector with different technical characteristics capable of capturing various track defects.

Aiming at improving inspection accuracy and automating the detection of both natural and harmful threat scenarios, an alternative to the use of the diagnostic systems described above can be the employment of a more advanced diagnostic system. Such a system

should combine multiple movable devices with distinct features such as drones [4], [5] that allow verifying the anomalies identified by the diagnostic train during the inspection process.

In the last decade, *unmanned aerial vehicles* (UAVs), commonly known as drones, have had a meaningful growth in several sectors and nowadays are having a great impact on railway operations worldwide. This is due to their ability to perform a detailed assessment of large physical structures with few units and their simplicity and flexibility of implementation, as well as low maintenance and instrumentation costs [4]. Although there are still some limitations characterizing drones, such as flying autonomy or payload weight, fleets of drones have become necessary for stable railway inspection systems guaranteeing railway operators' safety and reliability, alongside their trustworthy assistance. They are employed to assess high-voltage electrical lines, railway catenary lines, and even tracks and switching points. With the drone's feature of sensor/camera mobility, extensive imagery is obtained to rapidly amplify the process of detecting flaws, cracks, and additional hazards. Therefore, the use of drones increases productivity and efficiency of the entire diagnostic process by minimizing intervention times compared to more traditional methods and drastically reducing dangerous activities executed by humans [6].

The aim of this chapter is to define a hybrid movable railway diagnostic architecture based on the use of a diagnostic train and a fleet of drones for the identification and evaluation of anomalies in railway lines and surrounding areas. In particular, the diagnostic system is in charge of checking the condition of the tracks and reporting online the issues that require timely intervention by human maintainers.

## 5.2 Related Works and Contributions

In this chapter, we focus on the arising field of diagnostics by drones of the railway infrastructure. This aims at frequently and automatically checking railway infrastructure parameters, thus leading to the implementation of early warning systems that detect faults and threats, including natural hazards and intentional attacks [4]. Although the employment of drones is being increasingly investigated in different inspection scenarios (e.g., in the health assessment of civil engineering structures and infrastructures), their potentials have yet to be fully exploited for automated railway surveillance and inspection, as shown by the few articles present in the related literature. For instance, in [2] and in [6], the state-of-the-art and future directions of the railway diagnostic systems with drones are presented, highlighting opportunities (i.e, cost-effectiveness, flexibility) and actual technical limits (i.e., low endurance, difficulty in using drones in hostile weather conditions, lack of international standard regulations for drones with maximum take-off weight lower than 150 kg). In [5], Flammini *et al.* illustrate a proposal of an early warning system based on wireless sensor networks for railway infrastructure assessment, whereas in [7], Kochan *et al.* present the results of the "Drone-monitor" project that is launched to assess the possibility of using drones for automating the railway infrastructure inspection.

Aiming at filling the gap in the related research field, in our work we propose a hybrid movable railway diagnostic architecture that consists of a diagnostic train and a fleet of drones, which are quadrotors, optimally guided by a dedicated control system. In particular, we focus on the crucial phase of drones' return to and landing on the moving train, when the railway inspection mission is completed. For the flight formation phase, which allows the drones to follow the diagnostic train and to reach its position and velocity, we implement the well-known consensus technique in the leader-following mode. This technique is examined in several papers, such as in [8], where a new kind of distributed non-smooth control-based formation control algorithm is developed, and in [9], where an algorithm based on the combination of sliding mode control and *linear quadratic regulator* (LQR) is proposed to solve the problem in a leader-follower configuration. In the proposed architecture, the consensus algorithm is combined with the LQR [10] that aims at controlling the drones in the landing phase, subsequent to the flight formation phase. To the best of our knowledge, we develop a landing on a moving platform approach



suitable for quadrotors, where the moving platform is the diagnostic train, in a different way (both from an application and control point of view) compared to the few articles in the related literature [11]–[13]. These, in fact, rely mainly on vision-based and multi-sensor fusion approaches, which in some cases can present a high computational cost.

### 5.3 System Modelling and Tasks

This section describes the railway diagnostic system based on the combined use of 3D quadrotors and a train for inspecting railway lines. In particular, Section 5.3.1 and Section 5.3.2 present the dynamic models of the quadrotor and the train, respectively, whereas the operating scenario and tasks phases are illustrated in Section 5.3.3.

#### 5.3.1 Quadrotor Dynamics

As reported in Chapter 4, the quadrotor is a type of helicopter with four propellers at the extremities and an electronic board in the middle and its space motion can be defined through six *degrees of freedom* (DOF).

The quadrotor is modelled as a rigid body, with a symmetric structure and without ground effect, following the system [14] proposed in Chapter 4. To define the quadrotor's structure and position, two different reference frames are considered. We use the north-east-down (NED) for the first inertial coordinate system (fixed), whereas the aircraft body center (ABC) is used for the second reference system united with the quadrotor's barycenter (mobile).

By calling  $[x^d, y^d, z^d, \psi^d, \theta^d, \phi^d]^\top$  the vector containing the linear  $x^d, y^d, z^d$  and angular  $\psi^d, \theta^d, \phi^d$  positions of the quadrotor in the NED frame and  $[e^d, v^d, w^d, p^d, q^d, r^d]^\top$  the vector containing the linear  $e^d, v^d, w^d$  and angular  $p^d, q^d, r^d$  velocities in the ABC frame, we define the state's vector as follows:  $[x^d, y^d, z^d, \psi^d, \theta^d, \phi^d, e^d, v^d, w^d, p^d, q^d, r^d]^\top \in \mathbb{R}^{12}$ . Note that the two reference frames are put in relation by the following equation:

$$\begin{aligned} \mathbf{v} &= \mathbf{R} \mathbf{v}_B \\ \boldsymbol{\omega} &= \mathbf{T} \boldsymbol{\omega}_B \end{aligned} \quad (5.1)$$

where  $\mathbf{v} = [\dot{x}^d, \dot{y}^d, \dot{z}^d]^\top \in \mathbb{R}^3$ ,  $\boldsymbol{\omega} = [\dot{\psi}^d, \dot{\theta}^d, \dot{\phi}^d]^\top \in \mathbb{R}^3$ ,  $\mathbf{v}_B = [e^d, v^d, w^d]^\top \in \mathbb{R}^3$ ,  $\boldsymbol{\omega}_B = [p^d, q^d, r^d]^\top \in \mathbb{R}^3$ , and  $\mathbf{R}$  and  $\mathbf{T}$  are the rotation matrix and the matrix for angular transformations, respectively. Assuming small angles of movement [15], the quadrotor's dynamic model can be simplified by setting  $[p^d, q^d, r^d]^\top = [\dot{\psi}^d, \dot{\theta}^d, \dot{\phi}^d]^\top$ ; hence, we redefine the state's vector in the inertial frame as  $\mathbf{s}^d = [x^d, y^d, z^d, \psi^d, \theta^d, \phi^d, \dot{x}^d, \dot{y}^d, \dot{z}^d, \dot{\psi}^d, \dot{\theta}^d, \dot{\phi}^d]^\top \in \mathbb{R}^{12}$ . As a consequence, by using the state vector  $\mathbf{s}^d$ , the non-linear equations of the quadrotor's dynamics are written in the state space form as:

$$\dot{\mathbf{s}}^d = \mathbf{f}(\mathbf{s}^d) + \sum_{i=1}^4 \mathbf{g}_i(\mathbf{s}^d) u^{d,i} \quad (5.2)$$

where  $u^{d,1}, u^{d,2}, u^{d,3}, u^{d,4}$  are the four control inputs and:

$$\mathbf{f}(\mathbf{s}^d) = \begin{bmatrix} \dot{x}^d \\ \dot{y}^d \\ \dot{z}^d \\ \dot{\theta}^d \frac{\sin(\phi^d)}{\cos(\theta^d)} + \dot{\phi}^d \frac{\cos(\phi^d)}{\cos(\theta^d)} \\ \dot{\theta}^d [\cos(\phi^d)] - \dot{\phi}^d [\sin(\phi^d)] \\ \dot{\psi}^d + \dot{\theta}^d [\sin(\phi^d) \tan(\theta^d)] + \dot{\phi}^d [\cos(\phi^d) \tan(\theta^d)] \\ 0 \\ 0 \\ g \\ \frac{J_{yy} - J_{zz}}{J_{xx}} \dot{\theta}^d \dot{\phi}^d \\ \frac{J_{zz} - J_{xx}}{J_{yy}} \dot{\psi}^d \dot{\phi}^d \\ \frac{J_{xx} - J_{yy}}{J_{zz}} \dot{\psi}^d \dot{\theta}^d \end{bmatrix} \quad (5.3)$$

$$\mathbf{g}_1(\mathbf{s}^d) = [0 \ 0 \ 0 \ 0 \ 0 \ 0 \ g_1^7 \ g_1^8 \ g_1^9 \ 0 \ 0 \ 0]^\top \quad (5.4)$$

$$\mathbf{g}_2(\mathbf{s}^d) = [0 \ 0 \ 0 \ 0 \ 0 \ 0 \ 0 \ 0 \ 0 \ \frac{1}{J_{xx}} \ 0 \ 0]^\top \quad (5.5)$$

$$\mathbf{g}_3(\mathbf{s}^d) = [0 \ 0 \ 0 \ 0 \ 0 \ 0 \ 0 \ 0 \ 0 \ 0 \ \frac{1}{J_{yy}} \ 0]^\top \quad (5.6)$$

$$\mathbf{g}_4(\mathbf{s}^d) = [0 \ 0 \ 0 \ 0 \ 0 \ 0 \ 0 \ 0 \ 0 \ 0 \ 0 \ \frac{1}{J_{zz}}]^\top \quad (5.7)$$

where  $g$  is the gravity acceleration,  $J_{xx}$ ,  $J_{yy}$ ,  $J_{zz}$  are the components of the diagonal inertia matrix  $J$ , and:

$$g_1^7 = -\frac{1}{m^d} [\sin(\phi^d) \sin(\psi^d) + \cos(\phi^d) \cos(\psi^d) \sin(\theta^d)] \quad (5.8)$$

$$g_1^8 = -\frac{1}{m^d} [\cos(\psi^d) \sin(\phi^d) - \cos(\phi^d) \sin(\psi^d) \sin(\theta^d)] \quad (5.9)$$

$$g_1^9 = -\frac{1}{m^d} [\cos(\phi^d) \cos(\theta^d)] \quad (5.10)$$

with  $m^d$  the total mass of the quadrotor.

Often, starting from the non-linear quadrotor's dynamics in (5.2), the linearized version is considered for control purposes (see Section 5.4). By considering the four control inputs, one for the vertical thrust ( $f_t^d$ ) taken upwards and one for each of the angular motions ( $\tau_x^d, \tau_y^d, \tau_z^d$ ), and thus, by setting the control input vector  $\mathbf{u}^d = [f_t^d, \tau_x^d, \tau_y^d, \tau_z^d]^\top \in \mathbb{R}^4$ , through the linearization around the nominal point  $\mathbf{s}^{d,*}$  or trajectory  $\mathbf{s}_n^{d,*}$  and control input vector  $\mathbf{u}_n^{d,*}$ , using  $\Delta t$  for the time step in the discretization procedure, we obtain the following linear dynamics:

$$\bar{\mathbf{s}}_{n+1}^d = \mathbf{A} \bar{\mathbf{s}}_n^d + \mathbf{B} \bar{\mathbf{u}}_n^d \quad (5.11)$$

with  $\bar{\mathbf{s}}_n^d = \mathbf{s}_n^d - \mathbf{s}_n^{d,*}$  and  $\bar{\mathbf{u}}_n^d = \mathbf{u}_n^d - \mathbf{u}_n^{d,*}$ .

### 5.3.2 Train Model

The train model is formulated in the state space form as:

$$\mathbf{s}_{n+1}^t = f(\mathbf{s}_n^t, \mathbf{u}_n^t) \quad (5.12)$$

where the state vector is defined as  $\mathbf{s}^t = [x^t, y^t, z^t, \dot{x}^t, \dot{y}^t, \dot{z}^t]^\top \in \mathbb{R}^6$  with  $x^t, y^t, z^t$  the train's positions along the X, Y, Z axes and  $\dot{x}^t, \dot{y}^t, \dot{z}^t$  its linear velocities, and the control input vector as  $\mathbf{u}^t = [\ddot{x}^t, \ddot{y}^t, \ddot{z}^t]^\top \in \mathbb{R}^3$  with  $\ddot{x}^t, \ddot{y}^t, \ddot{z}^t$  the train's accelerations.

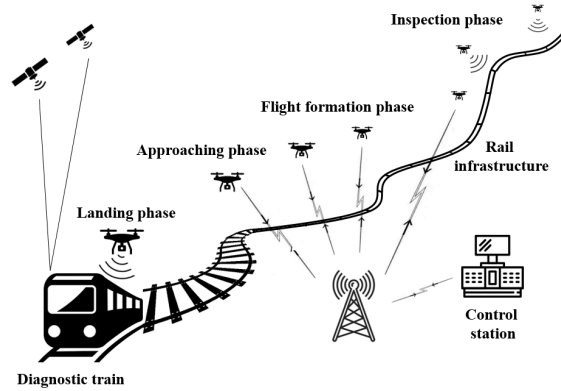


Figure 5.1: Railway diagnostic architecture with the operating tasks phases.

### 5.3.3 Operating Scenario and Tasks Phases

The operating scenario concerns the use of drones for the identification and evaluation of anomalies of the railway line and surrounding areas thanks to state-of-the-art sensors mounted on drones' board that allow to collect data quickly and easily. The architecture (Fig. 5.1) is composed of a diagnostic train on which the drones' charging base is positioned and a fleet of drones that initiate the inspection mission when some anomaly on a given railway line is identified by the train.

In this context, we focus on the crucial phase of the drones' returning to the train once the railway line has been inspected. The approach consists of these phases (Fig. 5.1):

**I) Inspection phase (pre-condition):** Once the fleet of drones notifies the control station of the end of the railway line inspection mission, it is ready to receive the current status of the train and the predicted trajectory in terms of position, velocity, and timestamp of the landing point situated in the barycentric position of the charging base.

**II) Flight formation phase:** In this phase, the fleet of drones aims at following the diagnostic train trajectory, in terms of position and velocity, in single file fleet formation, ensuring that each drone keeps a safe distance between the preceding and subsequent one placed in sequence, and aligns its attitude along the X and Y axis of the train at a given offset over the Z axis. The technique implemented for the flight formation phase is the consensus algorithm in the leader-following mode.

**III) Approaching phase:** Once the fleet of drones has aligned with the train, the starting point of the landing phase must be reached from each drone, one at a time. Then the drone that has started its approaching phase hovers in its starting point and then proceeds with the landing phase. Note that, while the first drone starts the landing phase, the subsequent drones continue following the train up to when their approaching phase can start. Then they proceed gradually in queue towards the estimated landing point.

**IV) Landing phase:** After reaching the starting point of the landing phase, the drone is ready to land and reach the landing area located on the roof of the diagnostic train. The landing phase can be performed in two different ways. More specifically, it can be solved as a *descent through a go to goal*, i.e., from a given point to the target along a vertical or oblique descent, by implementing a LQR with two Riccati equations, or as a *descent along a predefined path*, i.e., the tracking of an oblique given trajectory, by implementing a LQR with four Riccati equations.

Note that for both the approaching and landing phases, the estimate of the landing starting point is performed on the basis of the predicted trajectory (in terms of both position and velocity) of the train that is provided by the control station in accordance with a certain sampling step ( $\Delta t$ ). For the vertical landing, the drone initiates the descent phase from a point with a vertical and a forward horizontal offset with respect to the train's estimated position corresponding to the landing time. Conversely, for the oblique descent (both through a go to goal and along a predefined path), the drone is initially

aligned with the train along the X and Y axes, while keeping a given offset along Z, and reaches the landing point from behind. As a final remark, during the drone's inspection phase and subsequent return, the train, if necessary, slows down its velocity to adapt to the technical characteristics of the drones. The same holds for drones as well.

## 5.4 Control strategies

### 5.4.1 Consensus Algorithm in the Leader-Following Mode

The aim of the flight formation phase is to have the drones follow the train, after having finished their mission. In accordance with this goal, we implement the consensus algorithm in the leader-following mode [16] along the linear positions and velocities, viewing the train dynamics as a reference model. Applying the leader-following strategy to our scenario, the drones and train respectively act as the team followers, denoted as agents  $\{1, \dots, I\}$  (i.e., the number of drones is  $I$ ), and leader, denoted as agent  $I + 1$ , respectively. In particular, follower  $i$  has the state information  $\xi^{d,i} \in \mathbb{R}^3$  (i.e., the position of drone  $i$   $[x^{d,i}, y^{d,i}, z^{d,i}]^\top$ ) and its derivative  $\zeta^{d,i} \in \mathbb{R}^3$  (i.e., the velocity of drone  $i$   $[\dot{x}^{d,i}, \dot{y}^{d,i}, \dot{z}^{d,i}]^\top$ ), whilst the leader  $I + 1$  has the information state  $\xi^{I+1} \triangleq \xi^t \in \mathbb{R}^3$  (i.e., the train's position  $[x^t, y^t, z^t]^\top$ ) and its derivative  $\zeta^{I+1} \triangleq \zeta^t \in \mathbb{R}^3$  (i.e., the train's velocity  $[\dot{x}^t, \dot{y}^t, \dot{z}^t]^\top$ ) satisfying the following discrete-time reference model:

$$\xi_{n+1}^t = \zeta_n^t, \quad \zeta_{n+1}^t = \varphi(n, \xi_n^t, \zeta_n^t) \quad (5.13)$$

where  $\varphi(\cdot, \cdot, \cdot)$  is required to be piecewise continuous in  $n$  and locally Lipschitz in  $\xi_n^t$  and  $\zeta_n^t$ . We assume that the communication topology in the train-drone network – denoted as  $\mathcal{G}_{I+1}$  – is a directed spanning tree and allows the information to flow only from parents to children. Note that since the flow goes from parents to children, the reference model in (5.13) is directly available to the neighboring followers of the leader, i.e., the children of agent  $I + 1$ .

The basic idea of the consensus algorithm is to impose similar dynamics on the information states of each agent. In this case, the information states of the followers and their derivatives evolve according to the model in (5.13), by guaranteeing that, for each  $i$ ,  $\xi_n^{d,i} \rightarrow \xi_n^t$  and  $\zeta_n^{d,i} \rightarrow \zeta_n^t$ , as  $n \rightarrow \infty$ . By considering the equivalence between the second-order derivatives of the information states and control inputs  $\xi_{n+2}^{d,i} \equiv \zeta_{n+1}^{d,i} \equiv \alpha_n^{d,i}$  with  $\alpha_n^{d,i} \in \mathbb{R}^3$  the drone's acceleration vector in the X, Y, Z axes framework, we define the algorithm with bounded control inputs as follows:

$$\begin{aligned} \alpha_n^{d,i} = & \frac{1}{k_i} \left( \sum_{j=1}^I \omega_{ij} (\zeta_n^{d,j} - \zeta_{n-1}^{d,j}) + \omega_{i(I+1)} (\zeta_n^t - \zeta_{n-1}^t) \right) \\ & - \frac{1}{k_i} K_{ri} \tanh \left( \sum_{j=1}^I \omega_{ij} (\xi_n^{d,i} - \xi_n^{d,j}) + \omega_{i(I+1)} (\xi_n^{d,i} - \xi_n^t) \right) \\ & - \frac{1}{k_i} K_{vi} \tanh \left( \sum_{j=1}^I \omega_{ij} (\zeta_n^{d,i} - \zeta_n^{d,j}) + \omega_{i(I+1)} (\zeta_n^{d,i} - \zeta_n^t) \right), \end{aligned} \quad (5.14)$$

$$i = 1, \dots, I$$

where  $\omega_{ij}$  is the  $(i, j)$  entry of the adjacency matrix  $\mathbf{A}_{I+1} \in \mathbb{R}^{(I+1) \times (I+1)}$  associated with  $\mathcal{G}_{I+1}$ ,  $k_i \triangleq \sum_{j=1}^{I+1} a_{ij}$ ,  $K_{ri}$  and  $K_{vi}$  are  $6 \times 6$  symmetrical positive-definite matrices, and  $\tanh(\cdot)$  is defined componentwise. Note that each entity needs the information states and their first and second-order derivatives (i.e., the information control inputs  $\alpha_n^{d,j}$ ) from its neighbors.

### 5.4.2 Landing Optimal Control Problem

As discussed in Section 5.3.3, the landing phase can be solved as a descent through a go to goal along a vertical or oblique line or as descent along a predefined path which consists in following an oblique given trajectory. The quadrotor is controlled thanks to the implementation of a LQR with two and four Riccati equations for the first and second task, respectively. Note that for the sake of simplifying the notations, we refer to a single drone in this section and thus, superscript  $i$  is removed from the state and control variables.

On the one hand, in the descent through a go to goal line, linearization (5.11) is executed around a nominal point  $\mathbf{s}^{\text{d},*}$  and control input vector  $\mathbf{u}^{\text{d},*}$ , and given a control horizon whose length is  $N$ , the objective of the LQR is to find the  $\mathbf{u}_0^{\text{LQR2}}, \dots, \mathbf{u}_{N-1}^{\text{LQR2}}$  that minimize the following quadratic cost function subject to the model in (5.11) [17]:

$$\begin{aligned} F^{\text{G}} &= (\mathbf{s}_N^{\text{d}} - \mathbf{s}^{\text{d},*})^\top \mathbf{Q}_N^{\text{G}} (\mathbf{s}_N^{\text{d}} - \mathbf{s}^{\text{d},*}) \\ &+ \sum_{n=0}^{N-1} [(\mathbf{s}_n^{\text{d}} - \mathbf{s}^{\text{d},*})^\top \mathbf{Q}_n^{\text{G}} (\mathbf{s}_n^{\text{d}} - \mathbf{s}^{\text{d},*}) \\ &+ (\mathbf{u}_n^{\text{d}} - \mathbf{u}^{\text{d},*})^\top \mathbf{R}_n^{\text{G}} (\mathbf{u}_n^{\text{d}} - \mathbf{u}^{\text{d},*})] \end{aligned} \quad (5.15)$$

where  $\mathbf{Q}_N^{\text{G}} \in \mathbb{R}^{12 \times 12}$ ,  $\mathbf{Q}_n^{\text{G}} \in \mathbb{R}^{12 \times 12}$ , and  $\mathbf{R}_n^{\text{G}} \in \mathbb{R}^{4 \times 4}$  are the final, state, and input cost diagonal matrices to be tuned. Note that the three terms in (5.15) present the final state deviation, state deviation, and control input deviation, respectively.

By solving the minimization problem with the objective function  $F^{\text{G}}$ , the state constraint (5.11), and the initial state  $\mathbf{s}_0^{\text{d}}$ , we obtain the optimal control law:

$$\mathbf{u}_n^{\text{LQR2}} = \mathbf{K}_n^{\text{G}} (\mathbf{s}_n^{\text{d}} - \mathbf{s}^{\text{d},*}) + \mathbf{u}^{\text{d},*}, \forall n = 0, \dots, N-1 \quad (5.16)$$

where the feedback gain  $\mathbf{K}_n^{\text{G}} \in \mathbb{R}^{12 \times 12}$  is obtained through the following well-known two Riccati equations [18] that are solved recursively backwards:

$$\begin{aligned} \mathbf{K}_n^{\text{G}} &= -(\mathbf{R}_n^{\text{G}} + \mathbf{B}^\top \mathbf{P}_{n+1}^{\text{G}} \mathbf{B})^{-1} \mathbf{B}^\top \mathbf{P}_{n+1}^{\text{G}} \mathbf{A}, \\ \mathbf{P}_n^{\text{G}} &= \mathbf{Q}_n^{\text{G}} + \mathbf{A}^\top \mathbf{P}_{n+1}^{\text{G}} \mathbf{A} + \mathbf{A}^\top \mathbf{P}_{n+1}^{\text{G}} \mathbf{B} \mathbf{K}_n^{\text{G}}, \\ &\forall n = 0, \dots, N-1 \end{aligned} \quad (5.17)$$

being  $\mathbf{P}_N^{\text{G}} \in \mathbb{R}^{12 \times 12}$  the parameter matrix and initializing  $\mathbf{P}_N^{\text{G}} = \mathbf{Q}_N^{\text{G}}$ .

On the other hand, in the descent along a predefined path, the system is linearized around the nominal trajectory  $(\mathbf{s}_n^{\text{d},*}, \mathbf{u}_n^{\text{d},*})$  at each iteration step, and a quadratic approximation of the cost function is minimized.

Given a control horizon whose length is  $N$ , analogously to LQR with two Riccati equations, the optimal control vectors  $\mathbf{u}_0^{\text{LQR4}}, \dots, \mathbf{u}_{N-1}^{\text{LQR4}}$  are found by minimizing the following cost function [17] subject to the model in (5.11):

$$\begin{aligned} F^{\text{P}} &= (\mathbf{s}_N^{\text{d}} - \mathbf{s}_N^{\text{d},*})^\top \mathbf{Q}_N^{\text{P}} (\mathbf{s}_N^{\text{d}} - \mathbf{s}_N^{\text{d},*}) \\ &+ \sum_{n=0}^{N-1} [(\mathbf{s}_n^{\text{d}} - \mathbf{s}_n^{\text{d},*})^\top \mathbf{Q}_n^{\text{P}} (\mathbf{s}_n^{\text{d}} - \mathbf{s}_n^{\text{d},*}) \\ &+ (\mathbf{u}_n^{\text{d}} - \mathbf{u}_n^{\text{d},*})^\top \mathbf{R}_n^{\text{P}} (\mathbf{u}_n^{\text{d}} - \mathbf{u}_n^{\text{d},*})] \end{aligned} \quad (5.18)$$

where  $\mathbf{Q}_N^{\text{P}} \in \mathbb{R}^{12 \times 12}$ ,  $\mathbf{Q}_n^{\text{P}} \in \mathbb{R}^{12 \times 12}$ , and  $\mathbf{R}_n^{\text{P}} \in \mathbb{R}^{4 \times 4}$  are the final, state, and input cost diagonal matrices to be tuned.

By solving the minimization problem with the objective function  $F^{\text{P}}$ , the state constraint (5.11), and the initial state  $\mathbf{s}_0^{\text{d}}$ , we obtain the optimal control law:

$$\mathbf{u}_n^{\text{LQR4}} = \mathbf{K}_n^{\text{P}} (\mathbf{s}_n^{\text{d}} - \mathbf{s}_n^{\text{d},*}) + \mathbf{u}_n^{\text{d},*} + \mathbf{k}_n^{\text{P}}, \forall n = 0, \dots, N-1 \quad (5.19)$$

**Table 5.1:** Drone's dynamics parameters.

Description	Parameter	Value
Total mass	$m^d$ [kg]	1.38
Motors' mass	$m_m$ [kg]	0.06
Gravity acceleration	$g$ [m/s <sup>2</sup> ]	9.81
Length	$l_m$ [m]	0.175
Components of the diagonal inertia matrix	$J_{xx} = 2m_m l_m^2$ [kg m <sup>2</sup> ]	0.0037
	$J_{yy} = 2m_m l_m^2$ [kg m <sup>2</sup> ]	0.0037
	$J_{zz} = 4m_m l_m^2$ [kg m <sup>2</sup> ]	0.0073

**Table 5.2:** Tuning parameters in the consensus algorithm.

Parameter	Value
$k$	1.2
$K_r$	$I_6$
$K_v$	$diag(1.25, 1.3, 1, 1, 1, 1)$

where the feedback gain  $\mathbf{K}_n^P \in \mathbb{R}^{12 \times 12}$  and the feedforward gain  $\mathbf{k}_n^P \in \mathbb{R}^4$  (added for the trajectory tracking problem) are obtained through the following well-known four Riccati equations [18] that are solved recursively backwards:

$$\begin{aligned}
 \mathbf{K}_n^P &= -(\mathbf{R}_n^P + \mathbf{B}_n^T \mathbf{P}_{n+1}^P \mathbf{B}_n)^{-1} \mathbf{B}_n^T \mathbf{P}_{n+1}^P \mathbf{A}_n, \\
 \mathbf{P}_n^P &= \mathbf{Q}_n^P + \mathbf{A}_n^T \mathbf{P}_{n+1}^P \mathbf{A}_n + \mathbf{A}_n^T \mathbf{P}_{n+1}^P \mathbf{B}_n \mathbf{K}_n^P, \\
 \mathbf{k}_n^P &= -(\mathbf{R}_n^P + \mathbf{B}_n^T \mathbf{P}_{n+1}^P \mathbf{B}_n)^{-1} (\mathbf{B}_n^T \mathbf{p}_{n+1}^P + \mathbf{r}_n^P), \\
 \mathbf{p}_n^P &= \mathbf{q}_n^P + \mathbf{A}_n^T \mathbf{p}_{n+1}^P + \mathbf{A}_n^T \mathbf{P}_{n+1}^P \mathbf{B}_n \mathbf{k}_n^P, \\
 \forall n &= 0, \dots, N-1
 \end{aligned} \tag{5.20}$$

being  $\mathbf{P}_n^P$  and  $\mathbf{p}_n^P$  the parameter matrices,  $\mathbf{q}_n^P = -\mathbf{Q}_n^P \mathbf{s}_n^{d,*}$  and  $\mathbf{r}_n^P = -\mathbf{R}_n^P \mathbf{u}_n^{d,*}$ , and initializing  $\mathbf{P}_N^P = \mathbf{Q}_N^P$  and  $\mathbf{p}_N^P = \mathbf{q}_N^P$ . Note that the system is linearized at each state-control pair with the matrices  $\mathbf{A}_n$  and  $\mathbf{B}_n$  that, conversely to the descent through a goal, are time-variant.

## 5.5 Numerical experiments

### 5.5.1 System Setup

In this section, we describe the experimental setup of the proposed hybrid movable railway diagnostic architecture, consisting of a diagnostic train and a fleet of drones, employed for the identification and evaluation of anomalies of the railway infrastructure. We highlight that the architecture has been defined in the context of a collaboration with MERMEC S.p.A., an Italian company producer of railway diagnostic systems. The realistic scenario addressed in this work is shown in Fig. 5.2, that reproduces a curvilinear portion of a railway line situated in the Apulian region (Italy) [19]. The goal of our experiment from the control perspective is to optimally manage the re-entry of the drones on the moving train, where the drones' charging base is located, once the inspection mission is accomplished. Note that the trajectory of the train in terms of position, velocity, and timestamp of the landing point situated in the barycentric position of the charging base, is set based on data of the national Italian railway company "Ferrovie dello Stato italiane" [19].

The drones selected for the system simulation experiments are the well-known DJI Phantom 4 Pro [20], which have a maximum speed of 72 km/h and a flight autonomy of about 30 minutes, and are modeled in accordance with the dynamic parameters in Table 5.1. As for the fleet of drones, we refer to the state of the drone positioned in front of the fleet. As initial state's vector of train and drone, and thus as initial condition of the experiment, we consider  $\mathbf{s}_0^t = [500, 0, 3, 11.11, 0, 0]^T$  and  $\mathbf{s}_0^d = [0, 750, 6, 0, 0, 0, 1.39, 0.03, 0, 0, 0, 0]^T$



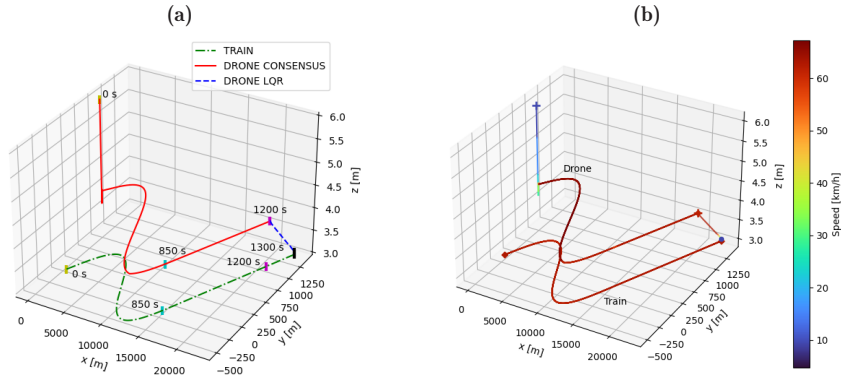


Figure 5.2: 3D train-drone trajectory with time reference (a) and colour-map based on speed (b).

Table 5.3: Tuning parameters in the landing optimal control problem.

Phase	Control	N	$\Delta t$ [s]	Q	R
Vertical descent through a go to goal	LQR with 2 Riccati eqs.	1000	0.01	$550 I_{12}$	$2 I_4$
Oblique descent through a go to goal	LQR with 2 Riccati eqs.	1000	0.01	$diag(100 I_6, 500, 100 I_5)$	$2 I_4$
Oblique descent along a predefined path	LQR with 4 Riccati eqs.	1000	0.1	$diag(500, 5000, 500, 100, 100, 100, 10^6, 10^3, 100, 100, 100, 100)$	$2 I_4$

Table 5.4: Position and speed error in the boarding point.

Phase	Position	Speed
Vertical descent through a go to goal	1.5017e-04	1.1452e-04
Oblique descent through a go to goal	6.1905e-04	0.0484
Oblique descent along a predefined path	0.0480	1.3164

which are the current state of the train and of the drone at the instant equal to 0, corresponding to the time when the inspection mission finalized, respectively. The drone control input vector is defined as  $\mathbf{u}^d = [m^d g, 0, 0, 0]$ .

As for the initialization of the consensus algorithm which is applied along the linear positions and velocities, we set the tuning parameters in Table 5.2. Instead, all the parameters employed for the landing optimal control problem are listed in Table 5.3. As can be seen from Fig. 5.2, through the consensus algorithm we bring the drones to 1 m along the Z axis from the train that we consider 3 m high. All the simulations of this experiment are implemented on Python.

## 5.5.2 Results

The goal is to control a fleet of drones during the return on the moving train by combining the consensus algorithm with the LQR employed in the flight formation phase and landing phase, respectively. For the sake of brevity, we insert in this chapter the results related to the landing executed as oblique descent along a predefined path for the drone positioned in front of the fleet. The results of the other two landing modes are fully available as supplementary material [21].

In particular, it is possible to observe the 3D train-drone trajectory with time and speed reference in Fig. 5.2a and Fig. 5.2b, respectively. The railway path consists of a curvilinear portion that ends in 850 s, followed by a straight line. As we can see from Fig. 5.2a, the total mission for this landing mode lasts 1300 s, i.e., sum of drone consensus (1200 s) and drone LQR (100 s), and thus, lasts 90 s longer than the other two landing modes (LQR's duration is equal to 10 s, i.e., product between the parameters in the third and fourth column of Table 5.3). The drone achieves the consensus with the train in about 700 s reaching a speed of 67 Km/h. In the landing phase the drone begins to decelerate at 1274 s to reach zero speed at the landing area located on the moving train. Since the descents performed as a go to goal last 10 s, the drone reaches a speed of 10 km/h in a sudden manner already from the first iterations.

With the aim of evaluating the effectiveness of the control system employed in this experiment, we compute for each landing mode the error both in position and in speed of the landing point with respect to the center of the charging area (see Table 5.4): it is apparent that negligible errors are generated in all the three landing modes. We finally remark that the vertical and oblique descent performed as go to goal are certainly faster than the oblique descent along a predefined path. This aspect is of significant practical use in the presence of obstacles along the line to be avoid (e.g., pylons), thus implying that a possible choice of the landing mode is up to the users according to their level of experience.

## 5.6 Conclusions

This chapter presents an innovative movable railway diagnostic system architecture that consists of a diagnostic train and a fleet of drones. We focus on the re-entry phase of drones on the moving train –once the inspection mission is finalized– that is optimally controlled by applying a combination of consensus algorithm in the leader-following mode for the flight formation phase and linear quadratic regulator for the landing phase.

Future works will focus on enhancing the estimation of the landing point’s position using a dynamic model of the train, comparing the optimal control system of this work with the model predictive control technique, and implementing the architecture on a real system with the train’s trajectory consisting of curves, climbs, and descents.

## References

- [1] Fan, J. and Saadeghvaziri, M. A., “Applications of drones in infrastructures: Challenges and opportunities,” *Int J Mech Mechatron Eng*, vol. 13, no. 10, pp. 649–655, 2019.
- [2] Ngamkhanong, C., Kaewunruen, S., and Costa, B. J. A., “State-of-the-art review of railway track resilience monitoring,” *Infrastructures*, vol. 3, no. 1, p. 3, 2018.
- [3] Falamarzi, A., Moridpour, S., and Nazem, M., “A review on existing sensors and devices for inspecting railway infrastructure,” *Jurnal Kejuruteraan*, vol. 31, no. 1, pp. 1–10, 2019.
- [4] Flammini, F., Pragliola, C., and Smarra, G., “Railway infrastructure monitoring by drones,” in *2016 International Conference on Electrical Systems for Aircraft, Railway, Ship Propulsion and Road Vehicles & International Transportation Electrification Conference (ESARS-ITEC)*, IEEE, 2016, pp. 1–6.
- [5] Flammini, F., Gaglione, A., Ottello, F., Pappalardo, A., Pragliola, C., and Tedesco, A., “Towards wireless sensor networks for railway infrastructure monitoring,” in *Electrical Systems for Aircraft, Railway and Ship Propulsion*, IEEE, 2010, pp. 1–6.
- [6] Flammini, F., Naddei, R., Pragliola, C., and Smarra, G., “Towards automated drone surveillance in railways: State-of-the-art and future directions,” in *International conference on advanced concepts for intelligent vision systems*, Springer, 2016, pp. 336–348.
- [7] Kochan, A., Rutkowska, P., and Wójcik, M., “Inspection of the railway infrastructure with the use of unmanned aerial vehicles,” *Archives of Transport System Telematics*, vol. 11, 2018.
- [8] Du, H., Zhu, W., Wen, G., Duan, Z., and Lü, J., “Distributed formation control of multiple quadrotor aircraft based on nonsmooth consensus algorithms,” *IEEE Trans Cybern.*, vol. 49, no. 1, pp. 342–353, 2017.
- [9] Ghamry, K. A. and Zhang, Y., “Formation control of multiple quadrotors based on leader-follower method,” in *2015 International Conference on Unmanned Aircraft Systems (ICUAS)*, IEEE, 2015, pp. 1037–1042.

- 
- [10] Proia, S., Cavone, G., Camposeo, A., Ceglie, F., Carli, R., and Dotoli, M., “Safe and ergonomic human-drone interaction in warehouses,” in *2022 IEEE/RSJ International Conference on Intelligent Robots and Systems (IROS)*, Kyoto, Japan, 2022, pp. 6681–6686. DOI: [10.1109/IROS47612.2022.9981469](https://doi.org/10.1109/IROS47612.2022.9981469).
- [11] Falanga, D., Zanchettin, A., Simovic, A., Delmerico, J., and Scaramuzza, D., “Vision-based autonomous quadrotor landing on a moving platform,” in *2017 IEEE International Symposium on Safety, Security and Rescue Robotics (SSRR)*, IEEE, 2017, pp. 200–207.
- [12] Hui, C., Yousheng, C., Xiaokun, L., and Shing, W. W., “Autonomous takeoff, tracking and landing of a uav on a moving ugv using onboard monocular vision,” in *Proceedings of the 32nd Chinese control conference*, IEEE, 2013, pp. 5895–5901.
- [13] Saripalli, S. and Sukhatme, G. S., “Landing on a moving target using an autonomous helicopter,” in *Field and service robotics*, Springer, 2003, pp. 277–286.
- [14] Sabatino, F., *Quadrotor control: Modeling, nonlinear control design, and simulation*, 2015.
- [15] Das, A., Subbarao, K., and Lewis, F., “Dynamic inversion with zero-dynamics stabilisation for quadrotor control,” *IET control theory & applications*, vol. 3, no. 3, pp. 303–314, 2009.
- [16] Ren, W. and Beard, R. W., *Distributed consensus in multi-vehicle cooperative control*. Springer, 2008, vol. 27.
- [17] Bemporad, A., Morari, M., Dua, V., and Pistikopoulos, E. N., “The explicit linear quadratic regulator for constrained systems,” *Automatica*, vol. 38, no. 1, pp. 3–20, 2002.
- [18] Bittanti, S., Laub, A. J., and Willems, J. C., *The Riccati Equation*. Springer Science & Business Media, 2012.
- [19] *Ferrovie dello Stato italiane*, <https://www.rfi.it/it/rete/la-rete-oggi.html>, Accessed: 2022-10-01.
- [20] *Phantom 4 Pro*, <https://www.dji.com/it/phantom-4-pro/info>, Accessed: 2022-10-01.
- [21] *CASE23 experimental results*, <http://dclab.poliba.it/Results-paper-CASE23.pdf>, Accessed: 2023-02-01.

## Chapter 6

# Optimal Control of Drones for a Hybrid Truck-Drone Delivery System

### Abstract

Last-mile delivery is one of the most discussed problems of the last decade due to the growing importance of e-commerce and the development of Industry 4.0. In particular, this problem regards the delivery of parcels from the warehouse to the final customers. In order to bring efficiency and innovation, in this chapter a hybrid delivery architecture is considered, which takes advantage of the combined use of a drone and a truck to perform a sequence of pick-ups and deliveries, and the problem of optimal control of the drones' missions is addressed. The reference scenario is the smart city where the drone of the hybrid delivery architecture is in charge of three different pick-up and delivery missions: truck to point (i.e., pick-up from the truck and delivery to the customer), point to point (i.e., delivery to a customer and pick-up from the subsequent customer), and point to truck (i.e., reentry from a customer to the truck). From the control point of view, the drone is optimally guided in all the operating modes, i.e., ascent and descent from/to truck mode, free flight mode with/without payload, and descent for pick-up/delivery mode, by a receding horizon *linear quadratic regulator* (LQR), which is able to manage the drone in the dynamic landing on a movable vehicle and to allow the changing in real time of the landing point on the truck. Simulation results of the truck-drone delivery architecture are presented and discussed in detail, proving the effectiveness of the proposed method.

### 6.1 Introduction

In recent years, logistics (i.e., the set of operations aimed at planning, implementing, and controlling the flow and the storage of goods and related services from external origin points to companies and from companies to consumption points or final customers) is becoming more and more important in the development of the industrial sector [1] and it largely impacts firms' performance [2], [3]. In this chapter, we focus on Logistics 4.0 (a branch of Industry 4.0) and in particular, on distribution logistics, which generates the highest percentage of the logistic operations costs [4]. One of the most challenging and expensive problems in this field, estimated to range from 13% to 73% of the total distribution costs [5], is the so-called last-mile delivery problem, which consists in the delivery of parcels from the warehouse to the customers (i.e., final destinations) and whose relevance has grown with the increase of the online commerce and the same-day deliveries to single customers. The main issues that trigger relevance for this problem are [6]: (i) the increasing volume of urbanization and e-commerce, (ii) the sustainability of the shipping process since the rise in urban parcel demands induces a higher number of delivery trucks entering the city centers creating congestion and having negative impacts on health, environment, and safety, (iii) costs, (iv) time pressure because most online retailers sell next- or even same-day deliveries as one of their basic service promises, (v) aging workforce that in many industrialized countries enlarges the problem of employers hiring the required manpower. The last-mile delivery operation is usually performed by humans or vehicles such as vans, bikes, trains, and autonomous vehicles such as autonomous vans and drones.

Innovative applications in the last-mile delivery field come with the use of drones (also known as *unmanned aerial vehicles* (UAVs)) as vehicles. In the last decade, the

research and the real field applications of these technologies in the logistic sector are growing exponentially. One of the first applications was developed by Amazon in 2013, with the shipping of small parcels turned into Amazon's drone delivery services Prime Air, i.e., a drone-only delivery system. Subsequently, other companies such as the Workhorse company, the "Project Wing" of Google, and the "Parcelcopter" of DHL proposed a hybrid architecture where drones and trucks cooperate. A typical architecture where a drone and a truck collaborate consists of a drone that autonomously departs from a truck, performs the delivery or the pick-up of the parcel, and then comes back to the truck, while the truck delivers items to the customers or serves as a mobile hub for other drones (in fact, when the drone is on the truck, its battery can be replaced or recharged while waiting for the next trip [7]). The related literature abounds with papers that focus on the design of hybrid drone-truck architectures and their planning. The majority of contributions regard the offline strategic scheduling and routing of trucks and drones in the hybrid truck-drone architecture, while only a few works specifically focus on the online control of the drones' missions in coordination with the truck travel. Therefore, with the aim of bridging this gap, in this chapter, we propose a hybrid automated architecture that consists of a truck and a drone, where the missions of the transportation means are coordinated and the drone is optimally guided in real-time by a receding horizon *linear quadratic regulator* (LQR). The remainder of this chapter is structured as follows. Section 6.2 presents an overview of the related literature and a discussion about the main contributions. In Section 6.3 the 3D quadrotor with its operating modes and the truck dynamic models are examined. The formulation of the receding horizon LQR controller is presented in Section 6.4, and the simulations setup and results are discussed in Section 6.5. Finally, Section 6.6 reports some concluding remarks.

## 6.2 Related Works and Contributions

Numerous studies highlight the importance of drones and their flexibility in different applications such as agriculture, logistics, disaster management, infrastructure, and many others. Thanks to their high speed, low energy consumption, lightweight, and ability to move in three dimensions, instead of along a discrete set of static roadways, drones can employ paths that are closer to straight-line connections and can circumvent traffic congestion or accidents [8]. However, in the external logistic sector, drones present some limits if compared to trucks, e.g., short delivery range, low supported weight, and limited capacity. Consequently, the combined use of drones and trucks for last-mile deliveries can bring several improvements with respect to the separate use of drones and trucks[7]. In the related literature, the majority of contributions deal with the strategic design of hybrid truck-drone delivery architectures and the offline planning of both trucks and drones tasks. In fact, the recent surveys by Chung *et al.* [7] and by Madani *et al.* [9] highlight that the existing works mainly present mathematical models aimed at offline planning, and they can be roughly divided into traveling salesman problems with drones and vehicle routing problems with drones. For instance, Weng *et al.* [10] focus on deliveries in smart cities where parcels have to be delivered in restricted traffic zones aiming at determining the path of the truck out of the restricted zone and the path of the drone inside the restricted zone minimizing the execution time of the delivery. Similarly, Wang *et al.* [11] propose a novel routing and scheduling algorithm, referred to as hybrid truck-drone delivery, to simultaneously employ trucks, truck-carried drones, and independent drones to construct a more efficient truck-drone parcel delivery system. As can be deduced, articles that focus on the online control of drone missions in a hybrid truck-drone delivery system are lacking, although this aspect is crucial for the successful completion of parcel delivery. In particular, the efficient control of the whole mission of the drone and the landing on a moving platform (i.e., the truck) are non-negligible problems. The majority of contributions focus on landing on a static platform, while a limited number of papers tackle the problem of landing on a dynamic platform. Promising contributions in this regard are presented in Paris *et al.* [12] and in Falanga *et al.* [13] where the control

strategy largely relies on the use of artificial vision, while not specifically focusing on hybrid truck-drone delivery systems applications.

Differently from the discussed literature, this work presents a novel control technique for the last-mile delivery problem, where a drone and a truck are able to autonomously collaborate in order to improve the efficiency of the delivery. The proposed approach uses the receding horizon LQR to control the drone in the dynamic landing managing the real-time changes of the positions of the landing point.

### 6.3 System Modelling and Tasks

This section describes the hybrid parcel delivery system based on the combined use of a 3D quadrotor and a truck. In particular, Section 6.3.1 and Section 6.3.2 present the dynamic models of the quadrotor and the truck, respectively, whereas the quadrotor operating modes during the sequence of pick-ups and deliveries tasks are illustrated in Section 6.3.3.

#### 6.3.1 Quadrotor Dynamics

The quadrotor's space motion can be described through six *degrees of freedom* (DOF) as reported in Chapter 5.

The quadrotor of a total mass  $m^d$  is modelled as a rigid body with a symmetric structure and without ground effect, following the system [14] proposed in the equations 5.1-5.10 in Chapter 5. Note that  $m^d$  varies according to the presence of the payload: in particular, it holds  $m^d = m_0^d$  without payload and  $m^d = m_0^d + m^p$  with a payload of mass  $m^p$  equal to the weight of the transported item.

Starting from the non-linear quadrotor's dynamics in (5.2) defined in Chapter 5, the linearized version is often considered in the literature for control purposes (see Section 6.4). Through the linearization around the nominal point  $\mathbf{s}^{d,*}$  and control input vector  $\mathbf{u}^{d,*}$ , and by using the sampling time  $\Delta t$  as a time step and the discrete time index  $n$  as a subscript of vectors and variables, we obtain the following discretized linear dynamics:

$$\bar{\mathbf{s}}_{n+1}^d = \mathbf{A}\bar{\mathbf{s}}_n^d + \mathbf{B}\bar{\mathbf{u}}_n^d \quad (6.1)$$

with the state's vector  $\mathbf{s}^d = [x^d, y^d, z^d, \psi^d, \theta^d, \phi^d, \dot{x}^d, \dot{y}^d, \dot{z}^d, \dot{\psi}^d, \dot{\theta}^d, \dot{\phi}^d]^\top \in \mathbb{R}^{12}$  composed of linear  $x^d, y^d, z^d$  and angular  $\psi^d, \theta^d, \phi^d$  positions and linear  $\dot{x}^d, \dot{y}^d, \dot{z}^d$  and angular  $\dot{\psi}^d, \dot{\theta}^d, \dot{\phi}^d$  velocities of the quadrotor, with the control input vector  $\mathbf{u}^d = [f_t^d, \tau_x^d, \tau_y^d, \tau_z^d]^\top \in \mathbb{R}^4$  composed of the vertical thrust  $f_t^d$  and the angular motions  $\tau_x^d, \tau_y^d, \tau_z^d$  and with  $\bar{\mathbf{s}}_n^d = \mathbf{s}_n^d - \mathbf{s}^{d,*}$  and  $\bar{\mathbf{u}}_n^d = \mathbf{u}_n^d - \mathbf{u}^{d,*}$ .

#### 6.3.2 Truck Model

The truck model is formulated in state space form as:

$$\mathbf{s}_{n+1}^t = f(\mathbf{s}_n^t, \mathbf{u}_n^t) \quad (6.2)$$

where the state vector is defined as  $\mathbf{s}^t = [x^t, y^t, z^t, \dot{x}^t, \dot{y}^t, \dot{z}^t]^\top \in \mathbb{R}^6$  with  $x^t, y^t, z^t$  the truck's positions along the X, Y, Z axes,  $\dot{x}^t, \dot{y}^t, \dot{z}^t$  its linear velocities, and the control input vector as  $\mathbf{u}^t = [\ddot{x}^t, \ddot{y}^t, \ddot{z}^t]^\top \in \mathbb{R}^3$  with  $\ddot{x}^t, \ddot{y}^t, \ddot{z}^t$  the truck's accelerations.

#### 6.3.3 Quadrotor Operating Modes

The considered truck-drone delivery system is composed of a truck on which the drone's charging base is positioned and a drone that performs the pick-up and delivery of parcels from/to the customers in the surrounding areas.

For the development of our truck-drone delivery system automation, we consider three operating modes for the drone that are defined as follows [15].



I) **Ascent from customer and from truck, and descent to truck mode:** Ascent and descent are performed along a vertical and oblique axis, respectively. In particular, for the ascent, the quadrotor starts from the landing point, which is situated near the customer or in the barycentric position of its charging base located on the roof of the truck, and reaches vertically a certain altitude where it begins to hover, while for descent the opposite occurs but in oblique.

II) **Free flight with/without payload mode:** In this operating mode, the quadrotor is in free flight and there is no contact with the road.

III) **Descent for pick-up/delivery mode:** Starting from a certain altitude with a non-zero velocity, the quadrotor descends with a gradually decreasing velocity as it approaches the customer.

## 6.4 Control Strategy

For all the drone's operating modes described in Section 6.3.3, a receding horizon LQR controller [16] is implemented to control the quadrotor. According to the receding horizon approach, given the sampling time  $\Delta t$ , the optimization problem must be solved iteratively at each  $j\Delta t$  time instants, until the end of the delivery mission. It has to be highlighted that the nominal landing point might vary during the mission, since a dynamical platform is considered, thus variables  $s_j^{d,*}$  and  $u_j^{d,*}$  are updated at each time step  $j$  and consequently marked by  $j$  as a subscript.

By assuming the lengths of the prediction horizon and control horizon coincident and equal to  $N$ , the receding horizon open loop optimization problem at time step  $j$  is defined by introducing the following objective function:

$$\begin{aligned} J_{(N)} = & (\mathbf{s}_{j+N}^d - \mathbf{s}_j^{d,*})^\top \mathbf{Q}_{j+N} (\mathbf{s}_{j+N}^d - \mathbf{s}_j^{d,*}) \\ & + \sum_{n=0}^{N-1} [(\mathbf{s}_{j+n}^d - \mathbf{s}_j^{d,*})^\top \mathbf{Q}_{j+n} (\mathbf{s}_{j+n}^d - \mathbf{s}_j^{d,*}) \\ & + (\mathbf{u}_{j+n}^d - \mathbf{u}_j^{d,*})^\top \mathbf{R}_{j+n} (\mathbf{u}_{j+n}^d - \mathbf{u}_j^{d,*})]. \end{aligned} \quad (6.3)$$

where  $\mathbf{Q}_{j+N} \in \mathbb{R}^{12 \times 12}$ ,  $\mathbf{Q}_{j+n} \in \mathbb{R}^{12 \times 12}$ , and  $\mathbf{R}_{j+n} \in \mathbb{R}^{4 \times 4}$  are the final cost, state cost, and input cost diagonal matrices to be tuned. Note that the three terms in (6.3) present the final state deviation, state deviation, and input size, respectively.

Given the initial state  $\mathbf{s}_j^d$ , let  $\mathbf{u}_{j+n}^{LQR}$ ,  $n = 0, \dots, N-1$  be the control sequence that minimizes the quadratic cost function  $J_{(N)}$  subject to the state equation:

$$\begin{aligned} \mathbf{s}_{j+n+1}^d = & \mathbf{A}(\mathbf{s}_{j+n}^d - \mathbf{s}_j^{d,*}) + \mathbf{B}(\mathbf{u}_{j+n}^{LQR} - \mathbf{u}_j^{d,*}) + \mathbf{s}_j^{d,*}, \\ \forall n = & 0, \dots, N-1. \end{aligned} \quad (6.4)$$

In particular, the optimal control law is computed by the following iterative scheme:

$$\mathbf{u}_{j+n}^{LQR} = \mathbf{K}_{j+n}(\mathbf{s}_{j+n}^d - \mathbf{s}_j^{d,*}) + \mathbf{u}_j^{d,*}, \forall n = 0, \dots, N-1 \quad (6.5)$$

where the state  $\mathbf{s}_{j+n}^d$  is updated in accordance with the model in (6.4) and the feedback gain  $\mathbf{K}_{j+n} \in \mathbb{R}^{12 \times 12}$  is obtained through the following well-known Riccati difference equations [17] that are solved recursively backwards:

$$\begin{aligned} \mathbf{K}_{j+n} = & -(\mathbf{R}_{j+n} + \mathbf{B}_j^\top \mathbf{P}_{j+n+1} \mathbf{B}_j)^{-1} \mathbf{B}_j^\top \mathbf{P}_{j+n+1} \mathbf{A}_j, \\ \mathbf{P}_{j+n} = & \mathbf{Q}_{j+n} + \mathbf{A}_j^\top \mathbf{P}_{j+n+1} \mathbf{A}_j + \mathbf{A}_j^\top \mathbf{P}_{j+n+1} \mathbf{B}_j \mathbf{K}_{j+n} \\ \forall n = & 0, \dots, N-1 \end{aligned} \quad (6.6)$$

being  $\mathbf{P}_{j+n} \in \mathbb{R}^{12 \times 12}$  the parameter matrix and initializing  $\mathbf{P}_{j+N} = \mathbf{Q}_{j+N}$ .

The receding horizon policy proceeds by implementing only the first control input vector  $\mathbf{u}_j^{LQR}$ , whilst the rest of the control sequence  $\mathbf{u}_{j+n}^{LQR}$ ,  $\forall n = 1, \dots, N-1$  is not considered and  $\mathbf{s}_{j+1}^d$  is employed to update the optimization problem as a new initial condition. The algorithm proceeds until the end of the delivery mission, by shifting the horizon ahead by one time step.

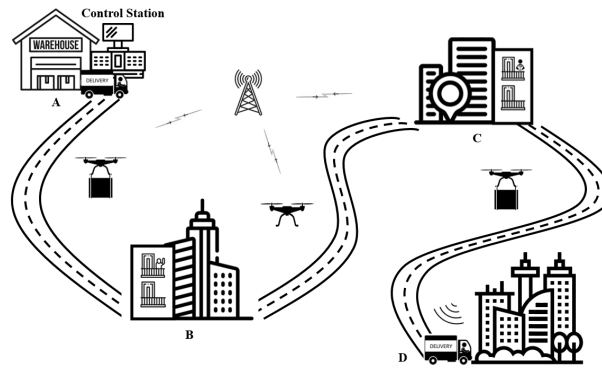


Figure 6.1: Parcels' last-mile delivery architecture with operating tasks phases.

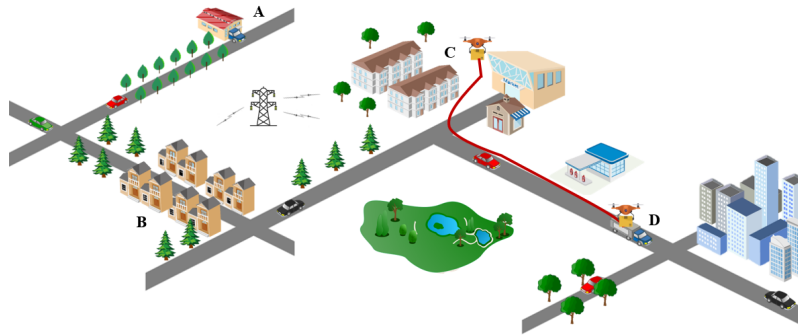


Figure 6.2: Last-mile delivery of parcels architecture with focus on the trajectory performed by the drone in the third operating task phase, i.e., Point (C) to Truck (D).

## 6.5 Numerical Experiments

### 6.5.1 System Setup

In this section, we describe the system setup and the simulation results of the proposed real-time control strategy for a hybrid truck-drone delivery system. We highlight that the quadrotor's control system is implemented on a Jupyter Notebook.

In the context of the last-mile delivery problem, i.e., delivery of items from the warehouse to the customers, the goal of our experiment is to efficiently perform a sequence of pick-up and delivery of parcels tasks in a smart city, by employing a hybrid truck-drone delivery architecture composed of a truck and a drone. Offline scheduled missions and depart/return together from/to the warehouse – where the truck is loaded with both its parcels and the ones of the drone – are assigned to the truck and the drone. The drone can recharge on the truck roof and must pick up and release from/to the truck light parcels, depending on its admissible payload. Differently, the truck is devoted to the delivery of heavier parcels. Pick-ups and deliveries can be assigned to both the truck and the drone, but at each mission, the truck departs and returns from/to the warehouse, while the drone departs/returns from/to the moving truck. Thanks to state-of-the-art sensors mounted on drones board that allow collecting data quickly and easily, the control station can communicate with the drone by notifying the trajectory (both position and velocity) of the truck in accordance with a certain sampling time  $\Delta t$  and thus, drone and truck rejoin along the fixed route of the truck.

More specifically, with the use of the three quadrotor's operating modes listed in Section 6.3.3, i.e., ascent and descent from/to truck mode, free flight mode with/without payload, and descent for pick-up/delivery mode, it is possible to perform a mission (see Fig. 6.1) through three phases, as detailed below.

1) **Truck (A) to Point (B)**: In this phase, once the truck has left the warehouse, the

**Table 6.1:** Quadrotor dynamics parameters.

Phase	$m^d$ [kg]	$\mathbf{I}$ [kg m <sup>2</sup> ]
Truck (A) to Point (B) Point (C) to Truck (D)	2.18	diag(0.0087,0.0087,0.0123)
Point (B) to Point (C)	1.38	diag(0.0037,0.0037,0.0073)

drone ascends from its charging base located on the roof of the truck with the parcel directed towards the customer placed at point B. Hence, the drone performs the route in free flight mode with payload and then executes the descent towards the customer.

2) **Point (B) to Point (C):** In this phase, after the drone has released the parcel to the customer located at point (B), it leaves in free flight mode without payload towards the second customer, i.e., point (C).

3) **Point (C) to Truck (D):** In this phase, after the drone picks up the customer parcel located at point (C), it receives the trajectory (both position and velocity) of the truck from the control station. Thus, the drone follows the trajectory of the truck in free flight mode with payload, and then, once reached, it is ready to descend towards the landing point situated in the barycentric position of the charging base, i.e., point (D). Note that, since the truck is moving, the drone is initially aligned with the truck along the X and Y axes, while keeping a given offset along Z, and reaches the landing point from behind. As a final remark, during the current phase, the truck, if necessary, slows down its velocity to adapt to the technical characteristics of the drone. The same holds for the drone as well. The realistic scenario addressed in this work is shown in Fig. 6.1, which reproduces the hybrid movable architecture that consists of a drone and a truck. In particular, Fig. 6.1 illustrates a portion of an entire daily truck-drone mission, i.e., the route followed by the truck transporting the items from the warehouse to the various customers located in different places and the drone that helps the courier to perform pick-ups and deliveries and once the assigned tasks are completed, it intercepts the truck on which the charging base is placed. The experiment is conducted considering the well-known DJI Phantom 4 Pro [18] drone, which has a maximum speed of 72 km/h and a flight autonomy of about 30 minutes. In particular, the quadrotor is modeled in accordance with the dynamic parameters in Table 6.1, where  $m^d$  and  $\mathbf{I}$  indicate the total mass of the quadrotor and the diagonal inertia matrix, respectively. The load of mass  $m^p$  carried by the vacuum gripper attached to the quadrotor base is equal to 0.8 kg. Instead, the drone' control input vector is defined as  $\mathbf{u}^d = [m^d g, 0, 0, 0]$  with the gravitational acceleration  $g$  set to 9.81 m/s<sup>2</sup>. To conclude the system setup, we set the sampling time  $\Delta t = 0.01$  s,  $N = 2000$ , as representing a good compromise between computational complexity and solution quality, the initial state cost matrix  $\mathbf{Q}_{j+N} = 200 \mathbf{I}_{12}$ , and the initial input cost matrix  $\mathbf{R}_{j+N} = 2 \mathbf{I}_4$  computed for each time step  $j$ .

## 6.5.2 Results

The goal of our work is to control a drone employed in the last-mile delivery problem in tandem with a truck with the aim of performing pick-ups/deliveries from/to customers in a smart city. In the proposed model, the truck works as a primary vehicle and follows a fixed route determined offline before the beginning of the mission. Instead, the drone departs from the roof of the truck (which is following its fixed route) and visits the customers according to the schedule. Then, in order to take other parcels from the truck and be ready for the next sortie, it returns to the moving truck whose position is notified by the control station.

The parcels' last-mile delivery architecture with the truck-drone combined operations is represented in a schematic configuration in Fig. 6.1 whereas in a 3D reconstruction in Fig. 6.2 to help the reader imagine the real scenario of an urban environment. For the sake of clarity, we highlight that the nodes (A), (B), (C), and (D) in Fig. 6.1 and Fig. 6.2 are coincident. As can be seen from the 3D view (Fig. 6.2), the truck leaves the warehouse to perform the scheduled deliveries of the heavier parcels and at the same time the drone carries out pick-ups and deliveries of parcels (i.e., Point (B) and Point (C))

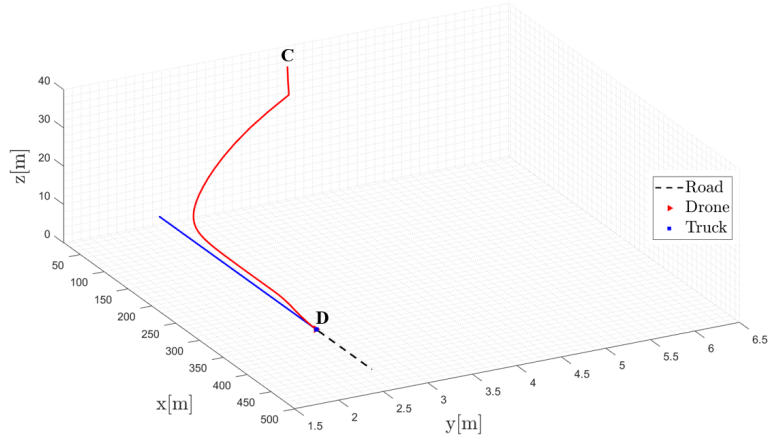


Figure 6.3: Drone’s trajectory from Point (C) to Truck (D).

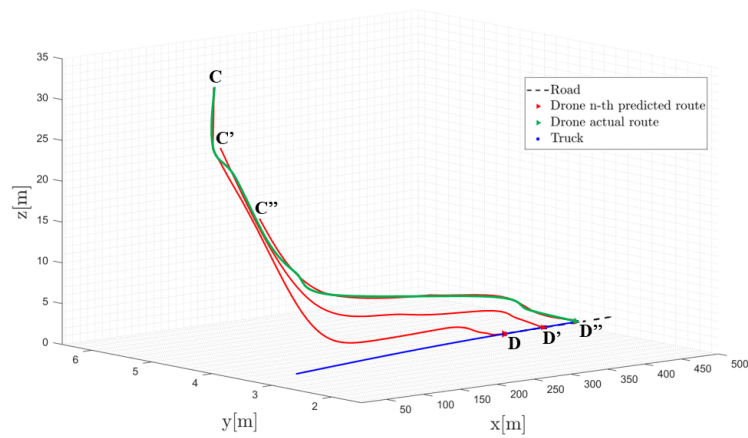


Figure 6.4: Drone’s trajectory variation with moving landing point located on the truck.

with a lower payload in the surrounding areas. Furthermore, Fig. 6.2 shows the trajectory followed by the drone to chase and catch up with the truck and then to perform the descent towards the landing point located on the roof of the moving truck. The trajectory from Point (C) to Truck (D) is also represented in red in Fig. 6.3, where it is possible to observe the perfect tracking executed by the drone of the truck’s trajectory (in blue) given at each sampling time  $\Delta t$  by the control station in terms of position and velocity.

The effectiveness of the implemented controller, i.e., the receding horizon LQR, lies in the possibility of changing online the position of the landing point located on the roof of the truck (i.e., the final cost in the objective function (6.3)). The drone can not only vary its speed, depending on the technical characteristics of the truck and vice-versa, but it can also change its trajectory towards the landing point in case there is an unexpected event, such as a slowdown of the truck due to traffic or merely a transmission error by the control station. Fig. 6.4 illustrates the trajectory followed by the drone as the position of the landing point varies from Point (D) to Point (D') and then to Point (D''). More specifically, it is possible to see the drone’s predicted routes in red from different starting points placed forward on the given prediction horizon whereas the drone’s actual route in green from Point (C) to Truck (D''), which intersects the n-th predicted routes.

## 6.6 Conclusions

This chapter presents an automatic real-time control approach for a hybrid truck-drone delivery system devoted to last-mile deliveries. In particular, the drone is used to help the

courier to perform a sequence of pick-ups and deliveries of parcels from/to the customers in the surrounding areas of the smart city and, once the scheduled tasks are finalized, it intercepts the moving truck and descends towards the charging base placed on its roof. To accomplish the desired mission, the drone is optimally guided by a receding horizon linear quadratic regulator in all its operating modes, which are classified as: ascent and descent from/to truck mode, free flight with/without payload mode, and descent for pick-up/delivery mode. In particular, the controller is able to manage in real-time the drone's landing on the moving truck and allow the online change of the landing point on the truck.

Future works will focus on enhancing the dynamical model of the drone, in order to consider the effects of the terrain and the airflow generated by the propellers, and on employing a dynamical model of the truck with the aim of enhancing the estimation of the landing point's position where the descent takes place. In addition, it will be useful to include the energy management objective in the current cost function, to compare the performance of the optimal control technique considered in this work with other receding horizon control strategies like model predictive control with constraints on the translational speed of the drone and on the flying elevation in a city environment or some visual-based control approaches and to implement the proposed architecture on a real system.

## References

- [1] Winkelhaus, S. and Grosse, E. H., "Logistics 4.0: A systematic review towards a new logistics system," *International Journal of Production Research*, vol. 58, no. 1, pp. 18–43, 2020.
- [2] Bag, S., Gupta, S., and Luo, Z., "Examining the role of logistics 4.0 enabled dynamic capabilities on firm performance," *The International Journal of Logistics Management*, 2020.
- [3] Boenzi, F., Digiesi, S., Facchini, F., Mossa, G., and Mummolo, G., "Sustainable warehouse logistics: A nip model for non-road vehicles and storage configuration selection," *Proceedings of the XX Summer School Operational Excellence Experience "Francesco Turco"*, 2015.
- [4] Tresca, G., Cavone, G., and Dotoli, M., "Logistics 4.0: A matheuristics for the integrated vehicle routing and container loading problem," in *2022 IEEE International Conference on Systems, Man, and Cybernetics (SMC)*, IEEE, 2022, pp. 333–338.
- [5] Cavone, G., Epicoco, N., Carli, R., Del Zotti, A., Paulo Ribeiro Pereira, J., and Dotoli, M., "Parcel delivery with drones: Multi-criteria analysis of trendy system architectures," in *2021 29th Mediterranean Conference on Control and Automation (MED)*, 2021, pp. 693–698. DOI: [10.1109/MED51440.2021.9480332](https://doi.org/10.1109/MED51440.2021.9480332).
- [6] Boysen, N., Fedtke, S., and Schwerdfeger, S., "Last-mile delivery concepts: A survey from an operational research perspective," *Or Spectrum*, vol. 43, no. 1, pp. 1–58, 2021.
- [7] Chung, S. H., Sah, B., and Lee, J., "Optimization for drone and drone-truck combined operations: A review of the state of the art and future directions," *Computers & Operations Research*, vol. 123, p. 105 004, 2020. DOI: <https://doi.org/10.1016/j.cor.2020.105004>. [Online]. Available: <https://www.sciencedirect.com/science/article/pii/S0305054820301210>.
- [8] Moshref-Javadi, M., Hemmati, A., and Winkenbach, M., "A truck and drones model for last-mile delivery: A mathematical model and heuristic approach," *Applied Mathematical Modelling*, vol. 80, pp. 290–318, 2020. DOI: <https://doi.org/10.1016/j.apm.2019.11.020>. [Online]. Available: <https://www.sciencedirect.com/science/article/pii/S0307904X19306936>.

- 
- [9] Madani, B. and Ndiaye, M., “Hybrid truck-drone delivery systems: A systematic literature review,” *IEEE Access*, 2022.
- [10] Weng, Y.-Y., Wu, R.-Y., and Zheng, Y.-J., “Cooperative truck–drone delivery path optimization under urban traffic restriction,” *Drones*, vol. 7, no. 1, p. 59, 2023.
- [11] Wang, D., Hu, P., Du, J., Zhou, P., Deng, T., and Hu, M., “Routing and scheduling for hybrid truck-drone collaborative parcel delivery with independent and truck-carried drones,” *IEEE Internet of Things Journal*, vol. 6, no. 6, pp. 10 483–10 495, 2019.
- [12] Paris, A., Lopez, B. T., and How, J. P., “Dynamic landing of an autonomous quadrotor on a moving platform in turbulent wind conditions,” in *2020 IEEE International Conference on Robotics and Automation (ICRA)*, IEEE, 2020, pp. 9577–9583.
- [13] Falanga, D., Zanchettin, A., Simovic, A., Delmerico, J., and Scaramuzza, D., “Vision-based autonomous quadrotor landing on a moving platform,” in *2017 IEEE International Symposium on Safety, Security and Rescue Robotics (SSRR)*, IEEE, 2017, pp. 200–207.
- [14] Lee, D., Burg, T. C., Dawson, D. M., Shu, D., Xian, B., and Tatlicioglu, E., “Robust tracking control of an underactuated quadrotor aerial-robot based on a parametric uncertain model,” in *2009 IEEE international conference on systems, man and cybernetics*, IEEE, 2009, pp. 3187–3192.
- [15] Proia, S., Cavone, G., Camposeo, A., Ceglie, F., Carli, R., and Dotoli, M., “Safe and ergonomic human-drone interaction in warehouses,” in *2022 IEEE/RSJ International Conference on Intelligent Robots and Systems (IROS)*, Kyoto, Japan, 2022, pp. 6681–6686. DOI: [10.1109/IROS47612.2022.9981469](https://doi.org/10.1109/IROS47612.2022.9981469).
- [16] Primbs, J. A. and Nevistic, V., “Constrained finite receding horizon linear quadratic control,” in *Proceedings of the 36th IEEE Conference on Decision and Control*, IEEE, vol. 4, 1997, pp. 3196–3201.
- [17] Bittanti, S., Laub, A. J., and Willems, J. C., *The Riccati Equation*. Springer Science & Business Media, 2012.
- [18] *Phantom 4 Pro*, <https://www.dji.com/it/phantom-4-pro/info>, Accessed: 2022-09-01.



## Chapter 7

# Conclusions

Over the years, the industry's primary objective has been straightforward: establish intelligent, automated production processes centered on digital communication and the systematic collection of data to perpetually enhance production efficiency.

The evolving landscape of industry is characterized by various emerging frontiers driven by technological advancements, shifting market dynamics, and innovative business models. These frontiers encompass on the one hand the integration of digital technologies, cyber-physical systems, artificial intelligence, and the internet of things into manufacturing processes, with the potential for future developments such as Industry 5.0 that focuses on enhanced collaborative robotic systems and in particular, on *human-robot collaboration* (HRC) by placing significant value on human input.

HRC democratizes the human touch, departing from traditional fenced-off industrial robots that replace human labor with automation. Instead, it augments human craftsmanship by providing the speed, accuracy, and precision needed to craft contemporary products while preserving that essential human element.

On the other hand, the cutting-edge frontiers include the integration of sensors and data analytics into smart infrastructure to enhance maintenance, reduce downtime, and improve safety, and thus, the use of cooperative robot-machine systems like drones and diagnostic trains for inspections of infrastructure, reducing costs and improving the efficiency of monitoring and maintenance. Within the industrial domain, a horizon of fresh possibilities is driven by emerging development of innovative last-mile delivery solutions, including drone delivery, autonomous delivery vehicles, and smart lockers, to streamline urban logistics.

In this thesis, two main research directions related to the implementation of control techniques for collaborative and cooperative robotic systems have been presented.

In the first part we analyze the emerging challenges in the related research field and we describe and design innovative HRC architectures and control methods in presence or absence of optimization in order to fill the literature identified gaps emerged from the extensive and complete reviews [1], [2] conducted by the author. The specific contributions of each chapter are reported hereafter.

- The analysis of the state-of-the-art of cobotic control systems presented in Chapter 2 is essential for researchers to identify gaps and future developments in the context of digital evolution. Thus, the categorization of the main works related to the existing decision and control techniques for a safe, ergonomic, and efficient HRC, which is the objective of the review, will certainly be useful to the scientific community to find a way to improve the current control approaches and seek alternative solutions.
- Undoubtedly, trajectory planning stands out as a pivotal concern explored in the realms of robotics and cobotics research. Its primary objective is to expedite real-world tasks, whether in experimental settings or industrial applications, ultimately bolstering a company's profitability and enhancing the comfort of human workers. Chapter 3 introduces a fresh perspective, presenting a multi-objective optimization method tailored for trajectory planning within the context of safe and ergonomic HRC. The aim is to strike an optimal balance between operator ergonomics and the time taken by the robot to traverse a predefined path. The effectiveness of this approach is assessed through an experimental case study.
- Chapter 4 illustrates an industrial use case of human collaboration with drone involving a quadrotor executing a pick-and-place operation within a warehouse 4.0 environment. Specifically, the quadrotor's role is to transport an item from the

---

picking bay to the palletizing area, ensuring a safe and ergonomically favorable collaboration with the operator. To achieve this, two key aspects are addressed: firstly, the paper identifies the ergonomic posture and the human collaboration with drone point by employing the *rapid upper limb assessment* (RULA) methodology. Secondly, it calculates the safety distance between the operator and the quadrotor, especially within the collaborative work zone, using the *speed and separation monitoring* (SSM) approach. By considering these factors, the study aims to facilitate safe and efficient human-quadrotor collaboration in a real-world industrial setting.

The research problems presented in the first part of this thesis have left open problems and paved the way for novel research directions.

- Future works will center on refining the HRC architecture to accommodate unforeseeable human behaviors. This will involve dynamic trajectory replanning in real-time, considering significant variations in the position and potentially the physical attributes of collaborating operators. Lastly, it might prove advantageous to assess the RULA index using a more sophisticated manikin that can better simulate real-world conditions.
- In upcoming research efforts, the emphasis will be on advancing the human collaboration with drone framework. This will involve accounting for operators who are in motion rather than stationary and predicting human movement within the warehouse 4.0 environment. This prediction will encompass aspects such as collision avoidance with human workers and objects during the ascent and descent phases. Furthermore, there will be an exploration of the quadrotor model equipped with a retractable gripper in the context of more intricate tasks.

In the second part of the thesis we focus on the cooperation between a fleet of drones or an individual drone and a ground mobile robotic system (i.e., train, truck) that entails these entities operating together in a synchronized fashion to accomplish defined goals or tasks. The two specific contributions are described hereafter.

- In Chapter 5, we introduce a novel architecture for a movable railway diagnostic system comprising a diagnostic train and a fleet of drones. The primary focus is on the re-entry phase of the drones onto the moving train, which occurs once the inspection mission is completed. To achieve optimal control during this process, a combination of consensus algorithm in a leader-following mode for the flight formation phase and a *linear quadratic regulator* (LQR) for the landing phase are employed.
- Chapter 6 introduces an automated real-time control strategy designed for a hybrid truck-drone delivery system primarily tailored for last-mile delivery. Specifically, the drone plays a supporting role by assisting the courier in executing a series of parcel pick-ups and deliveries from/to customers in the vicinity of a smart city. Upon completing the scheduled tasks, the drone intercepts the moving truck and descends towards a charging station located on the truck's roof. To accomplish this mission effectively, the drone's operations are optimally guided using a receding horizon LQR across various operating modes. Notably, the controller possesses the capability to manage the real-time landing of the drone onto the moving truck and allows for on-the-fly adjustments to the landing point on the truck.

The research problems presented in the second part of this thesis have left open problems and paved the way for novel research directions.

- Future research will prioritize improvements in conducting a comparative analysis between the optimal control system presented in this part and the model predictive control technique and in implementing the proposed architecture in a real-world system where the train's trajectory includes curves, inclines, and descents.

- 
- Future works will concentrate on improving the drone’s dynamical model and enhancing the accuracy of estimating the landing point during the descent process. Furthermore, it would be beneficial to integrate an energy management objective into the existing cost function to compare the performance of the optimal control method presented in this chapter with other receding horizon control strategies. Lastly, we plan to implement the proposed architecture in a real-world system, further validating its effectiveness and practicality in real applications.

## References

- [1] Proia, S., Carli, R., Cavone, G., and Dotoli, M., “Control techniques for safe, ergonomic, and efficient human-robot collaboration in the digital industry: A survey,” *IEEE Transactions on Automation Science and Engineering*, vol. 19, no. 3, pp. 1798–1819, 2022. DOI: [10.1109/TASE.2021.3131011](https://doi.org/10.1109/TASE.2021.3131011).
- [2] Proia, S., Carli, R., Cavone, G., and Dotoli, M., “A literature review on control techniques for collaborative robotics in industrial applications,” in *2021 IEEE 17th International Conference on Automation Science and Engineering (CASE)*, Lyon, France, 2021, pp. 591–596. DOI: [10.1109/CASE49439.2021.9551600](https://doi.org/10.1109/CASE49439.2021.9551600).